Alexander Tichai

Convergence Behaviour of Many-Body Perturbation Theory

Master Thesis

Supervisor Prof. Dr. Robert Roth
Second Advisor MSc. Joachim Langhammer

January 2014

TECHNISCHE
UNIVERSITÄT
DARMSTADT

Contents

List of Figures

List of Tables

Chapter 1

Introduction

The solution of the quantum many-body problem is the major goal of nuclear-structure theory and there is a great variety of *ab-initio* methods to provide accurate results on all kinds of observables going from ground-state energies over charge distributions and transition strengths up to the description of reactions. However, there is no superior method that is able to deal with all arising problems in a satisfactory way. Therefore, one must choose a particular approach to tackle specific problems. This investigation is mainly dedicated to the challenge of optimizing convergence properties of perturbative calculations.

Perturbation theory is a well-known attempt to solve the stationary Schrödinger equation

$$\hat{H}|\psi_n\rangle = E_n|\psi_n\rangle. \tag{1.1}$$

However, perturbation theory was known long before quantum mechanics was formulated. Orignially, this framework provides solutions to many ordinary differential equations. Lateron the framework was adapted for solving linear eigenvalue problems like (1.1). The main idea is very simple: one considers the solution to a problem given as an infinite power series in terms of a perturbation parameter λ and the coefficients of this power series arise from calculations specific to the particular problem. Ultimately one obtains an approximation to the solution by setting the parameter λ introduced to the problem to one. It is expected that calculating more contributions increases the accuracy of the approximation. Unfortunately this is only the case for a converging power series. In contrast, typically one is left with a divergent series expansion and one must think of an alternative way to obtain the solution.

Within this analysis we dealed with two different approaches. The initial ansatz was the use of so called resummation schemes, i.e., transformations that enable us to extract information from divergent series. Those schemes are very common in numerics and mathematical physics, when dealing with highly pathological problems, that are far away from providing an adequate description of nature. However, one attempt is the transfer of those methods to the description of realistic interactions and benchmarking their properties on a well-known example.

Secondly we analyzed perturbative results with respect to their partitioning. It is a well-known fact that perturbation problems are very sensitive to the underlying basis set in which the exact solution is expanded. We expect Hartree-Fock basis states, obtained via a variational procedure,

to yield better results compared to Harmonic Oscillator basis states, due to the optimized single-particle nature of the Hartree-Fock states.

All calculations for nuclei treat two-body interactions only. Those are constructed from chiral effective field theory. Furthermore, we always use the similarity renormalization group approach to evolve the Hamiltonian to improve the convergence properties with respect to the model spaces.

We start our investigation with a brief review of the nuclear interaction in chapter 2. Afterwards, we introduce the similarity renormalization group method on a basic level in chapter 3. We derive the flow equation for the evolution of the Hamiltonian and briefly discuss properties of the generator and induced higher particle-rank contributions. In chapter 4 we introduce the general concept of perturbation theory with help of basic examples like algebraic equations and conclude with a short treatment on the classification of perturbation problems. Next follows a discussion of the reasons for the failure of perturbative attempts and the derivation of low-order contributions to a first quantum problem.

The next sections are dedicated to perturbation theory in quantum mechanics. In chapter 5 we start with the general framework of Rayleigh-Schrödinger perturbation theory. We present a derivation of a recursive scheme for the derivation of high-order energy corrections. It follows a short introduction and derivation of the Hartree-Fock method in chapter 6 which provides the fundament of all subsequent calculations. Furthermore, we present in chapter 7 a treatment of both harmonic-oscillator perturbation theory and Hartree-Fock perturbation theory and discuss some special properties of the partitioning. After that we treat in chapter 8 a diagrammatic approach to low-order perturbation theory. The appearing Hugenholtz diagrams provide a concise derivation of formulas that are almost impossible to derive manually. Therefore, we investigate this in more depth, presenting a combinatorial approach in terms of graph theory.

After dealing with many-body methods, we show in chapter 9 a self-contained introduction to the basics of resummation theory. Starting with basic definitions we present some simple resummation methods and conclude with the treatment of asymptotic series. Next we investigate in more detail the wide field of sequence transformations in particular convergence acceleration. We conclude this section with a detailed discussion of Padé approximants with additional focus on their convergence theory.

In chapter 10 we briefly introduce the Coupled-Cluster approach, that is used lateron to test the perturbative results on consistency.

After providing the mathematical and phyiscal theory we give a description of the occuring difficulties from a computational point of view in chapter 11. We also present some strategies that were used in order to optimize both runtime and storage in low-order perturbation theory.

Chapter 12 presents the results of the performed calculations. Starting with the use of resummation schemes we investigate the quantum anharmonic oscillator and light nuclei and the effect of sequence transformations on the corresponding perturbation series. On the contrary we investigate the impact of HF basis states on the convergence properties both for high-order perturbation theory for light nuclei and low-order calculations for closed-shell nuclei over the whole mass range.

Finally, chapter 13 summarizes the obtained results and gives an outlook for future investigations and ongoing tasks.

Chapter 2

The Nuclear Hamiltonian

When analyzing the structure of nuclei, one is first left to find a model for the nucleonic interaction. In general, this is Quantum Chromodynamics (QCD). In principle nucleons are compound objects consisting of quarks as internal degrees of freedom, which are described in terms of colour and flavour. When formulating field theories one considers a Lagrangian that is consistent with certain symmetries. Those involve continous and discrete symmetries which may be described by their corresponding symmetry groups. An example for a continous symmetry group is Poincaré invariance, whereas parity is an example of a discrete symmetry. Next one is left with formulating a quantized field theory in terms of this Lagrangian.

Unfortunenately QCD has the property of a 'running coupling', meaning that its coupling constant is depend on the energy regime one is dealing with. The functional dependence is inverse to the coupling constant, so that the coupling is small for large energies and we may expand the occuring expressions in terms of that constant. On the other side nuclear structure theory takes place at low energies. In this regime the coupling constant can not be treated perturbatively. Therefore we use an effective field theory approach rather than solving QCD from first principles. We do not resolve the constituents of nucleonic matter but treat nucleons as effective degrees of freedom. This approach is known as chiral effective field theory (χEFT) [48, 20].

Effective approaches in general exhibit only a finite range of validility. The simplest model based from χEFT considers interactions between nucleon only by means of the lightest exchange-mesons, i.e., pions. In the case of massless quarks the interactions between up and down quarks are perfectly symmetric. This is referred to as the *chiral limit*. Nevertheless these quarks have rest masses of roughly 5MeV and therefore break the chiral symmetry explicitly. In addition not every property of nuclei maybe explained in terms of one-pion-exchanges only. In general one must include multi-pion exchanges [11, 24, 29].

Even though we restrict ourselves to the low energy regime there is still an infinite number of diagrams contributing to the action of the Lagrangian. However, it is possible to classify interactions by means of a so-called power counting scheme. In the 1980s Weinberg was able to show that there exist an expansion in powers of $(\frac{Q}{\Lambda})$. Here Q is a typical momentum, and $\Lambda = 1$ GeV a breakdown scale for the chiral symmetry to hold. Figure 2.1 depicts the lowest-orders contributions up to particle rank four. However, within this investigation we will only be concerned with two-body interactions. The Hamiltonian in use contains all diagrams up to N^3LO, i.e., fourth order in

powers of $(\frac{Q}{\Lambda})$ [10].

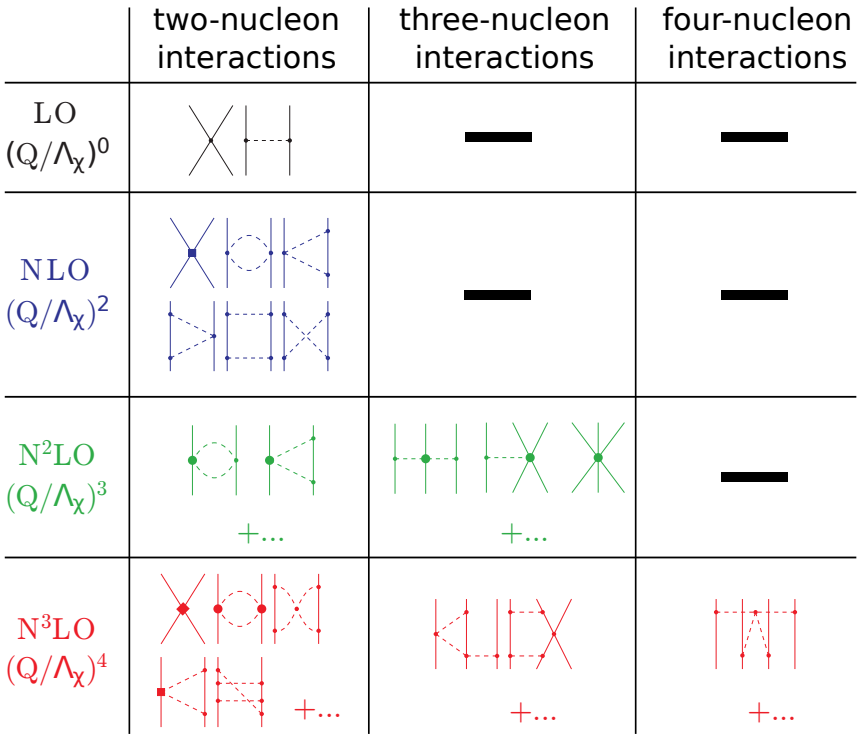

Figure 2.1: Hierarchy og the nucleonic interaction, taken from [24]

Chapter 3

Similarity Renormalization Group Transformation

One of the major challenges in nuclear structure theory is the treatment of short-range repulsions and tensor correlations in nuclear eigenstates. We use a Renormalization Group (RG) approach to soften the interaction and suppress these short-range correlations. These approaches will lead to an increased convergence behaviour with respect to the model space and consequently make the use of many-body-methods more feasible. We use a particular renomalization technique called Similiarity Renormalization Group (SRG) [19] [37]. This approach uses unitary transformations of the Hamiltonian resulting in a flow equation to evolve the interaction. This drives the Hamiltonian into band-diagonal structure and exponentially suppresses off-diagonal matrix elements. We start with deriving the flow equation. Therefore, consider an arbitrary Hamiltonian $\hat{H}$ and unitary operator $\hat{U}_\alpha$ depending on some parameter α. The transformed Hamiltonian is given by

$$\hat{H}_\alpha = \hat{U}_\alpha \hat{H} \hat{U}_\alpha^\dagger, \tag{3.1}$$

where α will be called the *flow parameter*. Next we will differentiate the above equation with respect to α. By the product rule we get

$$\frac{d\hat{H}_\alpha}{d\alpha} = \frac{d\hat{U}_\alpha}{d\alpha} \hat{H} \hat{U}_\alpha^\dagger + \hat{U}_\alpha \hat{H} \frac{d\hat{U}_\alpha^\dagger}{d\alpha}, \tag{3.2}$$

where the α-derivative on $\hat{H}$ vanishes sinces this operator does not depend on α. Since U_α is a unitary transformation, i.e $U_\alpha U_\alpha^\dagger = \mathbb{1}$ it follows that

$$\hat{U}_\alpha \frac{d\hat{U}_\alpha^\dagger}{d\alpha} = -\frac{d\hat{U}_\alpha}{d\alpha} \hat{U}_\alpha^\dagger, \tag{3.3}$$

or equivalently

$$\begin{aligned} \frac{d\hat{U}_\alpha^\dagger}{d\alpha} &= -\hat{U}_\alpha^\dagger \frac{d\hat{U}_\alpha}{d\alpha} \hat{U}_\alpha^\dagger, \\ \frac{d\hat{U}_\alpha}{d\alpha} &= -\hat{U}_\alpha \frac{d\hat{U}_\alpha^\dagger}{d\alpha} \hat{U}_\alpha. \end{aligned} \tag{3.4}$$

We will use in the following the notation

$$\hat{\eta}_\alpha = -\frac{d\hat{U}_\alpha}{d\alpha}\hat{U}_\alpha^\dagger. \tag{3.5}$$

By inserting (3.4) into (3.2) we obtain

$$\begin{aligned}
\frac{d\hat{H}_\alpha}{d\alpha} &= -\hat{U}_\alpha\frac{d\hat{U}_\alpha^\dagger}{d\alpha}\hat{U}_\alpha\hat{H}\hat{U}_\alpha^\dagger + \hat{U}_\alpha\hat{H}\hat{U}_\alpha^\dagger\frac{d\hat{U}_\alpha}{d\alpha}\hat{U}_\alpha^\dagger \\
&= -\hat{U}_\alpha\frac{d\hat{U}_\alpha^\dagger}{d\alpha}\hat{U}_\alpha\hat{H}\hat{U}_\alpha^\dagger + \hat{U}_\alpha\hat{H}\hat{U}_\alpha^\dagger U_\alpha\frac{d\hat{U}_\alpha^\dagger}{d\alpha} \\
&= [\hat{U}_\alpha\hat{H}\hat{U}_\alpha^\dagger, U_\alpha\frac{d\hat{U}_\alpha^\dagger}{d\alpha}] \\
&= [\hat{H}_\alpha, U_\alpha\frac{d\hat{U}_\alpha^\dagger}{d\alpha}] \\
&= [\hat{\eta}_\alpha, \hat{H}_\alpha].
\end{aligned} \tag{3.6}$$

where we used the definition of $\hat{\eta}_\alpha$ and the skewsymmetry of the commutator. Equation (3.6) is called *flow equation*. Note its similarity to a Heisenberg equation of motion. Furthmore it holds

$$\begin{aligned}
\hat{\eta}_\alpha^\dagger &= -(\frac{d\hat{U}_\alpha}{d\alpha}\hat{U}_\alpha^\dagger) \\
&= \hat{U}_\alpha\frac{d\hat{U}_\alpha^\dagger}{d\alpha}\hat{U}_\alpha\hat{U}_\alpha \\
&= \hat{U}_\alpha\frac{d\hat{U}_\alpha}{d\alpha} \\
&= -\hat{\eta}_\alpha,
\end{aligned} \tag{3.7}$$

i.e., the quantity η_α is *anti-Hermitian* and we refer to it as the *generator* of the flow equation.

Besides anti-Hermiticity there are no restrictions on choosing the generator η_α. A convenient choice of η_α is

$$\hat{\eta}_\alpha = (2\mu)^2[\hat{T}_{rel}, \hat{H}]. \tag{3.8}$$

This choice yields a evolved Hamiltonian if the eigenstates of $\hat{T}_{rel}$ and $\hat{H}$ coincide, i.e., if their commutator vanishes. Obviously this is not the case for a realisitc interaction and, therefore, evolving $\hat{H}$ results only in a band diagonal structure. The suppression of off-diagonal elements can be made arbitrary large, if we take the limit for $\alpha \to \infty$ and, therefore, completly decouple low momenta from high ones.

Nevertheless, with increasing α we end up with stronger contributions from higher particle rank, i.e., we can no longer neglect effects from induced higher-particle rank interactions. Those terms arise naturally when evolving the Hamiltonian [36] [32]. In general the SRG-evolution of a A-body-system will contain up to A-body contributions, i.e.

$$\hat{H}_\alpha = \sum_{i=1}^{A}\hat{H}_\alpha^{(i-body)}. \tag{3.9}$$

However, subsequent calculations become more involved when taking higher-particle rank contributions into account. So, in general we simple neglect contributions from particle rank three or higher.

Chapter 4

Perturbation Theory

This part is dedicated to the general framework of perturbation theory. Since this is the main tool for the study of the quantum-mechanical many-body problem within this investigation, it is discussed in quite detail. We start with perturbation theory without any regard to quantum mechanics at all. The conceptual understanding of a perturbative approach opens a much wider perspective than solving the eigenvalue problem of a associated Hamiltonian. In this context we will discuss algebraic equations and how to write their solution as an infinite series. Those provide not only well-known examples from quantum mechanics like the Schrödinger equation of the anharmonic oscillator in position space but admit a classification of perturbation problems in general. As we will see, the convergence properties of the resulting infinite series are closely related to the structure of the perturbation problem.
Afterwards, generic features of perturbative results in quantum mechanics are discussed and we provide a simple example that helps to understand how divergences can occur. In the subsequent sections we deal with the question of how to overcome the difficulties of diverging perturbation series.

4.1 Introduction

One of the fundamental problems in a broad variety of science is the fact, that most mathematical problems do not admit a solution in closed form. Even though an equation may look very simple it refuses a closed form solution. One of the first negative results is the fact that the zeros of an arbitrary polynomial of degree five or higher do not admit a representation in form of radicals, i.e., via elementary operations and roots. This is the seminal theorem of Abel and Ruffini which dates back to the 19th century [42]. This situation provides an example of a relatively easy mathematical problem which cannot be solved exactly. The situation does not change if the objects become more involved like differential equations rather than algebraic ones.
Unfortunately quantum mechanics is not the exception. There are very few problems which can be solved exactly and none of them provides a realistic description of nature. So we are left to find a strategy to solve such a problem. This is where perturbation theory comes into play. To solve a problem in terms of perturbation theory we first have to convert it into a perturbation problem. This is done as follows:

1. Introduce a so-called *auxilliary parameter* λ to the original problem
2. Assume that the solution of the original problem is given by power seris in λ
3. Derive recursively the coefficients of the perturbation series
4. Recover the solution by setting the parameter to appropriate value

It is noteworthy that those steps are not unique. The introduction of an auxilliary parameter may be done in several ways and depends on the particular problem under investigation and, therefore, the value of λ which recovers the original solution might be different.
At this point it is most instructive to go through an example in detail [2]. Let's reconsider the aforementioned problem of finding the zeros of a polynomial. We consider the equation

$$x^3 - 4.001x + 0.002 = 0. \tag{4.1}$$

Furthermore, recall that this is a cubic polynomial which thus admits a closed-form solution via the theorem of Vieta, which is a generalization of the known solution to a general quadratic polynomial. In principle there is no need of perturbation theory at all. But knowing the exact answer gives us the uportunity to compare the perturbative result to the exact one.

So the first step is the conversion step. We introduce λ via

$$x^3 - (4 + \lambda)x + 2\lambda = 0.$$

Furthermore, we assume the solution to this equation to be given by

$$x_n = \sum_{n=0}^{\infty} c_n \lambda^n, \tag{4.2}$$

where the coefficients c_n are calculated order by order. Since this is a third order polynomial we expect it to have three zeros over $\mathbb{C}$ by the fundamental theorem of algebra.

Next lets consider the equation when setting $\lambda = 0$. We will refer to this as the *unperturbed problem*. This yields

$$x^3 - 4x = 0.$$

This equation has the three zeros $x_1 = 0$, $x_2 = 2$ and $x_3 = -2$. We will now investigate more deeply the zero x_3, i.e., we want to determine higher-order corrections to the value -2 by taking higher orders of λ into account. For simplicity we restrict ourselves to second order corrections,

$$\tilde{x}_3 = -2 + c_1\lambda + c_2\lambda^2.$$

This is done by plugging the above expression into the polynomial equation

$$(12c_1 - 4c_1 + 2 + 2)\,\lambda + \left(12c_2 - c_1 - 6c_1^2 - 4c_2\right)\lambda^2 = O(\lambda^3).$$

We additionaly have grouped elements with equal powers of λ together. Now the perturbative corrections c_1 and c_2 may be calculated by matching orders, i.e., setting each bracket to zero. This

is justified rigourosly by the analysis of power series. Recall that to any given function there exists a *unique* power series representing this function. Therefore, both sides of the equation are equal in every order of λ and the brackets vanish identically. The next step is to determine first c_1 via the bracket corresponding to λ and subsequently c_2 recursively exploiting the knowledge of c_1. This yields

$$c_1 = \frac{1}{2}, \qquad c_2 = -\frac{1}{8} \tag{4.3}$$

and, therefore,

$$\tilde{x}_3 = -2 - \frac{1}{2}\lambda + \frac{1}{8}\lambda^2 + O(\lambda^3). \tag{4.4}$$

We obtain our initial problem by setting $\lambda = 0.001$ resulting in $\tilde{x}_3 = -2.00049987$. This value is exact up to 9 digits compared to the exact value, therefore, reflecting the huge potential of a perturbative approach.
As mentioned before, this is just one possible way to obtain a perturbation problem which is by far not unique. In general the accuracy of the obtained corrections may strongly depend on the chosen step of conversion, i.e., the way the perturbation parameter λ is introduced to the original problem. We refer to this freedom in choosing the unperturbed problem as *partitioning*. Furthermore, we call the terms carrying the λ-dependence *perturbation*. In the above problem $x + 0,002$ was the perturbation.
As we see lateron in chapter 12 a different partitioning may change the corrections not only quantitatively but also qualitatively.

4.2 Classification

Since we now understand the concept of perturbation theory on a basic level, we can move on to more complicated problems like the qualitative description of perturbation problems. Furthermore, we discuss the occuring perturbation series in depth with focus on convergence properties. In order to understand different perturbation problems we will discuss another example that is closely related to the discussion of the cubic equation in the last chapter. Consider the following perturbation problem

$$\lambda^2 x^6 - \lambda x^4 + x^3 + 1 = 0. \tag{4.5}$$

This is a polynomial equation of degree six. By the fundamental theorem of algebra we expect six, possibly complex, solutions to the equation. Let's now examine the limit $\lambda \to 0$

$$x^3 = 1, \tag{4.6}$$

whose solutions are given by the three roots of unity $x_k = e^{2\pi i k/3}$. Note that the number of solutions to the unperturbed problem is three. So three of the possible solutions disappeared. So the solution to the problem in the limit $\lambda \to 0$ does not only change quantitatively but *qualitatively*. The reason for this is the fact that the term $\lambda^2 x^6$ is no longer negligable compared to $x^3 + 1$. However, it is

possible to overcome this difficulty by using a *scale transformation*,

$$x = \lambda^{-2/3} y. \tag{4.7}$$

Substitution yields the expression

$$y^6 - y^3 + 8\lambda^2 - \lambda^{-2/3} = 0. \tag{4.8}$$

This is just a regular perturbation problem which has six solutions in the unperturbed case. So we will call a perturbation problem *singular* if its solution changes qualitatively in the limit $\lambda \to 0$.

4.3 Features of Perturbation Series

We now briefly discuss why our naive attempt using power series may fail. Consider an arbitrary function $f(z)$ and we want to represent it in a alternative way, in particular via a power-series expansion. Note that a function is nothing but an element of some function space, that is $f \in \mathcal{C}$ and we are interested in different representations of a function. As an example we consider the function f with representation

$$f(z) = \frac{1}{1-z}. \tag{4.9}$$

The right hand side is well defined for all $\{z \in \mathbb{C} : z \neq 1\}$. Now consider another representation given by

$$f(z) = \sum_{n=0}^{\infty} z^n. \tag{4.10}$$

The power series expansion converges for all $|z| < 1$ and its limit is given by the geometric sum as $\frac{1}{1-z}$. So the above representations coincide in the range where they both are well defined, but the first representation is defined on the punctured complex plane while the second one is defined only on the interiour of the unit disk. Therefore the first one has a wider range a validility.

If we are interested to the solution of a perturbation problem we assume that the answer is given in terms of a power series. In this case we choose a particular representation, for example for the energy of the ground state $E_0(\lambda)$. Unfortunately, in many cases the power series expansion we choose is evaluated outside its range of validility. Therefore, the value we obtain by setting the auxilliary parameter λ equal to one has no meaning at all. In particular we have to construct a representation of the solution of the perturbation problem which is valid at $\lambda = 1$. In most cases a mere power series expansion does not posses this property. One may wonder what is the reason for that. The answer is elementary. Whenever the domain of validility of a representation of a function is restricted it has to do with singularities. The problem lies in the very nature of a power series. Power series are constructed in such a way as that they approximate a function equally good in every direction, i.e., their domain of convergence is highly symmetric, that is a circle. Therefore the radius of convergence is limited by the singularity which is closest to the origin (This is of course only true if the series is of Maclaurin type, i.e., the point at which we expand the

function is the origin. Otherwise one has to analyze the functions behaviour of the function at this expansion point). Reconsider now the setting in a physical application where we want to evaluate the perturbation series at $\lambda = 1$. Even if there is no singularity in the neighborhood of λ equals one the power series may fail to converge since a singularity at a point, e.g., $\lambda = -\frac{1}{2}$ limits the radius of convergence to one half.

But why do perturbation series fail to converge in the presence of singularities? We can answer this question by simply reminding ourselves of the structure of power series. A power series is an infinite sum of monomials of arbitrary but *positive* degree. Since polynomials do not have singularities they are unable to imitate the functions behaviour. It is precisely the missing of terms like z^{-k} for $k \in \mathbb{N}$ that is responsible for the non-convergence of simple power series.

A great part of this investigation is spent on how to obtain a valid function representation for the perturbation series and we will see in later chapters that there exist an extensive apparatus of procedures that provide additional insight to the solution of the perturbation problem. But before considering particular methods we want to discuss on an example how the use of simple power series fails to give a solution to the Schrödinger equation.

4.4 The Anharmonic Oscillator

This section is dedicated to the discussion of the quantum anharmonic oscillator. First we will discuss the lowest order perturbative corrections and the behaviour of the coefficients of the perturbation series. Afterwards we will take a closer look on the asymptotic behaviour of the resulting solution. The importance of this problem is that it provides an analytically soluble example for a diverging perturbation series [6]. Therefore, it can serve as a benchmark problem for resummation methods.

First let's state the problem. A quantum anharmonic oscillator is a harmonic oscillator potential perturbed by some higher degree polynomial. For the sake of simplicty we will discuss a quartic perturbation λx^4 and restrict our treatment to one spatial dimension, i.e., the eigenvalue problem

$$(\frac{1}{2m}\hat{p}^2 + \frac{1}{2m}\omega\hat{x}^2 + \lambda\hat{x}^4)|\psi_n\rangle = E_n|\psi_n\rangle. \tag{4.11}$$

Now, setting all physical parameters equal to one we obtain

$$(\frac{1}{2}\hat{p}^2 + \frac{1}{2}\hat{x}^2 + \lambda\hat{x}^4|\psi_n\rangle = E_n|\psi_n\rangle. \tag{4.12}$$

Analogous to the harmonic oscillator we will solve the eigenvalue problem in terms of creation and annihilation operators. Recall their definition

$$\hat{a}^\dagger = (x - ip) \tag{4.13}$$

$$\hat{a} = (x + ip). \tag{4.14}$$

We write the above Schrödinger equation eq. (4.12) in second quantization as

$$\left(\hat{a}^\dagger\hat{a} + \frac{1}{2}\right)|\psi_n\rangle + \lambda\left(\hat{a}^\dagger + \hat{a}\right)^4|\psi_n\rangle = E_n|\psi_n\rangle. \tag{4.15}$$

So we can determine the first-order correction which is simply the expectation value of the perturbing potential, i.e.,

$$\begin{aligned}
E_n^{(1)} &= \lambda\langle n|x^4|n\rangle \\
&= \lambda\frac{1}{4}\langle n|(\hat{a}^\dagger\hat{a}^\dagger\hat{a}^\dagger\hat{a}^\dagger + \hat{a}^\dagger\hat{a}^\dagger\hat{a}^\dagger\hat{a} + \hat{a}^\dagger\hat{a}^\dagger\hat{a}\hat{a}^\dagger + \hat{a}^\dagger\hat{a}\hat{a}^\dagger\hat{a}^\dagger + \hat{a}^\dagger\hat{a}\hat{a}^\dagger\hat{a}^\dagger + \\
&\qquad \hat{a}\hat{a}^\dagger\hat{a}^\dagger\hat{a}^\dagger + \hat{a}\hat{a}\hat{a}^\dagger\hat{a}^\dagger + \hat{a}\hat{a}^\dagger\hat{a}\hat{a}^\dagger + \hat{a}\hat{a}^\dagger\hat{a}^\dagger\hat{a} + \hat{a}^\dagger\hat{a}\hat{a}\hat{a}^\dagger + \\
&\qquad \hat{a}^\dagger\hat{a}^\dagger\hat{a}\hat{a} + \hat{a}^\dagger\hat{a}\hat{a}^\dagger\hat{a} + \hat{a}\hat{a}\hat{a}^\dagger\hat{a} + \hat{a}\hat{a}^\dagger\hat{a}\hat{a} + \hat{a}^\dagger\hat{a}\hat{a}\hat{a}+ \\
&\qquad \hat{a}\hat{a}\hat{a}\hat{a})|n\rangle \\
&= \lambda\frac{1}{4}\langle n|(\hat{a}\hat{a}\hat{a}^\dagger\hat{a}^\dagger + \hat{a}\hat{a}^\dagger\hat{a}\hat{a}^\dagger + \hat{a}\hat{a}^\dagger\hat{a}^\dagger\hat{a} + \hat{a}^\dagger\hat{a}\hat{a}\hat{a}^\dagger + \hat{a}^\dagger\hat{a}^\dagger\hat{a}\hat{a} + \hat{a}^\dagger\hat{a}\hat{a}^\dagger\hat{a})|n\rangle \\
&= \lambda\frac{1}{4}\big((n+1)(n+2) + (n+1)^2 + n(n+1) + n(n+1) + n(n-1) + n^2\big) \\
&= \lambda\frac{1}{4}\big(6n^2 + 6n + 3\big).
\end{aligned} \tag{4.16}$$

The first perturbative coefficient for the groundstate energy is given by $\frac{3}{4}$. To see the specialness of the quartic perturbation lets evaluate the next energy correction. Recall that the the second order energy correction is given by

$$E_n^{(2)} = \sum_{n\neq m}^{\infty} \frac{\langle m|\hat{x}^4|n\rangle}{E_n - E_m}, \tag{4.17}$$

so we need an expression for the general matrixelement. This can be written by

$$\begin{aligned}
\langle m|\hat{x}^4|n\rangle = &\sqrt{n(n-1)(n-2))n-3)}\delta_{n-4,m} + \\
&\sqrt{n(n-1)}(4n-2)\delta_{n-2,m} + \\
&(\sqrt{(n+1)(n+2)}(2n+1) + (n+1)(2n+5))\delta_{n+2,m} + \\
&\sqrt{n(n+1)(n+2)(n+3)}\delta_{n+4,m}.
\end{aligned} \tag{4.18}$$

Now we see why the treatment of the anharmonic oscillator is so special: Its matrix elements have *band-diagonal* structure. So most of the matrix elements are zero and we are dealing with sparse matrices when evaluating higher-order corrections. Let's state the second order correction

$$E_n^{(2)} = \frac{1}{16}\sum_{n\neq m}^{\infty} \frac{\langle m|(\hat{a}^\dagger + \hat{a})^4|n\rangle}{n-m} \tag{4.19}$$

$$= -\frac{1}{16}\big(42 + 118n + 103n^2 + 68n^3\big). \tag{4.20}$$

The derivation involves some tedious algebra since the second-order correction involves the square of the matrix elements. The correction to the ground state is here given by the coefficient $a_2 = -\frac{21}{8}$. Observe that this coefficient is more than three times larger than the first corrections and five times larger than the zeroth-order energy of the unperturbed problem. So we intuitively wont expect the series to converge. As mentioned before it is because of the structure of the matrix elements very easy to obtain corrections up to order 100 with the use of an ordinary home computer and a simple

implementation with *Mathematica*. Table 4.1 gives an overview of the perturbation coefficients.

Index n	Coefficient
0	0.5
1	0.8
2	-2.6
3	$2.1 \cdot 10^{1}$
4	$-2.4 \cdot 10^{2}$
5	$3.6 \cdot 10^{3}$
10	$-2.1 \cdot 10^{10}$
15	$3.9 \cdot 10^{17}$
20	$-7.7 \cdot 10^{24}$

Table 4.1: Coefficients of the perturbation series of the anharmonic oscillator with quartic perturbation rounded to one decimal place.

Although we were able to derive first- and second-order corrections by explicitely solving the well-known formulas, there is still another more sophisticated way. The knowledge of high-order corrections dates back to the early 70s, a time when there was no oppurtunity to derive these numbers via excessive computations. The first approach used the derivation of a recursive formula from which one obtains higher-order corrections by knowing the first ones. The first people who achieved this where Carl Bender and Tsan Wu. They obtained corrections up to order 75. Most impressively they were not only able to derive the coefficients but to write down a closed expression for the asymptotic behaviour of the perturbation. Those results which were generalized to both higher order anharmonicities and excited states are nowadays known as *Bender-Wu formulas*[6, 16, 13].

Chapter 5

Rayleigh-Schrödinger Perturbation Theory

After investigating perturbation theory in general and analyzing certain properties of the resulting solution we now formulate a framework which is particularly suited for the determination of perturbative corrections of quantum-mechanical problems. This is the so called *Rayleigh-Schrödinger-Perturbation-Theory*. We will discuss in detail the derivation of high-order corrections. This yields a recursive formulation for both, energy corrections and corrections of states. Those formulas serve as an starting point for the determination of the ground-state energy of light nuclei with high precision [34].

Derivation of Recursion Scheme

We aim at the solution of the time-independent Schrödinger equation for a nuclear Hamiltonian $\hat{H}$,

$$\hat{H}|\psi_n\rangle = E_n|\psi_n\rangle, \tag{5.1}$$

where $|\psi\rangle$ denotes an eigenstate of $\hat{H}$ in the many-body Hilbert-space $\mathcal{H}$. In the following discussion we assume the potential to include two-body interactions only. Furthermore, we take the Hamiltonian to have the form

$$\hat{H} = \hat{T} - \hat{T}_{cm} + \hat{V}, \tag{5.2}$$

where the kinetic energy is absorbed into the first two parts and all interactions are absorbed in the potential $\hat{V}$ only.
Next, we choose the basis functions of the unperturbed problem to be Slater-determinants of single-particle states. Recall that a Slater-determinant $|\psi\rangle_a \in \mathcal{H}$ is a fully anti-symmetric linear combination of tensor-products of single-particle states $|\varphi_i\rangle$, i.e.,

$$|\psi\rangle_a = \frac{1}{\sqrt{A}} \sum_{\pi \in S_A} sgn(\pi)|\varphi_1 \cdots \varphi_A\rangle, \tag{5.3}$$

where $|\varphi_1 \cdots \varphi_A\rangle$ denotes the A-fold tensor-product

$$|\varphi_1\rangle \otimes \cdots \otimes |\varphi_N\rangle, \tag{5.4}$$

and S_A the symmetric group on A letters. In the following we drop the lower index a and assume anti-symmetry unless stated otherwise.
A particular partitioning fixes the single-particle basis. Convenient choices are harmonic-oscillator states or Hartree-Fock states. Therefore, the unperturbed Hamiltonian, denoted bei $\hat{H}_0$ consists of the kinetic-energy part and the harmonic oscillator,

$$\hat{H}_0 = \hat{T} - \hat{T}_{cm} + \hat{H}_{HO} \tag{5.5}$$

and therefore resulting in the perturbation $\hat{H}_1 = \hat{V}_0 - \hat{H}_{HO}$. Recall that in order to obtain a perturbation problem we must introduce an auxilliary parameter λ with

$$\hat{H}(\lambda) = \hat{H}_0 + \lambda \hat{H}_1. \tag{5.6}$$

This defines a one-parameter family of potentials for λ. Additionally, the computational basis is defined by

$$\hat{H}_0 |\Phi_n\rangle = E'_n |\Phi_n\rangle. \tag{5.7}$$

Now, we assume the energy and state correction to be given as a power series in terms of λ,

$$E_n(\lambda) = E_0^{(0)} + \lambda E_n^{(1)} + \lambda^2 E_n^{(2)} + ..., \tag{5.8}$$

$$|\psi_n\rangle(\lambda) = |\psi_n\rangle^{(0)} + \lambda |\psi_n\rangle^{(1)} + \lambda^2 |\psi_n\rangle^{(2)} + ..., \tag{5.9}$$

respectively. The lower index n accounts for the number of the basis state and the upper index denotes the order of perturbation correction. In the case of zeroth order contribution we set

$$E_n^{(0)} = E'_n, \qquad |\psi_n^{(0)}\rangle = |\Phi_n\rangle, \tag{5.10}$$

Furthermore, we will make the important restriction of considering only non-degenerate eigenvalues and, therefore, only investigating closed-shell nuclei. For a review on the derivation of corrections in degenerate perturbation theory compare [21].
The next step is completely analogous to the discussion of the general perturbation problems in the preceeding sections. By inserting the above expressions for the power-series expansion and the partitioning of $\hat{H}$ into the time independent Schrödinger equation (5.1) one obtains

$$\hat{H}_0 |\psi_n^{(0)}\rangle + \sum_{p=1}^{\infty} \lambda^p \left(\hat{V} |\psi_n^{(p-1)}\rangle + \hat{H}_0 |\psi_n^{(p)}\rangle \right) = E_n^{(0)} |\psi_n^{(0)}\rangle + \sum_{p=1}^{\infty} \lambda^p \left(\sum_{j=0}^{p} E_n^{(j)} |\psi_n^{(p-j)}\rangle \right). \tag{5.11}$$

We make the additional important assumption that the unperturbed basis states $\{|\psi_n\rangle\}_n$ form an orthonormal basis and use from now on the so-called intermediate normalization

$$\langle\psi_n^{(0)}|\psi_n\rangle = 1, \tag{5.12}$$

Therefore, all projections on higher-order contributions vanish, $\langle\psi_n^{(0)}|\psi_n^{(p)}\rangle = 0$ for $0 < p \in \mathbb{N}$. Multiplication of eq. (5.11) with the zeroth-order states $|\psi_n^{(0)}\rangle$ and using the eigenvalue relation for the unperturbed Hamiltonian yields a compact expression for the energy correction up to arbitrary order,

$$E_n^{(p)} = \langle\psi_n^{(0)}|\hat{V}|\psi_n^{(p-1)}\rangle. \tag{5.13}$$

Recall that it is the uniqueness of power series that assures the equality of both sides of the equation to every order in λ.
After obtaining a formula for the energy corrections, we go on with the state corrections. This is done in an analogous way. We take the stationary Schrödinger equation and multiply it with the m-th basis state $|\psi_m^{(0)}\rangle$. This yields an expansion of the p-th state correction in terms of the unperturbed basis

$$|\psi_n^{(p)}\rangle = \sum_m C_{n,m}^{(p)}|\psi_m^{(0)}\rangle, \tag{5.14}$$

where the coefficients are given by

$$C_{n,m}^{(p)} := \langle\psi_m^{(0)}|\psi_n^{(p)}\rangle \tag{5.15}$$

$$= \frac{1}{E_n^{(0)} - E_m^{(0)}}\left(\langle\psi_n^{(0)}|V|\psi_n^{(p-1)}\rangle - \sum_{j=1}^{p} E_n^{(j)}\langle\psi_m^{(0)}|\psi_n^{(p-j)}\rangle\right). \tag{5.16}$$

The above expression is well-defined since we assumed non-degenerate eigenvalues and therefore energies corresponding to different basis states n and m are different, such that the denominator does not vanish. Note that the sum on the right hand side consists of an infinite number of terms since m runs over all basis functions and the dimension of the Hilbert may even be overcountable. Making use of the intermediate normalization and the fact that eigenstates to different eigenvalues are orthonormal for self-adjoint operators one concludes

$$C_{n,n}^{(0)} = 0, \qquad C_{n,m}^{(0)} = \delta_{n,m}. \tag{5.17}$$

Finally, we want to derive formulas that use matrix elements with respect to the unperturbed basis only. For the energy corrections one plugs the expansion of $|\psi_n^{(p)}\rangle$ into eq. (5.13),

$$E_n^{(p)} = \sum_m \langle\Phi_n|\hat{V}|\Phi_m\rangle C_{n,m}^{(p-1)}. \tag{5.18}$$

Using the same procedure for the amplitudes one obtains,

$$C_{n,m}^{(p)} = \frac{1}{E_n^{(0)} - E_m^{(0)}} \left(\sum_{m'} \langle \Phi_n | V | \Phi_{m'} \rangle C_{n,m'}^{(p-1)} - \sum_{j=1}^{p} E_n^{(j)} C_{n,m}^{(p-j)} \right). \tag{5.19}$$

Note that all matrix elements in the above equations are with respect to the unperturbed basis. We finally arrived at a computational convient recursive scheme that one can use to obtain energy corrections up to arbitrary order. Note that for the determination of the p-th energy corrections we need all state corrections up to order $(p-1)$. Analogously we can derive the p-th state correction by knowing state corrections up to order $(p-1)$ and energy corrections up to order p. This iterative procedure enables us to evaluate perturbation series of light nuclei up to very high orders providing an analysis of the convergence behaviour in much greater detail than explicit calculations for low orders. However, the analysis is limited to light nuclei due to multiplication of large matrices arising from the recursion scheme.

Chapter 6

The Hartree-Fock Method

When improving the convergence properties of perturbation series by means of changing the partitioning one must find another suitable set of basis functions. In this section we will derive a different single-particle basis and construct a Hamiltonian whose eigenstates are given by Slater-determinants consisting of these particular single-particle states.

6.1 Introduction

Within this section we define a single-particle basis by means of a variational procedure. First recall the so-called *variational principle* that states, that the ground state is a stationary point of the energy functional. Variational principles apear often in physics like the principle of least action in classical mechanics, that states that trajectories of particles are geodesic lines. We come back to the calculus of variations when deriving the Hartree-Fcok equations.

When using variational procedures one takes the corresponding Hilbertspace $\mathcal{H}$ and searches for a stationary point of a given functional $\mathcal{L}$

$$\delta\mathcal{L}\left[\psi\right] = 0, \qquad \psi \in \mathcal{H} \tag{6.1}$$

However in terms of the Hartree-Fock method we restrict ourselves to a subspace of the Hilbertspace $\mathcal{H}$ containing only single Slater determinants. Of course not every function in $\mathcal{H}$ may be written as a single Slater determinant, so the space of testfunctions is strictly smaller that $\mathcal{H}$,

$$\mathcal{H}_{var} \subset \mathcal{H}. \tag{6.2}$$

This is the so called *Hartree-Fock approximation*. If the lowest state to a given potential is given by a single Slater determinant, then the Hartree-Fock method is exact. If not, this only yields an approximation to the real ground state. Nevertheless we can use this approximation as a starting point for perturbation theory. So the first step is minimizing the energy functional, i.e., finding the single-particle states $\{|\Phi_i\rangle\}$ such that

$$|\psi\rangle_a = \hat{\mathcal{A}}\left(|\varphi_1\rangle \otimes \cdots \otimes |\varphi_A\rangle\right) \tag{6.3}$$

is the best approximation to the ground-state energy. We can make this statement more precise by considering

Theorem 1 (Ritz [27]). *Let $\mathcal{H}_{var} \subset \mathcal{H}$ be the space of testfunctions for a given Hamiltonian H. Then it holds for $|\psi_{var}\rangle \in \mathcal{H}_{var}$ that*

$$E\left[|\psi_{var}\rangle\right] \geq E_0, \tag{6.4}$$

where E_0 denotes the exact ground-state energy.

Proof. Consider the expansion of the trial state $|\psi_{var}\rangle$ in terms of eigenstates $\{\langle|\Phi_i^H\rangle\}$ of $\hat{H}$,

$$|\psi_{var}\rangle = \sum_i c_i |\Phi_i^H\rangle. \tag{6.5}$$

This yields for the energy functional

$$\begin{aligned} E\left[\psi_{var}\rangle\right] &= \frac{\sum_{i,j} c_i^\star c_j \langle\Phi_i^H|H|\Phi_j^H\rangle}{\sum_{i,j} c_i^\star c_j \langle\Phi_i^H|\Phi_j^H\rangle} \\ &= \frac{\sum_i |c_i|^2 E_i}{\sum_i |c_i|^2} \\ &\geq \frac{\sum_i |c_i|^2 E_0}{\sum_i |c_i|^2} \\ &= E_0, \end{aligned} \tag{6.6}$$

where we used orthogonality of the states and the eigenvalue equation in the second equality and the fact that the ground state energy is the lowest energy eigenvalue in the inequality in the third line. □

The above theorem states that we always improve our approximation by lowering the value of the energy functional. We will deal with the explicit derivation of stationary points in the next section.

6.2 Variational Calculus

In the following, we derive the first variation of the energy functional. Consider an element $|\psi\rangle$ of the Hilbert space of trial functions $\mathcal{H}_{var}$. The energy functional is given by,

$$E\left[\psi_{var}\rangle\right] = \frac{\langle\psi|H|\psi\rangle}{\langle\psi|\psi\rangle}. \tag{6.7}$$

We now consider a small variation of the function,

$$|\psi\rangle \to |\psi\rangle + |\delta\psi\rangle. \tag{6.8}$$

Inserting this in the energy functional gives

$$\begin{aligned} E\left[|\psi+\delta\psi\rangle\right] &= \langle\psi+\delta\psi|H|\psi+\delta\psi\rangle \\ &= \langle\psi|H|\psi\rangle + \left(\langle\delta\psi|H|\psi\rangle + \langle\psi|H|\delta\psi\rangle\right) + O\left((\delta\psi)^2\right) \\ &= E\left[|\psi\rangle\right] + \delta E. \end{aligned} \tag{6.9}$$

We kept only terms involving first order variations in $|\psi\rangle$ and neglected higher order terms. We call δE the *first variation* of $E[\cdot]$. Furthermore the expression in brackets may be written as

$$\delta\langle\psi|\psi\rangle = \langle\delta\psi|\psi\rangle + \langle\psi|\delta\psi\rangle. \tag{6.10}$$

This is just the product rule, an analouge to the calculus of real variable functions. Additionaly, we call a point in $\mathcal{H}_{var}$ *stationary*, if

$$\delta E = 0. \tag{6.11}$$

Note that in principle this is not a minimum, since it may appear that it is a maximum or a saddle point. Ultimately we need to check the definiteness of the corresponding Hessian. In the derivation of the Hartree-Fock equation we will need the following

Theorem 2 (Fundamental Theorem of Calculus of Variations)**.** *Let f be an integrable function and g be a testfunction such that*

$$\int dx f(x)g(x) = 0 \tag{6.12}$$

for all g, then $f(x)$ vanishes identically.

This theorem states that if a particular integral vanishes on every testfunction, then the function to be integrated over is already the zero function itself. We will see how this can be ueful.

6.3 Derivation of the Hartree-Fock Equations

After dealing with the variational calculus in general we may apply it to derive the so called Hartree-Fock equations. Therefore, we consider a single Slater-determinant describing a A-body system

$$\begin{aligned} |\psi\rangle &= |\varphi_1 \cdot ... \cdot \varphi_A\rangle, \\ &= \hat{a}_1^\dagger ... \hat{a}_A^\dagger |0\rangle, \end{aligned} \tag{6.13}$$

where $|0\rangle$ denotes the vacuum vector. This will serve as a starting point for an energy minimization by varying the single-particle states $|\varphi_i\rangle = \hat{a}_i^\dagger|0\rangle$. First we choose a complete and orthonomal computational basis with single-particle states $\{|\chi_i\rangle\}$ and corresponding creation operators $\{\hat{c}_i^\dagger\}$.

This yields the following expansionn

$$|\varphi_i\rangle = \sum_{j=1}^{\infty} D_{ij}|\chi_j\rangle, \tag{6.14}$$
$$\hat{a}_i^\dagger = \sum_{j=1}^{\infty} D_{ij}\hat{c}_j^\dagger,$$

where the expansion coefficients are defined by the overlap $D_{ij} = \langle\chi_j|\varphi_i\rangle$.Since the two basis sets $\{|\chi_i\rangle\}$ and $\{|\varphi_i\rangle\}$ are complete and orthonomal it follows that the basis transformation is unitary. Slater-determinants are, up to a global phase factor, invariant under unitary transformations. Therefore, the variational procedure only yields a single-particle subspace. We represent this subspace by a single-particle density matrix

$$\rho_{ij}^{(1)} = \langle\chi_i|\rho^{(1)}|\chi_j\rangle. \tag{6.15}$$

We rewrite the single-particle density matrix in terms of the computational basis

$$\rho_{ij}^{(1)} = \langle\psi|\hat{c}_j^\dagger\hat{c}_i|\psi\rangle = \sum_{k,l} D_{ik}D_{jl}^\star\langle\psi|\hat{a}_l^\dagger\hat{a}_k|\psi\rangle = \sum_{k,l}^{A} D_{ik}D_{jl}^\star, \tag{6.16}$$

where we used diagonality of $\rho^{(1)}$ with respect to the single-particle basis $\{\hat{a}_i^\dagger\}$ with eigenvalues one for occupied and zero for unoccupied states. Additionally we must impose further restrictions to ensure that the many-body state is still a single Slater-determinant after performing a variation within the testspace. Therefore, we require idempotency and hermiticity

$$(\rho^{(1)})^2 = \rho^{(1)}, \qquad (\rho^{(1)})^\dagger = \rho^{(1)}. \tag{6.17}$$

Now we write down a generic two-body operator in second quantization with respect to the computational basis

$$\hat{H}_{NN} = \sum_{ij}^{\infty} t_{ij}\hat{c}_i^\dagger\hat{c}_j + \frac{1}{4}\sum_{ijkl} v_{ijkl}^{(2)}c_i^\dagger\hat{c}_j^\dagger\hat{c}_k\hat{c}_l, \tag{6.18}$$

with kinetic energy matrix-elements

$$t_{ij} = \langle\chi_i|\hat{T}|\chi_j\rangle \tag{6.19}$$

and anti-symmetrized two-body matrix elements of the nucleonic two-body interaction

$$v_{ijkl}^{(2)} = \frac{1}{\sqrt{2}}(\langle\chi_i\chi_j|\hat{V}_{NN}|\chi_k\chi_l\rangle - \langle\chi_i\chi_j|\hat{V}_{NN}|\chi_l\chi_k\rangle). \tag{6.20}$$

Hence, the energy functional yields

$$E[|\psi\rangle] = \sum_{ij} t_{ij}\langle\psi|\hat{c}_i^\dagger\hat{c}_j|\psi\rangle + \frac{1}{4}\sum_{ijkl} v_{ijkl}^{(2)}\langle\psi|\hat{c}_i^\dagger\hat{c}_j^\dagger\hat{c}_k\hat{c}_l|\psi\rangle. \tag{6.21}$$

By defining the two-body density matrix $\rho^{(2)}_{kl,ij} = \langle\psi|\hat{c}^\dagger_i\hat{c}^\dagger_j\hat{c}_l\hat{c}_k|\psi\rangle$ and changing summation indices, we write this more conveniently as

$$E[|\psi\rangle] = \sum_{ik} t_{ik}\ \rho^{(1)}_{ji} + \frac{1}{4}\sum_{ijkl} v^{(2)}_{ijkl}\rho^{(2)}_{kl,ij}. \tag{6.22}$$

By using Slater-rules we break the two-particle density down into a product of one-particle density matrices,

$$\rho^{(2)}_{kl,ij} = \rho^{(1)}_{ki}\rho^{(1)}_{lj} - \rho^{(1)}_{kj}\rho^{(1)}_{li}. \tag{6.23}$$

Plugging eq. (6.23) into the expression for the energy functionals eq. (6.21) yields

$$E[\rho^{(1)}] = \sum_{ik} t_{ik}\rho^{(1)}_{ki} + \frac{1}{2}\sum_{ijkl} v^{(2)}_{ijkl}\rho^{(1)}_{li}\rho^{(1)}_{kj}. \tag{6.24}$$

From the variation of the energy functional and neglecting terms of order two or higher in $\delta\rho^{(1)}$ we obtain

$$\begin{aligned}\delta E[\rho^{(1)}] &= \sum_{ik} t_{ik}\ \delta\rho^{(1)}_{ki} + \frac{1}{2}\sum_{ijkl} v^{(2)}_{ijkl}(\delta\rho^{(1)}_{li}\rho^{(1)}_{kj} - \rho^{(1)}_{li}\delta\rho^{(1)}_{kj}) \\ &= \sum_{ik}(t_{ik}\ + \sum_{kl} v^{(2)}_{ijkl}\rho^{(1)}_{lj})\delta\rho^{(1)}_{ki}.\end{aligned} \tag{6.25}$$

By defining

$$\begin{aligned}h_{ik}[\rho^{(1)}] &= t_{ik} + u_{ik}[\rho^{(1)}], \\ u_{ik}[\rho^{(1)}] &= \sum_{jl} v^{(2)}_{ijkl}\rho^{(1)}_{lj},\end{aligned} \tag{6.26}$$

we write the stationarity condition more compactly

$$\sum_{ik} h_{ik}[\rho^{(1)}]\delta\rho^{(1)}_{ki} = 0, \tag{6.27}$$

where $u_{ij}[\rho^{(1)}]$ is a one-body potential depending on the one-body density. Reconsider the imposed idempotency and Hermiticity conditions that must be fulfilled for arbitrary variations, i.e., $\left(\rho^{(1)} + \delta\rho^{(1)}\right)^2 = \left(\rho^{(1)} + \delta\rho^{(1)}\right)$ leading to

$$\rho^{(1)}\delta\rho^{(1)}\rho^{(1)} = 0, \tag{6.28}$$

$$\left(1 - \rho^{(1)}\right)\delta\rho^{(1)}\left(1 - \rho^{(1)}\right) = 0. \tag{6.29}$$

With respect to the basis $\{|\varphi_i\rangle\}$ the density matrix $\rho^{(1)}$ is diagonal. Therefore, the only possibile variation, that fulfills the above conditions, takes place between occupied and unoccupied states respectively. In contrast we know from equation eq. (6.27) that non-vanishing matrix elements between two particles or two holes, respectively, can only occur in HF basis. Equivalently this

means that the commutator between the single-particle Hamiltonian and $\rho^{(1)}$ vanishes,

$$[\hat{h}[\hat{\rho}^{(1)}], \hat{\rho}^{(1)}] = 0. \tag{6.30}$$

We deduce that there exists a simultaneous eigenbasis for $\hat{h}[\rho^{(1)}]$ and $\hat{\rho}^{(1)}$ and formulate the operator-valued equation eq. (6.30) into an eigenvalue equation

$$h[\rho^{(1)}]|\varphi_n\rangle = \epsilon_n|\varphi_n\rangle, \tag{6.31}$$

defining the Hartree-Fock single-particle states $|\varphi_n\rangle$ and the corresponding single-particle energies ϵ_n. Transformation to the computional basis yields

$$\sum_k \hat{h}_{ik}[\rho^{(1)}]D_{nk} = \epsilon_n D_{nk}, \tag{6.32}$$

Making use of the single-particle Hamiltonian and the density matrix we obtain

$$\sum_k (t_{ik} + \sum_r^A \sum_{jl} v^{(2)}_{ij,kl} D^\star_{rj} D_{rl}) D_{kn} = \epsilon_n D_{in} \tag{6.33}$$

Eq.(6.33) is called *Hartree-Fock equation*. This non-linear eigenvalue problem may be solved in terms of a iterative procedure. The A lowest single-particle states are used for the definition of the Hartree-Fock ground-state

$$|HF\rangle = \hat{a}^\dagger_1 ... \hat{a}^\dagger_A |0\rangle. \tag{6.34}$$

Chapter 7

Partitioning

In chapter 5 we formulated many-body perturbation without specifying a particular basis. To perform calculations we must choose a computational basis, i.e., a model space of states to expand the state corrections in. In the derivation of the recursive formulas we already encountered the splitting of the many-body Hamiltonian $\hat{H}_{\text{nucl}}$ according to

$$\hat{H}_{\text{nucl}} = \hat{H}_0 + \hat{H}_1. \tag{7.1}$$

We can rewrite the nuclear Hamiltonian

$$\hat{H}_{\text{nucl}} = \hat{H}_{\text{nucl}} + \hat{H}_0 - \hat{H}_0. \tag{7.2}$$

by simply adding and substracting an arbitrary operator $\hat{H}_0$. Comparing the above equations we deduce that the perturbation is given by $\hat{H}_1 = \hat{H}_{\text{nucl}} - \hat{H}_0$ and the unperturbed problem is given by $\hat{H}_0$. Recall that it is important in perturbation theory to be able to solve the unperturbed problem exactly, i.e.,

$$\hat{H}_0|\psi_n^{(0)}\rangle = E_n^{(0)}|\psi_n^{(0)}\rangle, \tag{7.3}$$

where $|\psi_n\rangle$ denotes an eigenstate of $\hat{H}_0$ and $E_n^{(0)}$ the corresponding eigenvalue. We discuss two particular choices for $\hat{H}_0$.

7.1 Harmonic-Oscillator Perturbation Theory

A convenient choice for the unperturbed problem is the spherical harmonic oscillator $\hat{H}_0 = \hat{H}_{HO}$,

$$\hat{H}_{\text{HO}} = \sum_r^A \hat{h}_{r,\text{HO}}, \tag{7.4}$$

where the single-particle Hamiltonian is given by

$$h_{r,\text{HO}} = \frac{1}{2} m\omega^2 \hat{r}^2 \tag{7.5}$$

The eigenvalues of $\hat{h}_{r,\mathrm{HO}}$ are given by

$$\epsilon_{n,HO} = \hbar\omega \left(2n + l + \frac{3}{2}\right), \tag{7.6}$$

and the single-particle eigenstates are given by

$$|\varphi_n\rangle = |n, l\rangle, \tag{7.7}$$

where n denotes the radial quantum number and l the orbital angular-momentum quantum number [38]. Furthermore, it holds

$$\begin{aligned} \langle\psi_n^{(0)}|\hat{H}_1|\psi_m^{(p)}\rangle &= \langle\psi_n^{(0)}|\hat{H}_{\mathrm{nucl}} - \hat{H}_{HO}|\psi_m^{(p)}\rangle \\ &= \langle\psi_n^{(0)}|\hat{H}_{\mathrm{nucl}}|\psi_m^{(p)}\rangle - \langle\psi_n^{(0)}|\hat{H}_{HO}|\psi_m^{(p)}\rangle \\ &= \langle\psi_n^{(0)}|\hat{H}_{\mathrm{nucl}}|\psi_m^{(p)}\rangle - \epsilon_{n,HO}\delta_{nm}\delta_{0p}. \end{aligned} \tag{7.8}$$

Therefore, the subtraction of the harmonic oscillator Hamiltonian has only an impact on diagonal matrix elements.

7.2 Hartree-Fock Perturbation Theory

Another choice for $\hat{H}_0$ is the Hartree-Fock Hamiltonian

$$\hat{H}_{HF} = \sum_r^A \hat{h}_{r,\mathrm{HF}}, \tag{7.9}$$

where the matrix elemts of $\hat{h}_{\mathrm{HF}}$ are given in terms of the one-body density matrix

$$h_{ik}[\rho^{(1)}] = t_{ik} + \sum_{jl} v^{(2)}_{ijkl}\rho^{(1)}_{lj}. \tag{7.10}$$

Therefore, the perturbation is given by

$$\hat{H}_1 = \hat{H}_{\mathrm{nucl}} - \hat{H}_{\mathrm{HF}}. \tag{7.11}$$

The Slater-determinant $|\psi\rangle_{\mathrm{HF}}$ constructed from the single-particle states $|\varphi_i\rangle$ obtained from the Hartree-Fock procedure yields an exact eigenstate to the Hartree-Fock Hamiltonian

$$\hat{H}_{\mathrm{HF}}|\psi\rangle_{\mathrm{HF}} = E^{(0)}_{\mathrm{HF}}|\psi\rangle_{\mathrm{HF}}, \tag{7.12}$$

where the eigenvalue is given by the sum of the single-particle energies

$$E^{(0)}_{\mathrm{HF}} = \sum_i^A \epsilon_i, \tag{7.13}$$

with single-particle energies given by eq. (6.31). We consider now the first energy correction

$$\begin{aligned} E_0^{(1)} &=_{\mathrm{HF}} \langle\psi|\hat{H}_1|\psi\rangle_{\mathrm{HF}} \\ &=_{\mathrm{HF}} \langle\psi|\hat{H}_{\mathrm{nucl}}|\psi\rangle_{\mathrm{HF}} - \sum_r^N {}_{\mathrm{HF}}\langle\psi|\hat{u}_r|\psi\rangle_{\mathrm{HF}} \\ &= \frac{1}{2}\sum_{a,b}^N \langle ab|\hat{H}_{\mathrm{nucl}}|ab\rangle - \sum_r^N \langle a|\hat{u}|a\rangle \\ &= -\frac{1}{2}\sum_{a,b}^N \langle ab|\hat{H}_{\mathrm{nucl}}|ab\rangle, \end{aligned} \tag{7.14}$$

We see that the Hartree-Fock energy $E[|\psi\rangle_{HF}]$ is given by

$$\begin{aligned} E_{\mathrm{HF}} &= E_0^{(0)} + E_0^{(1)}, \\ &= \sum_i^A \epsilon_i - \frac{1}{2}\sum_{a,b}^N \langle ab|\hat{H}_{\mathrm{nucl}}|ab\rangle, \end{aligned} \tag{7.15}$$

which is not just the sum of the single particle energies. The Hartree-Fock energy includes already the first-order correction. Therfore, the first correction to the Hartree-Fock energy arises in second-order perturbation theory. The general formula is given by

$$E_0^{(2)} = \sum_{n\neq 0}^{\infty} \frac{|\langle 0|\hat{H}_1|n\rangle|^2}{E_0^{(0)} - E_n^{(0)}}, \tag{7.16}$$

where $|0\rangle$ denotes the ground-state, which is in our case the Hartree-Fock state $|\psi\rangle_{HF}$. To determine the second-order contribution we need to evaluate matrix elements between the Hartree-Fock state and excited states. Since we are dealing with a two-body operator, matrix elements between states that differ in three or more single-particle states vanish,

$$\langle\psi_{abc}^{rst}|V_{NN}|\psi_{def}^{uvw}\rangle = 0, \tag{7.17}$$

where we introduced the notation

$$|\psi_{abc}^{rst}\rangle = \hat{a}_t^\dagger \hat{a}_s^\dagger \hat{a}_r^\dagger \hat{a}_c \hat{a}_b \hat{a}_a |\psi\rangle_{\mathrm{HF}}. \tag{7.18}$$

We are left with so-called singly- and doubly-excited Slater determinants, that differ by one or two single-particle states from the Hartree-Fock ground-state respectively. First consider single excitations, i.e. , matrix elements of the form

$${}_{\mathrm{HF}}\langle\psi|\hat{H}_1|\psi_a^r\rangle =_{\mathrm{HF}} \langle\psi|\hat{H}_{\mathrm{nucl}}|\psi_a^r\rangle -_{\mathrm{HF}} \langle\psi|\hat{H}_{\mathrm{HF}}|\psi_a^r\rangle. \tag{7.19}$$

The second term vanishes due to ortogonality of HF single-particle states, whereas the first one vansihes due to Brillouins theorem.

Theorem 3 (Brillouin)**.** *Let $\hat{H}$ be a two-body operator. A single excited determinant $|\psi_a^r\rangle$ does not*

mix with the Hartree-Fock ground state,

$$ {}_{HF}\langle\psi|\hat{H}|\psi_a^r\rangle = 0. \tag{7.20}$$

We see that for the aforementioned matrix elements only double excitations contribute in the case of a two-body interaction. Note that for double excitations we have

$$\hat{H}_0|\psi_{ab}^{rs}\rangle = (E_0^{(0)} - (\epsilon_a + \epsilon_b - \epsilon_r - \epsilon_s))|\psi_{ab}^{rs}\rangle. \tag{7.21}$$

We can write the second-order correction by

$$\begin{aligned} E_0^{(2)} &= \sum_{a<b,r<s} \frac{|\langle ab|\hat{H}_1|rs\rangle|^2}{(\epsilon_a + \epsilon_b - \epsilon_r - \epsilon_s)}, \\ &= \frac{1}{4}\sum_{a,b,r,s} \frac{|\langle ab|\hat{H}_1|rs\rangle|^2}{(\epsilon_a + \epsilon_b \epsilon_r - \epsilon_s)}, \end{aligned} \tag{7.22}$$

where we inserted the factor $\frac{1}{4}$ to account for double counting. In general one proceeds analogously to obtain higer order corrections, but the algebraic manipulations become quite cumbersome. We state without derivation the third order contribution

$$\begin{aligned} E_0^{(3)} = &\frac{1}{8}\sum_{a,b,c,d,r,s} \frac{\langle ab|\hat{V}|rs\rangle\langle rs|\hat{V}|cd\rangle\langle cd|\hat{V}|ab\rangle}{(\epsilon_a + \epsilon_b - \epsilon_r - \epsilon_s)(\epsilon_c + \epsilon_d - \epsilon_r - \epsilon_s)} + \\ &\frac{1}{8}\sum_{a,b,r,s,t,u} \frac{\langle ab|\hat{V}|rs\rangle\langle rs|\hat{V}|tu\rangle\langle tu|\hat{V}|ab\rangle}{(\epsilon_a + \epsilon_b - \epsilon_r - \epsilon_s)(\epsilon_a + \epsilon_b - \epsilon_t - \epsilon_u)} + \\ &\sum_{a,b,c,r,s,t} \frac{\langle ab|\hat{V}|rs\rangle\langle cs|\hat{V}|tb\rangle\langle rt|\hat{V}|ac\rangle}{(\epsilon_a + \epsilon_b - \epsilon_r - \epsilon_s)(\epsilon_a + \epsilon_c - \epsilon_r - \epsilon_t)}. \end{aligned} \tag{7.23}$$

We see within the next section how to derive such expressions more conveniently in terms of diagrams.

Chapter 8

Diagrammatic Perturbation Theory

When we discussed energy corrections in terms Rayleigh-Schrödinger Perturbation Theory we always were in need of the knowledge of state corrections in order to obtain, via recursion, the next order energy correction. In this section we will discuss a completely different but very powerful approach to determine explicit expressions for low order energy corrections with respect to arbitrary single-particle bases. This ansatz is in some way comparable to the use of Feynman diagrams in quantum field theory although Feynman diagrams do not provide a framework to calculate energy corrections. It is related in the way that we will use a pictorial notation to write down certain energy contributions in terms of graphs. By using a set of rules one is able to deduce the corresponding terms much faster than with the explicit use of Slater-Gordon rules.
We will also discuss how to obtain corrections beyond 3rd order simply by making combinatorial considerations and close with an discussion of the derivation of contributions that also include 3N-interactions.

8.1 Hugenholtz Diagrams

In the following we will discuss a so-called *diagrammatic* approach for the derivation of higher order energy corrections [43]. We will write down in a pictorial way certain configurations of points and interpret the way they are connected in terms of mathematical formulas. Thereforee we provide a set of rules that makes it easy to derive higher order contributions much faster than by the use of algebraic manipulations. We will call those diagrmas after their inventer *Hugenholtz diagrams*.

The use of diagrammatic expressions to derive mathematical formulas is not rigoros. We really need to *conjecture* a one-to-one correspondence between diagrams and perturbative corrections. But we will see that within this framework we will be able to get consistent results.

Consider yourself now in the position to derive the second order energy correction. When using diagrammatic perturbation theory we will proceed as follows.

1. Draw two dots on the plane
2. Connect these two dots such that four lines go into each dot and there are no lines coming in and out the same dot
3. Do this in every possible way

The only configuration to do so is the following:

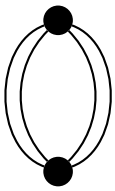

In the sequel we will call a dot *vertex* for reasons that become clear shortly. Next we choose orientations on the lines, such that at every vertex there are two lines going in and two lines going out. Furthermore every line gets a labels. Lines going from up to down are labeled by letters $a, b, c, ...$ and lines which are going up by $r, s, t, u, ...$ This yields

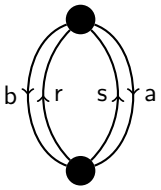

The general rules for the derivation of the perturbative contribution are now as follows

1. Each vertex contributes an antisymmetrized matrix element where the labels of the lines going in correspond to bra states and outgoing lines to ket states

2. Consider a imaginary horizontal line between two verties. Every horizontal lines contributes a energy denominator whose value is given by

$$\sum_h \epsilon_h - \sum_p \epsilon_p \tag{8.1}$$

   where the first sum runs over lables from downgoing lines and the second sum over the labels of the upgoing lines

3. The overall sign of the expression is given by the factor $(-1)^{h+l}$, where h corresponds to the number of downgoing lines and l is the number of so called *closed loops*. We will give a description on how to derive this number soon.

4. Sum over all labels

5. Introduce a factor 2^k, where k is the number of lines connecting the same vertices.

Reconsider now the second order diagram given above. First of all we get the following string of matrix elements

$$\langle ab|\hat{H}|rs\rangle\langle rs|\hat{H}|ab\rangle. \tag{8.2}$$

Secondly the introduction of the imaginary horizontal line gives a denominator

$$(\epsilon_a + \epsilon_b - \epsilon_r - \epsilon_s). \tag{8.3}$$

There are two downgoing lines so $h = 2$ and there are two pair of lines joining the same vertices so $k = 4$, which leaves us with an overall expression

$$E_0^{(2)} = (-1)^l \frac{1}{4} \sum_{abrs} \frac{\langle ab|\hat{H}|rs\rangle\langle rs|\hat{H}|ab\rangle}{(\epsilon_a + \epsilon_b - \epsilon_r - \epsilon_s)}. \tag{8.4}$$

Now are only left to determine the number of closed loops. To do so we consider contractions of the labels of the matrix element string. That is we take for instance the first single particle states in the first matrix element. This is the state a. We construct it with the corresponding ket state, which is r and start the next contraction at the other r arriving at,

$$\langle \overbrace{ab|\hat{H}|r}s\rangle\langle \overbrace{rs|\hat{H}|a}b\rangle. \tag{8.5}$$

This forms a sequence of labels $a \to r \to a$. Similarly

$$\langle ab|\hat{H}|\overbrace{rs}\rangle\langle a\overbrace{b|\hat{H}|rs}\rangle \tag{8.6}$$

yielding the sequence $b \to s \to b$. We refer to such a sequence as *closed loop*. Obviously there are two of them so the overall number of closed loops $l = 2$. Finally we get for the second order perturbation

$$E_0^{(2)} = \frac{1}{4} \sum_{abrs} \frac{\langle ab|\hat{H}|rs\rangle\langle rs|\hat{H}|ab\rangle}{(\epsilon_a + \epsilon_b - \epsilon_r - \epsilon_s)}. \tag{8.7}$$

a result we are already familiar with from the algebraic derivation.

Finally we will use the above technique to derive the afore mentioned third order energy correction (7.23). The procedure is the same. We draw three vertices on the plane and form every configuration consistent with the above mentioned rules. The only diagram is

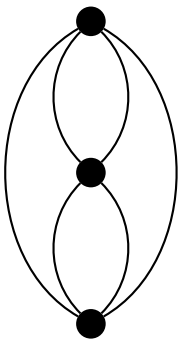

But in contrast to the second order diagram, one can choose different orientations on the above diagram:

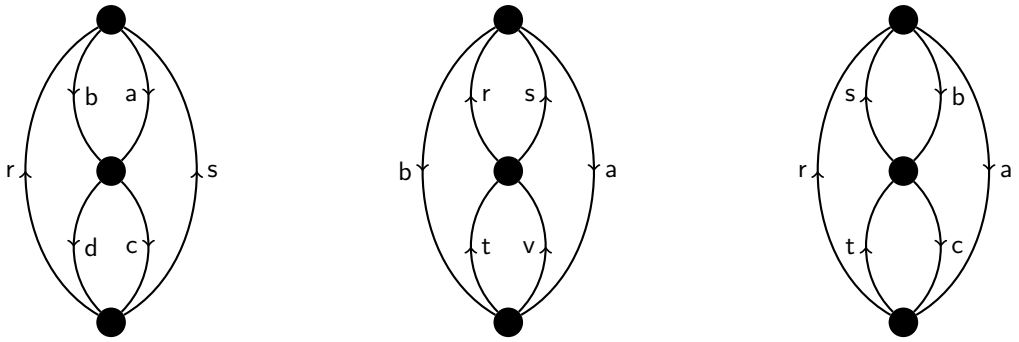

We will now derive each of the diagrams contribution to the third order energy direction. The left diagrams contributes

$$\frac{1}{2^3}(-1)^{4+l}\sum_{a,b,c,d,r,s}\frac{\langle ab|V|rs\rangle\langle rs|V|cd\rangle\langle cd|V|ab\rangle}{(\epsilon_a+\epsilon_b-\epsilon_r-\epsilon_s)(\epsilon_c+\epsilon_d-\epsilon_r-\epsilon_s)}, \tag{8.8}$$

where $l=2$ since we have two paths $a\to r\to c\to a$ and $b\to s\to d\to b$.

Analogously one gets for the middle diagram

$$\frac{1}{2^3}(-1)^{2+l}\sum_{a,b,r,s,t,u}\frac{\langle ab|V|rs\rangle\langle rs|V|tu\rangle\langle tu|V|ab\rangle}{(\epsilon_a+\epsilon_b-\epsilon_r-\epsilon_s)(\epsilon_a+\epsilon_b-\epsilon_t-\epsilon_u)} \tag{8.9}$$

where $l=2$ by $a\to r\to t\to a$ and $b\to s\to u\to b$.

The last diagramm yields

$$(-1)^{2+l}\sum_{a,b,c,r,s,t}\frac{\langle ab|V|rs\rangle\langle cs|V|tb\rangle\langle rt|V|ac\rangle}{(\epsilon_a+\epsilon_b-\epsilon_r-\epsilon_s)(\epsilon_a+\epsilon_c-\epsilon_r-\epsilon_t)}, \tag{8.10}$$

where $l=3$ by $a\to r\to a$, $b\to s\to b$ and $c\to t\to c$.

Thus we finally arive at

$$\begin{aligned}E_0^{(3)}=&\frac{1}{8}\sum_{a,b,c,d,r,s}\frac{\langle ab|V|rs\rangle\langle rs|V|cd\rangle\langle cd|V|ab\rangle}{(\epsilon_a+\epsilon_b-\epsilon_r-\epsilon_s)(\epsilon_c+\epsilon_d-\epsilon_r-\epsilon_s)}+\\&\frac{1}{8}\sum_{a,b,r,s,t,u}\frac{\langle ab|V|rs\rangle\langle rs|V|tu\rangle\langle tu|V|ab\rangle}{(\epsilon_a+\epsilon_b-\epsilon_r-\epsilon_s)(\epsilon_a+\epsilon_b-\epsilon_t-\epsilon_u)}+\\&\sum_{a,b,c,r,s,t}\frac{\langle ab|V|rs\rangle\langle cs|V|tb\rangle\langle rt|V|ac\rangle}{(\epsilon_a+\epsilon_b-\epsilon_r-\epsilon_s)(\epsilon_a+\epsilon_c-\epsilon_r-\epsilon_t)}\end{aligned} \tag{8.11}$$

which is exactly (7.23).

We see that diagrammatic perturbation theory is a very elegant way of deriving perturbative corrections to the ground-state energy. When facing the problem of deriving further contributions the growing number of possible diagramms makes it general impossible to write down all diagramms. For example in perturbation order four it is known that there are 39 contributing Hugenholtz diagrams and in perturbation order five even 840. In the next section we will investigate this more systematically and derive a formalism which enables us to perform those derivation algorithmically and particularly to implement it on a computer making higher orders more accesible to those

calculations.

8.2 Reformulation in Terms of Graph Teory

The goal of this section is to provide a more systematical treatment of the contributing diagrams for a given order in perturbation theory. At first sight the overwhelming amount of diagrams for higher order corrections might make a derivation of higher order corrections impossible. If one must draw every possible configuration and deduce the associated energy contribution from the diagram the derivation gets quite lenght. Besides this is very susceptible to human failure. So we are looking for a scheme that makes use of the combinatorial nature of the diagrams and therefore makes it accesible to computers [28, 52, 23]. We will explain how this is done in great detail.

8.2.1 Notation and Definitions

First of all note that a diagram can be described by a graph [9], which itself is a combinatorial object, namely

Definition 1 (Graph)**.** *A* graph *G is a triple (V, E, I) consisting of a set of vertices V and set of edges E and an incidence relation I. A* loop *is an edge that starts and ends at the same vertex. If G contains no loops we call G simple. Furthermore we call G* finite *if V is finite.*

The incidence relation tells us, which vertices are connected by which edges. If two vertices are connected by a edge, we call them adjacent. Furthermore we say that an edge $e \in E$ is incident to a vertex $v \in V$ if v is one of the endpoints of e. The number of incident edges is called the *degree* of a vertex v and is denoted by $deg(v)$. Note that a drawing of a graph, i.e., a diagram, is an *embedding* of a graph into a vector space, in our case just $\mathbb{R}^2$. There are many interesting questions about graphs that involve such embeddings. For example what is the simplest surface on which a particular graph may be drawn withou any lines crossing. However none of the properties we use in diagrammatic perturbation theory makes use of such geometries properties - except for the fact that we cannot interchange the order of the vertices in a diagram. But once we choose a labeling for the vertices we are left with a pure combinatorial problem. Within the next pages we will rephrase the problem of finding a particular energy contribution in terms of combinatorics.

First of all we must discuss on how to encode the information of the incidence relation. Basically there are two ways to encode a graph. We will deal with this problem via the so called *adjacency matrix*.

Definition 2 (Adjacency Matrix)**.** *Let $G = (V, E, I)$ be a simple finite graph. Fix a labeling of the vertices $\{e_n\}_{n=0}^{|V|}$. The adjacency matrix of a graph G is the matrix A with entries,*

$$a_{ij} = \{\textit{number of edges connecting } e_i \textit{ with } e_j\} \tag{8.12}$$

This allows us to take a look at first example. Consider the matrix

$$A = \begin{pmatrix} 0 & 1 & 1 & 0 \\ 1 & 0 & 1 & 1 \\ 1 & 1 & 0 & 1 \\ 0 & 1 & 1 & 0. \end{pmatrix} \tag{8.13}$$

The corresponding graph is given by

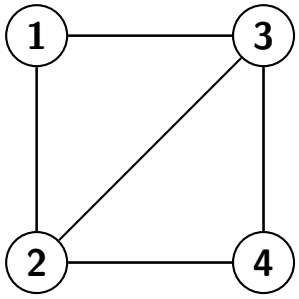

Recall that until now we are only dealing with unoriented graphs, i.e., we do not mind about orientation on the edges. Note that in the treatment of Hugenholtz diagrams it is important to distinguish between several orientations on the egde since they correspond to particle-states and hole-states respectively. Since the adjacency matrix yields a symmetric matrix we can not resolve the difference between any two graphs that only differ in the orientation of their edges.

In order to extract the information of the orientation we have to generalize our definition of the adjacency matrix.

Definition 3 (Generalized Adjacency Matrix)**.** *Let $G = (V, E, I)$ be a simple finite graph. Fix a labeling of the vertices $\{e_n\}_{n=0}^{|V|}$. The* generalized adjacency matrix *of a graph G is the matrix $\tilde{A}$ with entries,*

$$\tilde{a}_{ij} = \{\textit{number of edges starting in } e_i \textit{ and ending in } e_j\} \tag{8.14}$$

To see the difference lets reconsider the above example with a chosen orientation, e.g. the following graph:

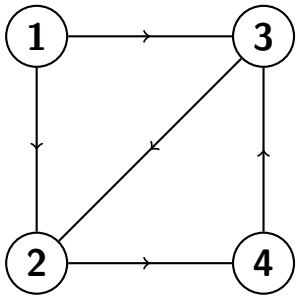

In this case the generalized adjacency matrix is given by

$$\tilde{A} = \begin{pmatrix} 0 & 1 & 1 & 0 \\ 0 & 0 & 0 & 1 \\ 0 & 1 & 0 & 0 \\ 0 & 0 & 1 & 0. \end{pmatrix} \tag{8.15}$$

In the absence of loops, the adjacency matrix A and the generalized adjacency matrix $\tilde{A}$ are related in a very simple way,

$$a_{ij} = \tilde{a}_{ij} + \tilde{a}_{ji}. \tag{8.16}$$

The last equation is the very reason why it suffices to consider the matrices instead of the graphs itself. In the following we need the notion of a k-partition.

Definition 4. *Let n be a natural number. A k-partitioning of n is a k-tuple $(v_1, ..., v_k)$, such that*

$$\sum_{i=1}^{k} v_i = n. \tag{8.17}$$

Now we are able to see, how we can obtain a directed graph from a undirected graph in terms a their adjacency matrices .

Algorithm 1. *Let G be a finite undirected graph without loops and A its corresponding adjacency matrix. One can construct a directed graph by*

1. *Take an element a_{ij} of the adjacency matrix A*
2. *Consider a 2-partition of a_{ij} and call their values r and s respectively*
3. *Set $\tilde{a}_{ij} = r$ and $\tilde{a}_{ji} = s$*
4. *Iterate this procedure for all $1 \leq i < j \leq |V|$*

Note that assuming the graph to have no loops leads to vanishing diagonal entries in both A and $\tilde{A}$. Additionally it suffices to check $i < j$, i.e. the entries of the lower triangluar matrix of A, due to the symmetry of A. One can construct all possible orientations on a directed graph by considering all possible 2-partitions on the entries of the adjacency matrix A.

8.2.2 Applications to Hugenholtz Diagrams

All considerations that we made are valid for arbitrary graphs. Next we will specify this concepts to Hugenholtz diagrams. First of all we must reformulate them in graph theoretical language. Recall that we proposed certain properties for the diagrams. We will restate them in the following

Definition 5. *A* Hugenholtz diagram *for a two-body interaction with respect to k-th order perturbation theory is a connected simple graph on k vertices, where every vertex v has degree $deg(v) = 4$.*

Recall from the construction of Hugenholtz diagrams in the preceeding section that the two-body nature of the interaction implies that there are going two lines in and out of every vertex. Furthermore the number of vertices is the number of matrixelements of a certain energy contribution. The terminology of graph theory allows us to investigate Hugenholtz diagrams more deeply. Therefore lets reconsider a diagram that we have already seen in the derivation of the third order contribution.

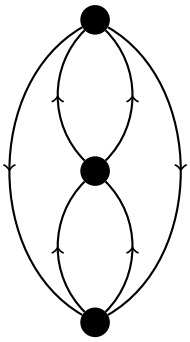

Its generalized adjacency matrix $\tilde{A}$ is given by

$$\tilde{A} = \begin{pmatrix} 0 & 0 & 2 \\ 2 & 0 & 0 \\ 0 & 2 & 0 \end{pmatrix} \tag{8.18}$$

Since the graph has no loop there are no non-vanishing diagonal entries. Furthermore one can reconstruct the adjacency matrix of the undirected graph,

$$A = \begin{pmatrix} 0 & 2 & 2 \\ 2 & 0 & 2 \\ 2 & 2 & 0 \end{pmatrix} \tag{8.19}$$

Note that we obtain the directed graph using our algorithm via choosing the 2-partition $(1, 1)$. On top we would have obtained the other two contributions taking the partition $(2, 0)$ or $(0, 2)$ respectively.

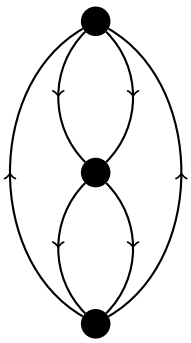

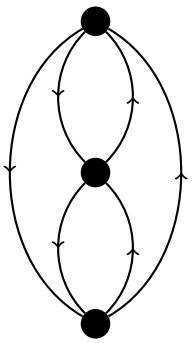

Their generalized adjacency matrices are given by

$$\tilde{A}_{(2,0)} = \begin{pmatrix} 0 & 2 & 0 \\ 0 & 0 & 2 \\ 2 & 0 & 0 \end{pmatrix} \qquad \tilde{A}_{(1,1)} = \begin{pmatrix} 0 & 1 & 1 \\ 1 & 0 & 1 \\ 1 & 1 & 0 \end{pmatrix} \tag{8.20}$$

This gives us a first clue of how in general to obtain an adjacency matrix of a corresponding Hugenholtz diagram. Note that in the above cases the sum of the entries in each row and each column is given by two. Of couse this is the case since those matrices arise from a partition of the entries of a adjacency matrix of an undirected graph, with entries $a_{ij} = 2$. This does not contradict the definition of a Hugenholtz diagram where we claimed $deg(v) = 4$ for all $v \in V$. Recall that the

degree counts both in- and outcoming edges and therefore the sum of the row and column entries being equal to two is completely consistent.

Since we discussed properties of Hugenholtz diagrams we simply have to translate them into properties of the generalized adjacency matrix. The entries of a fixed column of $\tilde{A}$ give the number of edges going from the correspondig vertex into another vertex. Since every vertex has two outgoing edges the sum over all entries of a given column must be equal to two. Analogously the sum of the entries per row must be equal to two since these correspond to incoming edges which are also two. So we have two additional conditions for the entries of the matrix $\tilde{A}$,

$$\begin{aligned} \sum_{i=1}^{n} \tilde{a}_{ij} &= 2 \\ \sum_{j=1}^{n} \tilde{a}_{ij} &= 2, \end{aligned} \tag{8.21}$$

where n denotes the number of vertices. This heavily restricts the number of possible matrices that might correspond to a particular Hugenholtz diagram. For example

$$\begin{pmatrix} 0 & 2 & 2 \\ 0 & 0 & 2 \\ 0 & 0 & 0 \end{pmatrix} \tag{8.22}$$

is not a valid adjacency matrix for a Hugenholtz diagram because it violates (8.21), although it is a valid 2-partition of a undirected graph. Furthermore there are some difficulties that do not arise in third perturbation order. In the description of Hugenholtz diagrams we restrict ourselves to connected graphs. Recall that a we call a graph *connected* if for two arbitrary vertices $v_1, v_2 \in V$ there exists a sequence of edges $\{e_i\}_{i=1}^{N}$ where v_1 is the starting point of e_1 and the endpoint of e_j is the starting point of e_{j+1} such that the endpoint of e_n is v_2.

In the case of graphs on three vertices there is only one configuration, up to permutation of the vertices, that is disconnected:

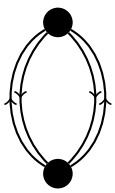

However this configuration is already forbidden because of the occurring loops at the lowest vertex. This changes in perturbation order four or higher. Consider the diagram

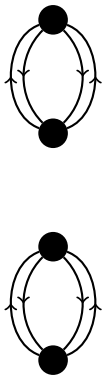

The above graph is disconnected and simple and it therefor does not suffice to check the adjacency matrices for loops. Fortunately there is an easy way of determining whether a graph is connected or not.

Theorem 4 (Connectedness of Graphs)**.** *A graph G is connected if there exists no permutation matrix $P \in Mat_n(\mathbb{R})$ such that the adjacency matrix may be cast into the following form*

$$PAP^T = \begin{pmatrix} A_{rr} & 0 \\ A_{rs} & A_{ss} \end{pmatrix} \tag{8.23}$$

where A_{rr} anf A_{ss} are block matrices.

The adjacency to the last example from perturbation order four is given by

$$\tilde{A} = \begin{pmatrix} 0 & 2 & 0 & 0 \\ 2 & 0 & 0 & 0 \\ 0 & 0 & 0 & 2 \\ 0 & 0 & 2 & 0 \end{pmatrix} \tag{8.24}$$

Obviously we can choose $P = 1_{4\times 4}$ and therefore the above graph is disconnected.

We are now able to summarize the procedure that concludes the first step of the combinatorial derivation of the perturbative corrections.

Algorithm 2 (Generation of valid Hugenholtz diagrams)**.** *The contributing Hugenholtz diagrams in terms of their generalized adjacency matrices for a two-body interaction for a given perturbation are constructed as follows*

1. *1. Fill a $n \times n$ matrix $\tilde{A}$ under the condition*

$$\tilde{a}_{ij} + \tilde{a}_{ji} = 2 \qquad \tilde{a}_{ij} \in \mathbb{N}, i \neq j$$

2. *2. Set $\tilde{a}_{ii} = 0$ for all $1 \leq i \leq n$.*

3. 3. Check if

$$\sum_{i=1}^{n} \tilde{a}_{ij} = 2$$
$$\sum_{j=1}^{n} \tilde{a}_{ij} = 2,$$

4. 4. Check if $\tilde{A}$ is irreducible and save $\tilde{A}$ if all conditions are satisfied

5. 5. Loop over all possible 2-partitions and repeat steps 1 to 4

If one runs this algorithm one gets one diagram in the case of second order perturbation theory, three in third order and 39 in fourth order. This rapidly increasing number of diagrams makes it in pratical applications almost impossible to determine corrections beyond third order corrections in closed form. However this treatment is not restricted to a given perturbation order and, therefore, completely general. For a treatment of the number of Hugenholtz diagrams and related sequences compare the Online Encyclopedia of Integer Sequences OEIS.

8.2.3 Information Extraction from Incidence Matrices

After determining all contributing Hugenholtz diagrams for a given order we are now in need of a scheme that enables us to translate the information hidden in the generalized adjacency matrix into energy corrections as we did for Hugenholtz diagrams. To do so we switch notation and use another way of presenting a graph that is more convenient for our pourposes. The description which we used until now was *vertex-based* and we will now make use of a *edge-based* notation.

Definition 6 (Incidence Matrix)**.** *Let $G = (V, E, I)$ be a finite simple directed graph. The* incidence matrix *B is the $|E| \times |V|$-matrix given by*

$$b_{ij} = \begin{cases} 1, & \text{if } e_j = (v_i, n) \\ 0, & \text{if } v_i \notin e_j \\ -1, & \text{if } e_j = (n, v_i) \end{cases}$$

where n denotes an arbitrary node.

Again lets consider the by now well-known example of a third order Hugenholtz diagram

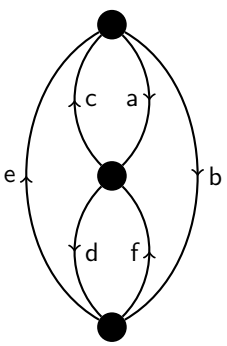

Its incidence matrix is given by

$$B = \begin{pmatrix} 1 & 1 & -1 & 0 & -1 & 0 \\ -1 & 0 & 1 & 1 & 0 & -1 \\ 0 & -1 & 0 & -1 & 1 & 1. \end{pmatrix} \tag{8.25}$$

Recall that this offers no additional insight, compared to the generalized adjacency matrix but we now can obtain more information with respect to the edges. Besides it is no conincidence that we label the edges by letters. This makes the resulting expression look more familiar.

Now lets try to extract the energy contribution directly from the matrix without making use of the diagram itself. We start with the first row. Two of its entries are given by $+1$ and two by -1. We will write the letters of the edges corresponding to the entries with $+1$ in the bra-state of a two-body matrix element and the one correspondig to -1 in the ket-state respectively, i.e.

$$V_1 = \langle ab|H|ce\rangle. \tag{8.26}$$

Analogously the other two rows yields

$$V_2 = \langle cd|H|af\rangle \tag{8.27}$$

$$V_3 = \langle ef|H|bd\rangle. \tag{8.28}$$

Obiously every variable appears once in a ket-state and once in a bra state, just as in the case of Hugenholtz diagrams. The evaluation of the energy denominators is a little bit more involved. There are two of those denominators which are determined by evaluating the lines crossing an the imaginary line between the first and second and second and third vertex respectively. To see how this is done in this particular case note that considering the first row, which corresponds to the edge a, the value of the sum changes from 1 to $1 - 1 = 0$. This corresponds to a hole state, i.e., a downgoing line (Recall that the entry -1 corresponds to the endpoint of the edge a). We must iterate this procedure for every column. There may appear five cases

1. Case 1: The sum was given by 1 and changes to 0
2. Case 2: The sum was given by -1 and changes to 0
3. Case 3: The sum was given by 1 and does not change
4. Case 4: The sum was given by -1 and does not change
5. Case 5: The sum was given by 0

The cases one and three correspond to hole states, since they are associated with downgoing lines. Cases 2 and 4 represent particle, i.e., upgoing, lines. The last case which does not appear in our example does not contribute to the energy denominator. With this in mind we can evaluate both energy denominators by considering the change of the sums from the first to the second row or

from the second to the third row respectively. The result is

$$E_1 = \epsilon_a + \epsilon_b - \epsilon_c - \epsilon_e$$
$$E_2 = \epsilon_b + \epsilon_d - \epsilon_e - \epsilon_f. \tag{8.29}$$

The number of equivalent edges is simply given by the number of identical columns, which is one in this case, so $1/N! = 1$. Now we are only left with determining the relative minus sign. This depends on the number of hole states. This quantity is easy to read of the incidence matrix. We must simply count the number of columns in which there first appears 1 before -1 when going down a fixed column. This is true for the edges a, b, d and the number of holes states is given by three.

The last remaining quantity is given by the number of closed loops. This can again be read from the string of matrix elements as we did in the previous sections yielding an overall plus sign. Putting all together we get

$$E^{(3)}_{partial} = \sum_{abd} \sum_{cef} \frac{\langle ab|H|ce\rangle\langle cd|H|af\rangle\langle ef|H|bd\rangle}{(\epsilon_a + \epsilon_b - \epsilon_c - \epsilon_e)(\epsilon_b + \epsilon_d - \epsilon_e - \epsilon_f)}, \tag{8.30}$$

which is just the familiar particle-hole correction from third order perturbation theory. Note that the variables a, b, d are holes states and we have to rename the summation indices to obtain eq. (7.23).

So we see that we are able to deduce the energy correction just from the combinatorial data of a graph which we can produce algorithmically. Again lets summarize the derivation of the energy contributions in form of

Algorithm 3 (Derivation of Energy Contributions via Graph Theory)**.** *The following algorithm needs as input data the perturbation order and gives back the energy contribution from the corresponding diagrams*

1. *Use Algorithm* 2 *to construct all valid generalized adjacency matrices*

2. *Transform the generalized adjacency matrix into a incidence matrix I. Every colum of the incidence matrix corresponds to an edge and every row to a vertex.*

3. *Label the edges by $a, b, c, d, ...$*

4. *Fix a row j and go trough it starting from the left. If the matrix elent of I is* 1 *write the label of the corresponding edge in the bra-state of a two-body matrix element. Write it in the ket state if it is -1. If it is* 0 *do nothing.*

5. *Fix two successive rows i and $i+1$. Fix a column and determine its sum for the first i entries. Then add the $i+1$th entry. If the sum was* 1 *(-1) then the corresponding edge is a hole-line (particle-line). Do this for all columns. Particle lines corresponding to an edge a contribute a summand ϵ_a hole lines $-\epsilon_a$.*

6. *Iterate step 5 for every pair of successive rows.*

7. *Count the number of columns where the entry $+1$ appears before the entry -1. This number gives the number of hole states h. They contribute a facotr of $(-1)^h$*

8. *Count the number N of identical columns. They contribute a factor $1/N!$*

9. *Write down the string of matrix elements and evaluate the number of closed loops l. They contribute a number $(-1)^l$*

10. *Iterate this step for all valid generalized adjacency matrices*

The above algorithm has the huge advantgae that it may be implemented on a computer and yields a treatment of the derivation of high order corrections that is robust to human failure. On top the classification of diagrams, e.g., by means of their hole-states, can be done much more effectively in terms of properties of the adjacency matrix. This task must be content of further investigations since it may provide a deeper understanding of problems which can be formulated diagrammatically.

8.3 Generalization to 3N-Interactions

When diagrammatic perturbation theory was first used to derive energy corrections there was no attempt to include $3N$-interactions into the discription. Over the last decades the view on higher particle-rank interactions changed drammaticaly and the treatment of $3N$-interactions becomes inevitable in modern nuclear structure theory. To account this for we will briefly discuss on how to generalize the framework derived so far. If we want do derive the contributing diagrams to a given perturbation order n, we draw again n vertices in the plane. The first difference appears in the degree of the vertices. The degree of each vertex changes from four to twice the number of the particle rank of the interaction, i.e. for a $3N$ interaction the degree is now six. Furthermore it may appear that there are three line joining the same vertex. In this case this contributes a prefactor of $1/(n!)$ which is just $1/6$ in this particular case. Additionaly one must account for the particle rank when formulating the conditions of the adjaceny matrix. This is generalized to

$$\sum_{i}^{n} \tilde{a}_{ij} = P \qquad \sum_{j}^{n} \tilde{a}_{ij} = P, \tag{8.31}$$

where n is again the perturbation order and P the particle rank. Unfortunately investigations within this thesis were based on two-body interactions and we will leave a precise treatment of this topic to future analysis. Even though we believe that a investigation of diagrammatic perturbation theory of three-body interactions might reveal further information on the importance of certain classes of diagramms.

Chapter 9

Resummation Theory

Derivation of high-order perturbative corrections for light nuclei provides a foundation to discuss convergence properties of the resulting perturbation series. There are several investigations using harmonic oscillator bases, that show that the energy corrections diverge with increasing perturbation order. Additionaly we have seen, that even simplest potentials lead to diverging series like in the case of the anharmonic osciillator. Therefore we are in great need of methods that enable us to extract meaningful quantities from a divergent expression. This branch of applied mathematics is called *Resummation Theory*.
We start with the treatment of generic properties and different concepts of infinite series. This leads to the concept of *Asymptoticity*. By precise analysis of the partial sums one is able to form models of series which one uses to motivate the transformation to a new series. This often leads to much better convergence properties [2]. Lateron many different types of resummation schemes are presented and the underlying theory is discussed briefly.

9.1 Infinite Series

As already discussed in the treatment of perturbation theory in general, the solution of a perturbative problem is given as an infinite power series. This is of course a problem since in order to use any information from this series directly one must proof that the power series converges inside the domain to be evaluated. Recall that we define an infinite series to be convergent if and only if the corresponding sequence of partial sums converges. Unfortunately this requires an infinite amount of information, i.e., an analytic expression of all coefficients in the power series. Of course at this point there arises the problem that this is very rarely fulfilled in any physical application in nuclear structure theory. This means that we can not talk about convergence at all. But we ignore this problem within this chapter and assume complete knowledge of all coefficients of a infinite series. In the sequel another notion of convergence will be more convient.

Definition 7. *A power series* $\sum_{n=0}^{\infty} a_n x^n$ *converges to* $f(x)$ *if and only if for* fixed x *it holds that,*

$$\left| f(x) - \sum_{i=0}^{N} a_i x^i \right| \to 0, \ N \to \infty.$$

The above statement is equivalent to the definition of convergence via partial sums. But in this case it becomes much clearer that convergence means to control the error between function and power series.
It is interesting to compare convergence to a similar, yet less-known concept. This concept is called asymptoticity, and to define it we must introduce some supplementory notation. First we need to know so-called asymptotic relations [6].

Definition 8. *A function $f(x)$ is asymptotic to $g(x)$ as x goes to x_0 if*

$$\lim_{x \to x_0} \frac{f(x)}{g(x)} = 1.$$

Obviously, the above defintion is just a statement about the asymptotic behaviour of the quotient of two functions. Note that such a relation is not unique. To see this consider, for example, $f(x) = x^4$ and $g(x) = x^4 + x^2$. Obviously it holds that

$$f(x) \sim g(x) \to \infty, \tag{9.1}$$

but we could have added a subdominant function like $\sin(x)$ to the right hand side of the equation and it would still be a valid asymptotic relation.
Furthermore, a word of caution must be a said. For most of the usual arithmetic operations asymptotic relations behave well. But there there are two important exceptions: differentiation and exponentiation. Reconsider the above example but add a particular subdominant function

$$x^4 \sim x^4 + x^3 + \sin(x^{10}) \tag{9.2}$$

as $x \to \infty$. Since the sine is subdominant this is a valid expression. Differentiation of both sides yields

$$4x^3 \sim 4x^3 + 3x^2 - 10x^9 \cos(x^{10}) \tag{9.3}$$

as $x \to \infty$. We see that the contributions from the inner derivative blow up much faster than the cubic monomial and violate the definition of an asymptotic relation.
In general, there are many very deep theorems which assure under certain technicalties the validility of differentiating an asymptotic relation. Those theorems are called *Tauberian*. A rigoros treatment may be found in the classical book by Hardy [14].
Now we are ready to define asymptoticity for power series.

Definition 9. *A power series is* asymptotic *to a function $f(x)$ for $x \to x_0$, if for fixed N*

$$\left| f(x) - \sum_{i=0}^{N} a_i (x - x_0)^i \right| \sim a_{N+1} (x - x_0)^{N+1}$$

Note that this definition does not make any assertions about the absolute magnitude of the error after a finite number of terms of the power series are included. It only states that the error within the first N terms is asymptotic to the $(N+1)$-th term in the series if we take the limit x goes to x_0. This does not necesserily mean that the error tends to zero. But there is a feature

that both convergent ans asymptotic series have in common. In both cases an infinite ammount of information is needed to check the defining property. Therefore one can only rarely prove in a physical setting wether the perturbation series is convergent or asymptotic. Even though a perturbation series diverges, it can still be an asymptotic series. So we are in need of a method that extracts information from an asymptotic series. We see in the subsequent sections how this can be achieved. But first we take a look on divergent series in general.

9.2 Divergent Series

After introducing the notion of convergence and asymptoticity we want to discuss the meaning of divergent series and how to deal with divergences in general. When facing a divergent series one cannot obtain a meaningful expression for the infinite sum by considering the sequence of partial sums, since the limit of that sequence does not exist. In the following we will some basic resummation methods that allow for defining the sum of a divergent series in a meaningful way. We start with two more elementary examples and define the so called Euler-sum and Borel-sum of a series and show their consistency on a well-known example.

9.2.1 Euler-Summation

The summation scheme which we work out here dates back to the 17th century and was first discussed by Leonhard Euler [12]. Consider a divergent series $\sum_{n=0}^{\infty} a_n$. The main idea is very simple: We take the divergent series and convert it into a power series by introducing a real-valued variable x, i.e.,

$$E(x) = \sum_{n=0}^{\infty} a_n x^n. \tag{9.4}$$

This is just a geometric series, and we can use for $q < 1$,

$$\sum_{n=0}^{\infty} q^n = \frac{1}{1-q}. \tag{9.5}$$

With this in mind we can define the Euler-sum S_{Euler} as

$$S_{Euler} = \lim_{x \to 1^-} \sum_{n=0}^{\infty} a_x x^n. \tag{9.6}$$

Note that the use of this summation method is restricted to so called *algebraically divergent series*. This means that the coefficients a_n do not grow faster than some polynomial of finite order. This is important since the exponential factor x^n cannot suppress exponentially diverging coefficients which ultimately would yield a non-convergent power series expansion.
Although Euler-Summation is strictly limited in its use it provides a simple but powerful method when dealing with bounded coefficients. To see this consider the series

$$S = \sum_{n=0}^{\infty} (-1)^{(n+1)}. \tag{9.7}$$

This series diverges because the sequence of partial sums has two accumulation points -1 and 0. Next, we use the Euler method to obtain a meaningful expression from the infinite series. The conversion to a power series yields

$$E(S) = \sum_{n=0}^{\infty} (-x)^n, \tag{9.8}$$

which is a abolute convergent power series for $|x| < 1$. Therefore, we obtain via the geometric series

$$\sum_{n=0}^{\infty} (-x)^n = \frac{1}{1+x}. \tag{9.9}$$

By taking the limit $x \to 1^-$ we obtain the value $E(S) = \frac{1}{2}$. This is the arithmetic mean of the partial sums. Therefore Euler summation performs some kind of averaging process. There are more elaborate procedures like Cesaro resummation that use similar principles. For the use and restrictions of those methods see the book from Hardy.

The above series was a positive example for Euler summability. We will additionally discuss the possibility of the failure of Euler summation. Therefore we consider a slight modification of the previous example namely $S = \sum_{n=0}^{\infty} (-1)^n n!$, which is the so called *Stirling series* [51]. Note that this series is not algebraically divergent since the factorial has superexponential growth.
Again, conversion yields

$$E(S) = \lim_{x \to 1^-} \sum_{n=0}^{\infty} (-1)^n n!. \tag{9.10}$$

We see that the Euler sum is not defined since the sum does only conververge for $n = 0$ and we can not perform the limit process. In order to resum the Stirling series we need a more powerful scheme to handle such superpolynomial growth rates.

9.2.2 Borel-Summation

As we have seen there are series which diverges too fast to be resummed by means of Euler summation. We present a more sophisticated method called *Borel Resummation*. Let's again assume we were given a infinite series $S = \sum_{n=0}^{\infty} a_n$. The first step is similar to the one in Euler summation. We will define a power series by

$$\phi(x) = \sum_{n=0}^{\infty} \frac{a_n x^n}{n!}. \tag{9.11}$$

The above expression is convergent even for exponentially diverging coefficients, which makes it applicable to more general situations than Euler-summation. Next we perform an integral transformation

$$B(x) = \int_0^{\infty} e^{-t/x} \Phi(xt) dt, \tag{9.12}$$

and define the value $B(1)$ to be the Borel-sum of S. The above integral is of Laplace type and convergent in a neighborhood of the origin. Compare for example [15] for an exhausting discussion

on the Laplace transformation and additionaly [14] on the Borel summation.
The next step involves an asymptotic relation, i.e.,

$$B(x) \sim \sum_{n=0}^{\infty} \frac{a_n}{n!} \int_0^{\infty} e^{-t/x} t^n \frac{dt}{x} \tag{9.13}$$

$$= \sum_{n=0}^{\infty} a_n x^n, \; x \to 0^+. \tag{9.14}$$

This justifies the definition of the Borel sum by means of Watson's Theorem (Appendix A). Recall the integral in the above equation is just the definition of the gamma function

$$\Gamma(x) = \int_0^{\infty} t^{x-1} e^{-t} dt, \tag{9.15}$$

which is convergent for positive real values of x and reduces to the factorial function for $x \in \mathbb{N}$.
Now we reconsider again the series $S = \sum_{n=0}^{\infty}(-1)^n$ and determine its Borel sum. The transformed sum is given by

$$\phi(x) = \sum_{n=0}^{\infty} \frac{1}{n!}(-x)^n \tag{9.16}$$

$$= e^{-x}. \tag{9.17}$$

So we can analytically solve the Laplace integral,

$$B(x) = \int_0^{\infty} e^{-t} \sum_{n=0}^{\infty} \frac{(-xt)^n}{n!} dt \tag{9.18}$$

$$= \int_0^{\infty} e^{-t(1+x)} dt \tag{9.19}$$

$$= \frac{1}{1+x}. \tag{9.20}$$

So the Borel-sum is $B(1) = \frac{1}{2}$. Recall that this is consistent with the Euler sum of the series.
Next we apply this method to the Stirling series where Euler summation failed, i.e., choose $S = \sum_{n=0}^{\infty}(-1)^n n!$. This yields

$$\phi(x) = \sum_{n=0}^{\infty}(-x)^n = \frac{1}{1+x}. \tag{9.21}$$

So the additional $n!$ from the Borel sum cancels the factorial divergences of the Stirling series. The Laplace integral is given by,

$$B(x) = \int_0^{\infty} \frac{e^{-t}}{1+xt}$$

and, thereforee the Borel sum is

$$B(1) = \int_0^{\infty} \frac{e^{-t}}{1+t}.$$

This integral can be solved numerically and $B(1) = 0.596$. Recall that the Stirling series was not Euler summable and Borel summation is indeed more powerful in this case. Of course, there are series that diverge much faster, like

$$S = \sum_{n=0}^{\infty} (2n)!. \tag{9.22}$$

For those series even the Borel method is not applicable. Even though one can perform a generalized procedure called Borel-Leroy summation. In that case one divides the series not only by $n!$ but $(mn)!$ for some fixed m. By choosing $m = 2$ one could resum even series like $\sum_{n=0}^{\infty}(2n)!$. For additional information and further generalizations see [40] and for some rigoros treatment of Borel summability see [31] [25].

9.3 Treatment of Asymptotic Series

In the treatment of infinite series we introduced the notion of asymptoticity. Assuming we were given an asymptotic series we need a scheme that enables to extract information from the series by using its defining property. This is done by so called *Optimal Asymptotic Truncation*. Besides we discuss a general result that gives an explicit construction for an object that is asymptotic to a given series. Lateron we treat a numerically determination of an infinite sum with the help of the mentioned procedures.

9.3.1 The Euler-MacLaurin Formula

In the following we present a way of obtaining certain asymptotic expressions. Consider an infinite series $\sum_{n=0}^{\infty} a(k)$ where we interpret the coefficients as functions. We can write its k-th partial sum as

$$P_k = \sum_{n=0}^{k} a(n). \tag{9.23}$$

We are trying to find a expression that is asymptotic to P_k as x goes to infinity. We rather discuss the result than prove it. The statement is the following

$$P_k \sim \frac{1}{2}a(k) + \int_0^k a(t)dt + \sum_{l=0}^{\infty}(-1)^{(l+1)}\frac{B_{l+1}}{(l+1)!}a^{(l)}(k) + C, \tag{9.24}$$

for $n \to \infty$. Here C is some constant and B_i is the i-th Bernoulli number. The Bernoulli numbers are given recursively by the zeros of the corresponding Bernoulli polynomial $B_i(x)$, which is defined by

$$B_i(x) = \frac{d^i}{dt^i}\frac{te^{xt}}{e^t - 1}. \tag{9.25}$$

One can prove an important property of the Bernoulli numbers,

$$B_{2i+1} = 0 \ \forall i \geq 1. \tag{9.26}$$

This shows that the infinite sum on the right hand side of the Euler-Maclaurin formula only involves odd derivatives of the function $a(k)$. It is precisely the existence of an expression involving another integral and another infinite sum that makes this formula useful. We will discuss its application lateron.

9.3.2 Optimal Asymptotic Truncation

By now we have not discussed how to extract information from a asymptotic series. Recall that, by definition, the error of the N-th term is asymptotic to the $(N+1)$-th term in the series. Therefore, the error is minimal when the next coefficient is minimal. So, the first thing to do is to form a sequence from the coefficients of an asymptotic series. Next we are looking for the index N in the sequence of the coefficients that gives the smallest coefficient. Last we will sum up the first $(N-1)$ terms. This algorithm provides a technique that uses asymptoticity to obtain an upper bound on the error for every value of a power series. Of course the index depends on the value of the power series to be evaluated at. Since this gives rise to minimal error for a given x we call the scheme *optimal asymptotic truncation* (OAT) [6, 5].
There are a few things to mention on OAT. First of all one needs a asymptotic series. Proving asymptoticity in general is difficult, and requires, just as the discussion of convergence, an infinite amount of information, namely an expression for every coefficient in the series. In typical applications one is not able to show that a perturbation series is asymptotic. So the use of OAT is rather justified by means of its succes rather than being provable. Secondly, the formulation of this rule is based on empirical experience. Even if one has proven that a certain series is an asymptotic series one cannot prove in general that OAT works and lead to precise results. But it has been shown to be very useful in the discussion of certain infinite series, and provides a new strategy to tackle infinite sums by means other than classical resummation schemes like Euler or Borel summation.

9.3.3 On the Resummation of the ζ-Function

We show on an example how to use OAT and why it is so powerful. We use the ζ-function as an testcase. Recall that this funtion is defined via

$$\zeta(s) = \sum_{n=1}^{\infty} \frac{1}{n^s}, \text{ Re } s > 1,$$

yielding a convergent expansion for all complex numbers whenever $\mathrm{Re}(s) > 1$. Furthermore, this function is not only interesting because we to use it as an example for OAT. It has many applications in both theoretical physics and pure mathematics like number theory. Values of this function occur in different contexts as prefactors of integrals in quantum field theory - just as the gamma function is related to the volume of higher dimensional spheres.
But what makes it important for us is the fact that the above expression is *very* slowly convergent. One needs more than 10^{20} terms in order to achieve one percent accuracy. Unfortunately, one needs much more computational power than is available on a single computer. In fact this series was used as a benchmark problem for supercomputers. Because of this slow convergence, the above expression is practically without any use, except for proving algebraic identities. In the following we show how to determine the sum of this series with the help of OAT.

The first step in the procedure is the replacement of the above convergent series expansion. Recall the Euler-Maclaurin formula and that in our example $a(k)$ is given by $\frac{1}{k^s}$, therefore yielding

$$P_k \sim \frac{1}{2k^s} + \frac{1}{(s-1)K^{s-1}} - \frac{1}{2k^s} + \frac{B_2 s}{k^{s+1}} + \frac{B_4 s(s+1)(s+2)}{2k^{s+3}} + ..., k \to \infty, \tag{9.27}$$

and, therefore,

$$\zeta(s) \sim \sum_{i=1}^{k} \frac{1}{i^s} + \frac{1}{2k^s} + \frac{1}{(s-1)K^{s-1}} - \frac{1}{2k^s} + \frac{B_2 s}{k^{s+1}} + \frac{B_4 s(s+1)(s+2)}{2k^{s+3}} + ..., \tag{9.28}$$

as $k \to \infty$.
This expression allows for obtaining much more accurate results via using OAT than by the use of the direct summation of the convergent expansion of the function. The following table shows the results for different partial sums.

Partial sum	Value of OAT	Number of terms
1	10.581720833333333333333333	5
2	10.584451922653952985003529 0	9
3	10.584448469577813110695320 3	14
4	10.584448464943248378747081 3	18
5	10.584448464950822569464200 9	22
10	10.584448464950809826386400 8	43

Table 9.1: Values of OAT for ζ-function. Underlined figures are in agreement to the exact result

The first column corresponds to the number of terms in the partial sum, i.e., the value of k. When k increases one must determine the smallest value of P_n and sum up the first $n-1$ terms. The number of terms is shown in the last column. The second column shows the value of the series by means of OAT. Underlined figures are ine agreement with the exact result. Therefore, one sees that by using only ten terms in the partial sum and 43 terms in the truncation of P_n we obtain a result that is precise up to 27 decimal places.
The last example shows the power of asymptotic analysis. By performing OAT on an asymptotic series one can obtain highly accurate values for slowly convergent series. Unfortunately, the use of such a scheme is limited because we need an exact expression for every term in the series. Since we are solving physical problems we are in need of schemes that require only finite information. This leads to the discussion of sequence transformations and the constructions of approximants.

9.4 Sequence Transformation

We have presented several methods that make use of an explicit expression for the coefficients of perturbation series. Next we discuss the possibility to improve the perturbative corrections by means of certain transformation. There is a highly developed branch in applied mathematics called *convergence acceleration*. We show some elementary routines that are applied lateron to physical

problems.

9.4.1 Introduction

The concept of sequence transformations is to obtain a new sequence that has better convergence properties. Recall that every infinite sum can be interpreted as a sequence of its partial sums. So consider a series $\sum_{n=0}^{\infty} a_n$ with $p_k = \sum_{n=0}^{k}$ and the sequence,

$$p_0, p_1, p_2, p_3, ... \tag{9.29}$$

and a mapping T with $T(p_i) = p_i'$. We will call T a *sequence transformation* [49]. At first sight one would postulate some properties to be fulfilled by a meaningful transformation. The most obvious is *regularity*, i.e., when p_i converges to some limit p than $T(p_i)$ converges to the same value. The power of sequence transformations is the fact that the convergence is accelerated, and less terms are needed to obtain a given accuracy. Additionaly, one might require linearity,

$$T(\alpha p_i + \beta q_i) = \alpha T(p_i) + \beta T(q_i). \tag{9.30}$$

Combining thoses properties leads to

$$\lim_{i\to\infty} T(\alpha p_i + \beta q_i) = \alpha p + \beta q, \tag{9.31}$$

for $p_i \to p$, $q_i \to q$. It turns out that the above requirements can be weakened. One drops the assumptions, and only requires *translational invariance*,

$$T(\alpha p_i + d) = \alpha T(p_i) + d. \tag{9.32}$$

Since this requirement is less restrictive we have more freedom in constructing a transformation. Experience shows that it is the non-linear character of the methods that is the reason for their succes. However, in most cases it does not suffice to use any arbitrary resummation scheme. Most impressive results are obtained if one takes as much information into account as possible. One of the most important features is the use of so called *remainder estimates*. It is not always possible to get this information. But if they are available they can be used to construct resummations chemes which are particularly well suited for a certain sequence. To see how this works let's consider an arbitrary sequence of partial sums

$$p_n = p + r_n, \tag{9.33}$$

where p denotes the limit and r_n is the so called remainder. Recall that it is equivalent that p_n converges to p and that r_n converges to zero. However, the strategy is the transformation to a new sequence where the remainder vanishes faster,

$$p_n' = p + r_n'. \tag{9.34}$$

Now we further assume the sequence of partial sums to have the following structure

$$p_n = p + \omega_n z_n. \tag{9.35}$$

We use this equation as a starting point to form a model of our sequence, i.e., we make explicit assumptions on the functional form of ω_n and z_n. This enables us to derive transformations that lead to improved convergence properties for an entire *class* of functions, namely those sharing a certain behaviour of their remainder terms. It is important to note that this involves a modelling process and not a derivation. The succes of a particular transformation tells whether the assumptions on the remainder terms were precise or not. An concept which is important in the derivation of a particular transformation involves so called *annihilation operators*. We say that an operator $\hat{A}$ is an annhihilation operator if it is linear and

$$\hat{A}(z_n) = 0, \forall n \in \mathbb{N}. \tag{9.36}$$

With this we are able construct a sequence transformation which is exact for (9.35) since

$$\begin{aligned} \frac{\hat{A}(p_n)}{\hat{A}(\omega_n))} &= \frac{\hat{A}(s)}{\hat{A}(\omega_n)} + \hat{A}(\omega_n) \\ &= \frac{1}{A(\omega_n)} s, \end{aligned} \tag{9.37}$$

and, therefore,

$$\mathcal{A}(p_n, \omega_n) = \frac{\hat{A}(p_n/\omega_n)}{\hat{A}(1/\omega_n)}. \tag{9.38}$$

This gives us a transformation $\mathcal{A}$ that involves both, the sequence and its remainder terms. Furthermore, this contruction is *exact* in the sense that

$$\mathcal{A}(p_n, \omega_n) = p. \tag{9.39}$$

In applications it is complicated to deal with the most general remainder estimates, so we restrict ourselves to the situation where z_n is after multiplication with a suited function ω_n only a finite polynomial. In this case a particular annihilation operator comes into play that enables to deduce closed formulas for a certain resuammtion scheme. Within the last decades there was spend much effort in the derivation and deeper understanding of resummation processes. For example Brezinski and Matos were able to show, that every known extrapolation procedure arises from a representation via annihilation operators [8]. For further information the interested reader finds the exhaustive treatment of sequence transformations by Ernst Jochim Weniger in reference [50].

9.4.2 Shanks Transformation

Having understood the concept of sequence transformation we are now able to introduce a first example which is called *Shanks transforamtion* [41]. Daniel Shanks proposed his method of accelerating certain series already in the 1950s. To motivate his approach consider a sequence of partial

sums p_n where the n-th term has the following form,

$$p_n = p + \alpha q^n, \tag{9.40}$$

where p and α are some constants and $|q| < 1$. This implies that p_n converges to p. We call such a term *transient*. Next we try to eliminate this term, since is the slowest decaying. Therefore, consider the three following equations

$$A_{n-1} = A + \alpha q^{n-1} \tag{9.41}$$

$$A_n = A + \alpha q^n \tag{9.42}$$

$$A_{n+1} = A + \alpha q^{n+1}. \tag{9.43}$$

Solving the above system for A yields

$$A = \frac{A_{n+1}A_{n-1} - A_n^2}{A_{n+1} + A_{n-1} - A_n^2}.$$

We use this to define the Shanks transformation

$$S(A_n) = \frac{A_{n+1}A_{n-1} - A_n^2}{A_{n+1} + A_{n-1} - A_n^2}. \tag{9.44}$$

Recall that we explicitly build a model for the sequence of partial sums to construct a transformation scheme. Besides the above assumptions seem rather restrictive. Nevertheless, it is sufficient that the most pronounced transient term is of the above form. To see this assume that

$$p_n = \tilde{p}(n) + \alpha q^n, \tag{9.45}$$

where $\tilde{p}(n)$ carries additional n-dependece. Anyhow, it is only important that $\tilde{p}(n)$ is more slowly varying than $\alpha(q)^n$. In that case we assume that $\tilde{p}(n-1)$, $\tilde{p}(n)$ and $\tilde{p}(n+1)$ being equal is a justified approximation.

Note that we can obtain a new transformed sequence by applying the Shanks transformation twice on the partial sums. This procedure is called *iterated Shanks transformation* and we will see on an example how well this works.

To see how Shanks transformation works consider

$$f(z) = \frac{1}{(1+z)(2+z)}. \tag{9.46}$$

One can show that

$$f(z) = \sum_{n=0}^{\infty} (-1)^n \left(1 - \frac{1}{2^{n+1}}\right) z^n, \tag{9.47}$$

and, therefore, the n-th partial sum to be given by

$$p_k = \sum_{n=0}^{k} (-1)^n \left(1 - \frac{1}{2^{n+1}}\right) z^n \tag{9.48}$$

$$= \frac{1}{(1+z)(2+z)} - \frac{(-z)^{n+1}}{z+1} + \frac{(-z/2)^{n+1}}{z+2}. \tag{9.49}$$

Further note that due to the poles at $z = -1, -2$ the domain of convergence is the unit circle. If we would like to evaluate the series at a point near boundary, say $z = 0.99$, we must take roughly 1000 terms into account to obtain five digits accuracy. With the help of the Shanks transformation we can do better. Figure(9.1 shows the absolute error for low order iterated Shanks in depence of the number of terms in the transformed series.

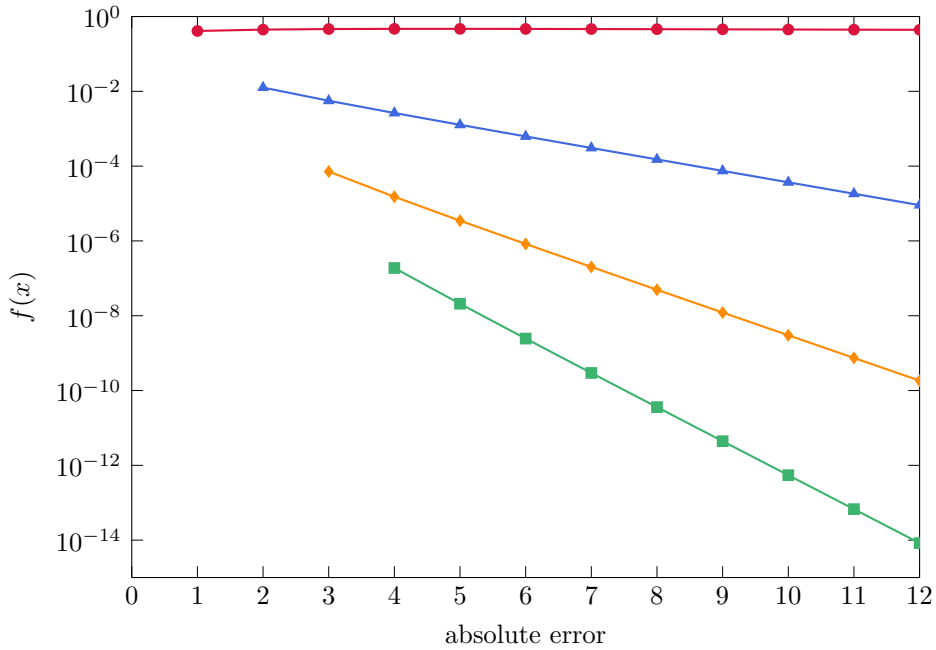

Figure 9.1: Semilogarithmic plot of the absolute error for different iterated Shanks transformations plotted over the number of terms in the transformed sequence for the function $f(z) = \frac{1}{(1+z)(2+z)}$ with partial sums given $\sum_{n=0}^{k}(-1)^n \left(1 - \frac{1}{2^{n+1}}\right) z^n$ for a value of $z = 0.99$. Shown are partial sums (●), Shanks-transformed partial sums $S(p_k)$ (▲), and the iterated Shanks-transformed partial sums $S^{(2)}_{(p_k)}$ (◆) and $S^{(3)}_{(p_k)}$ (■)

9.4.3 Levin-Weniger Transformations

Finally, we give an example of a more sophisticated resummation scheme which is named after its inventors Levin and Weniger [22] [50]. As we have already seen the properties of a sequence to be resummed determines the success of a certain resummation scheme. In general there does not exist a transformation that is equally well suited for every application. Quite contrary it is the special model that provides a powerful resummation scheme. In the case of the Shanks transformation we made use of a transient decay of the remainder term. Now, we will provide another example.

Consider the following model of a sequence

$$p_n = p + \omega_n \sum_{j=0}^{k-1} \frac{c_j}{(n+\beta)^j}. \tag{9.50}$$

This is again just another model for a sequence of partial sums. Recall that in this case the sum on the r.h.s. is just a polynomial of degree $k-1$ in the variable $\frac{1}{(n+\beta)}$. Those series arise naturally if we take them as finite approximations to an asymptotic expansion of the form

$$p_n \sim p + \omega_n \sum_{j=0}^{\infty} \frac{c_j}{(n+\beta)^j}. \tag{9.51}$$

The above model has $k+1$ unknown quantities - the limit p and the coefficients $c_0, ..., c_{k-1}$. So we need $k+1$ terms of the series to solve this system of equations.

In the following, we cast eq. (9.51) into a more convenient form to derive, in an analogous way to the Shanks transformation, a particular resummation scheme. We multiply both sides by a polynomial of degree $k-1$ of the form $(n+\beta)^{k-1}$, i.e.,

$$(n+\beta)^{k-1}(p_n - p) \cdot \frac{1}{\omega_n} = \sum_{j=0}^{k-1} \frac{c_j}{(n+\beta)^{k-j-1}} \tag{9.52}$$

The next step involves the iterated forward difference operator Δ^k, which is the discrete analogon to the well-known differential operator. It is recursively defined via

$$\begin{aligned} \Delta^0 f(n) &= f(n), \\ \Delta\ f(n) &= f(n+1) - f(n), \\ \Delta^k f(n) &= \Delta(\Delta^{k-1} f(n)), \qquad k \geq 1. \end{aligned} \tag{9.53}$$

It can be shown that this operator is linear and annihilates polynomials, more preciseley

$$\Delta^k P(n) = 0, \qquad \forall P \in \Pi_{k-1} \tag{9.54}$$

where Π_{k-1} denotes the vectorspace of polynomials of degree $k-1$. Since the right-hand side of (9.52) is a polynomial of degree $k-1$ applying Δ^k yields

$$\begin{aligned} \Delta^k \left[(n+\beta)^{k-1}(p_n - p) \cdot \frac{1}{\omega_n} \right] &= \Delta^k \left[\sum_{j=0}^{k-1} \frac{c_j}{(n+\beta)^{k-j-1}} \right] \\ &= 0. \end{aligned} \tag{9.55}$$

Additionally, linearity implies

$$p = \frac{\Delta^k \left[(n+\beta)^{k-1} p_n/\omega_n \right]}{\Delta^k \left[(n+\beta)^{k-1}/\omega_n \right]}. \tag{9.56}$$

Furthermore, we can write the k-th forward difference of an arbitrary sequence s_n as

$$\Delta^k s_n = \sum_{j=0}^{k} (-1)^{k-j} \binom{k}{j} s_{k+j}. \tag{9.57}$$

Applying this to (9.56) yields

$$p = \frac{\sum_{j=0}^{k} (-1)^j \binom{k}{j} (\beta + n + j)^{k-1} \frac{p_{n+j}}{\omega_{m+j}}}{\sum_{j=0}^{k} (-1)^j \binom{k}{j} (\beta + n + j)^{k-1} \frac{1}{\omega_{m+j}}}. \tag{9.58}$$

Details of the derivation of the last equation can be found in [].This motivates the so called *Levin-Weniger transformation* $\mathcal{L}(\beta)$. For numerical reasons this is often written more conveniently as

$$\mathcal{L}(\beta) = \frac{\sum_{j=0}^{k} (-1)^j \binom{k}{j} \frac{(\beta+n+j)^{k-1}}{(\beta+n+k)^{k-1}} \frac{p_{n+j}}{\omega_{m+j}}}{\sum_{j=0}^{k} (-1)^j \binom{k}{j} \frac{(\beta+n+j)^{k-1}}{(\beta+n+k)^{k-1}} \frac{1}{\omega_{m+j}}}, \tag{9.59}$$

where the additional denominator is introduced to prevent numerical overflow. The parameter β may be adjusted to improve the convergence properties of the transformed sequence. This transformation provides a powerful tool in improving convergence of certain factorial divergent series. Lateron we will use the perturbation series of the anharmonic oscillator as a benchmark to test this particular resummation scheme.

9.5 Padé Approximants

After constructing sequence transformations, we will now discuss an approach that is closely related. Instead of transforming the perturbation series after it has been evaluated for $\lambda = 1$, we transform the power series itself. This uses the concept of so called approximants, i.e., functions that approximate the power series.

9.5.1 Concept

As already mentioned in the discussion of generic features of perturbation series, their main disadvantage comes from the fact that they involve only positive powers of the perturbation parameter λ and therefore become useless in the presence of a singularity. In the next step we will take a truncated power series, i.e.

$$f_N(\lambda) = \sum_{j=0}^{N} c_j \lambda^j, \tag{9.60}$$

and construct an approximant. An *approximant* is another function that coincides with the truncated series in a sense that is made precise below. By choosing a suited approximant we hope to overcome the convergence difficulties of the original power series and obtain more accurate results if we increase the truncation index N. Therefore a sequence of truncated power series is transformed into a sequence of approximants, a concept which we are familiar with, from the last chapter.

Note that we will choose the approximants such that they posses the ability to imitate singu-

larities. However, it is desirable to work with functions as simple as possible in order to obtain a closed-form expression for their construction. It has shown that the use of rational functions leads to very good results. An approximants that is constructed by means of rational functions is called *Padé approximant* [1, 17]. We discuss in great detail both, their construction and convergence theory and show their great value in physical applications.

9.5.2 Construction

We now discuss the construction of Padé approximants from the corresponding power series. First recall that a rational function is a function

$$R(z) = \frac{\sum_{j=0}^{L} a_j z^j}{\sum_{j=0}^{M} b_j z^j} \tag{9.61}$$

that is given as a quotient of two finite polynomials in the variable z. We denote

$$\begin{aligned} P_L(z) &= \sum_{j=0}^{M} a_j z^j, \\ Q_M(z) &= \sum_{j=0}^{N} b_j z^j. \end{aligned} \tag{9.62}$$

Futhermore, we choose the coefficients $\{a_j\}$ and $\{b_j\}$ such that for $z \to 0$

$$f(z) - R(z) = O(z^{L+M+1}) \tag{9.63}$$

where $f(z)$ is the function to be approximated. Therefore the Taylor series of $f(z)$ and $R(z)$ coincide up to order $L + M + 1$. We will call the particular rational function for that (9.63) is fulfilled the Padé approximant and denote it by $P_f[L, M](z)$.

Note that that the value of a rational function does not chance if both numerator and denominator ar multiplied with the same number. Therefore one of $L + 1 + M + 1 = L + M + 2$ coefficients may be set to one. We follow the convention of setting $b_0 = 1$. By now we only discussed desireable properties of the approximant but we do not know how to construct it. Note that we can rephrase (9.63) in the way that for $z \to 0$

$$Q_M f(z) - P_L(z) = O(z^{L+M+1}). \tag{9.64}$$

This enables us to derive a system of equalities whose solution yields the coefficients of the Padé

approximant,

$$\begin{aligned}
c_0 &= b_0,\\
c_1 + c_0 a_1 &= b_1,\\
c_2 + c_1 a_1 + c_0 a_2 &= b_2,\\
&\vdots \qquad\qquad \vdots\\
c_L + c_{L+1} a_1 + \cdots + c_0 a_L &= b_L,\\
c_{L+1} + c_L a_1 + \cdots + c_{L_M+1} a_M &= 0,\\
&\vdots \qquad\qquad \vdots\\
c_{L+M} + c_{L+M-11} a_1 + \cdots + c_L a_M &= 0.
\end{aligned} \tag{9.65}$$

The solution to (9.65) is given by

$$P_f[L/M](z) = \frac{\begin{Vmatrix} c_{L-M+1} & c_{L-M+2} & \cdots & c_L \\ c_{L-M+2} & c_{L-M+3} & \cdots & c_{L+1} \\ \vdots & \vdots & \cdots & \vdots \\ c_L & c_{L+1} & \cdots & c_{L+M} \\ \sum_{j=M}^{L} c_{j-M} z^j & \sum_{j=M-1}^{L} c_{j-M+1} z^j & \cdots & \sum_{j=0}^{L} c_j z^j \end{Vmatrix}}{\begin{Vmatrix} c_{L-M+1} & c_{L-M+2} & \cdots & c_L \\ c_{L-M+2} & c_{L-M+3} & \cdots & c_{L+1} \\ \vdots & \vdots & \cdots & \vdots \\ c_L & c_{L+1} & \cdots & c_{L+M} \\ z^M & z^{M-1} & \cdots & 1 \end{Vmatrix}} \tag{9.66}$$

By determining the solution of the both determinants, we can write down a fractional function $P_f[L/M](z)$ whose Taylor expansion coincides with the truncated power series expansion $f_N(z)$, where $N = L + M + 1$. From this point of view this is just a transformation of one function to another. The advantage is that the Padé approximants often posses much better convergence properties than ordinary power series. More precisely this means, that even if a power series expansion of a function $f(z)$ fails to converge due to singularities, the Padé approximants might converge anyway. Besides Padé approximants have another important advantage. There are certain kinds of functions for which exist a highly developed convergence theory which enables us to actually prove that they succeed in approximating certain perturbation series. We discuss this in the next section.

Finally, let's discuss an example of a Padé approximant in the case of an analytical function. Consider the function

$$f(z) = \sqrt{\frac{1 + \frac{1}{2}x}{1 + 2x}}. \tag{9.67}$$

Its Taylor series expansion is given

$$T_n(f)(z) = 1 - \frac{3}{4}x + \frac{39}{32}x^2 + ... \tag{9.68}$$

Note that the radius of convergence is given by $\frac{1}{2}$ due to the zero in the denominator. Constructing the Padé approximant $P_f[1/1]$ yields

$$\begin{aligned} P_f[1/1] &= \frac{\begin{Vmatrix} -\frac{3}{4} & \frac{39}{32} \\ x & 1 - \frac{3}{4}x \end{Vmatrix}}{\begin{Vmatrix} -\frac{3}{4} & \frac{39}{32} \\ x & 1 \end{Vmatrix}} \\ &= \frac{1 + \frac{7}{8}x}{1 + \frac{13}{8}x}. \end{aligned} \tag{9.69}$$

The following plot shows a comparison between the orignal function and its Taylor and Padé approximation.

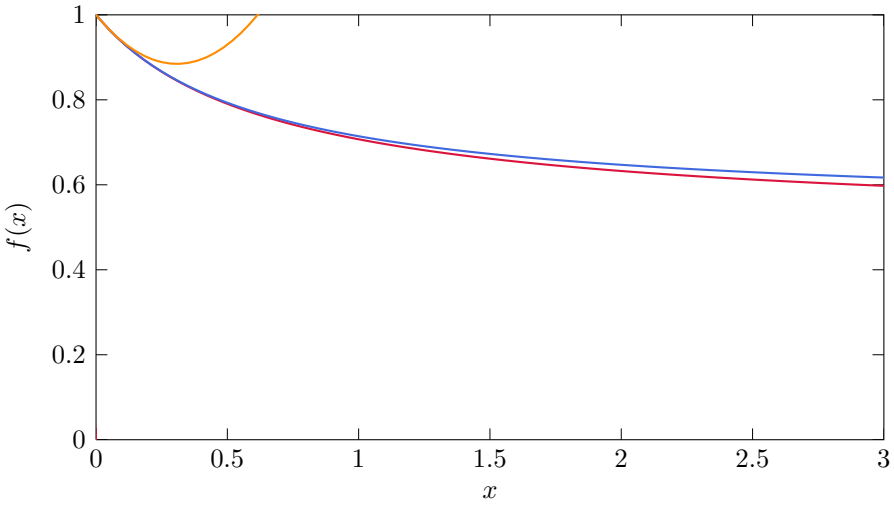

Figure 9.2: Plot of the function $f(z) = \sqrt{\frac{1+\frac{1}{2}x}{1+2x}}$ (●) with its truncated Taylor series $T_2(z)$ (●) and the Padé approximant $P_f[1/1](z)$ (●). Note that both approximations involve only third order information.

Oberserve that, although using the same amount of information, the truncated Taylor series is unable to provide an accurate approximation to the function due to the pole located at $z = \frac{1}{2}$, while the Padé approximant could even nearly fit the asymptotics of the functions. The asymptotic values of $f(z)$ and $P_f[1/1](z)$ differ only by 8% for $z \to \infty$.

9.5.3 Stieltjes Functions

In a general setting one is in only few able to prove that a particular resummation scheme works and that the convergence of the transformed series yield the same limit as the original one. But there are certain class of functions for which one can show that a particular method works and derive rigorous results on their convergence properties. This is the case for so called *Stieltjes functions*

and the corresponding *Stieltjes series*.

Definition 10. *Let* $f(z) = \sum_{n+0}^{\infty} a_n z^n$ *a function with its formal power series expansion.* $f(z)$ *is said to be a* Stieltjes function *if*

$$a_n = (1)^n \mu_n \tag{9.70}$$

where μ_n *has the following representation,*

$$\mu_n = \int_0^\infty t^n d\lambda(t), \tag{9.71}$$

where $\lambda(t)$ *is unique positive measure on* $[0, \infty)$ *that takes infinitely many different values. Furthermore* $f(z)$ *has a convergent integral representation via*

$$f(z) = \int_0^\infty \frac{1}{1+zt} d\lambda(t). \tag{9.72}$$

The corresponding power series expansion

$$f(z) = \sum_{n=0}^{\infty} (-1)^n \mu_n z^n, \tag{9.73}$$

is called Stieltjes series*.*

Before stating some of the important features of the convergence theory of Stieltjes series, let's recall how to deal with this property in physical applications. To prove the Stieltjes property one must determine every of the coefficients and compare them to the definition. First of all, as already mentioned many times before, we are typically not in the situation to have this infinite amount of information and are rather restricted to the knowledge of a few coefficients of the perturbation series. This shows that we are never able to prove that a series arising from many-body perturbation theory is a Stieltjes series. Even if we knew a closed formula for the coefficients, the Stieltjes property is hard to check from the definition. We will state without proof simple necessary condition for the convergence of Padé approximants.

Theorem 5. *Let* $\{\mu_n\}_{n=0}^{\infty}$ *be the sequence of the Stieltjes moments. If*

$$\sum_{n=0}^{\infty} \mu_n^{-1/(2n)} = \infty, \tag{9.74}$$

then the sequence $P_f[N + J/N]$ *of Padé approximants converges for* $N \to \infty$ *and fixed* $J \geq -1$ *to the value of the corresponding Stieltjes function* $f(z)$*.*

A very important implication is the following:

Theorem 6 (Carleman [7])**.** *The condition* (9.74) *is fulfilled if*

$$\mu_n \leq C^{n+1}(2n)!, \tag{9.75}$$

where C *is a positive constant.*

We will use the last statement in the discussion of the qunatum anharmonic oscillator in terms of Padé approximants.

Interstingly, in the case of Stieltjes series we can construct bounds on the elements of the sequence. Consider the sequences $P_f[N/N]$ and $P_f[N/N+1]$. We will refer to them as *diagonal* and *subdiagonal* Padé sequences respectively. One can prove that

$$P_f[N/N](z) \geq f(z) \geq P_f[N/N+1](z). \tag{9.76}$$

This provides upper and lower bounds for the limit the function $f(z)$. But we can do even better. On top of that the diagonal Padé sequence converges in a strictly monotone decreasing fashion to $f(z)$ while contrary the subdiagonal Padé sequence converges strictly monotone increasing. This means that via constructing more and more Padé approximants those new elements in the Padé sequence give us more and more accurate bounds on the error between the Padé approximants and the limiting function.

Chapter 10

The Coupled-Cluster Method

In the discussion of the results we use Coupled-Cluster (CC) methods to check perturbation theory on consistency with the CC approach. This section is dedicated to a brief introduction of the Coupled-Cluster technique [39, 26]. CC theory was known long before it became a standard technique in modern nuclear structure. Quantum chemistrists used the CC approach in the 1950s to study correlations between electrons. With the growing computational power nucleonic interactions became tractable as well [33].

Calculation of the Ground-State Energy

The CC approach yields an exact solution of the stationary Schrödinger equation. Let $|\psi\rangle$ denote the ground state of an A-body system. We write this in terms of a reference state $|\Phi\rangle$ via the ansatz

$$|\psi\rangle = e^{\hat{T}}|\Phi\rangle, \tag{10.1}$$

where $\hat{T}$ denotes the so-called cluster operator, defined by

$$\hat{T} = \sum_{n}^{A} \hat{T}_n, \tag{10.2}$$

where $\hat{T}_n$ is a n-p-n-h excitation operator. We write the excitation operator in second quantization by

$$\hat{T}_n = \left(\frac{1}{n!}\right)^2 \sum_{\substack{a_1,\dots,a_n \\ r_1,\dots,r_n}} t_{a_1\dots a_n}^{r_1\dots r_n}\ \hat{a}_{r_1}^{\dagger}\dots\hat{a}_{r_n}^{\dagger}\hat{a}_{a_n}\dots\hat{a}_{a_1}, \tag{10.3}$$

with cluster amplitudes $t_{a_1\dots a_n}^{r_1\dots r_n}$. Recall that indices starting from a correspond to particle-indices, whereas indices starting from r are hole-indices. Ultimately we need to solve the Schrödinger equation

$$\hat{H}|\psi\rangle = E_0|\psi\rangle, \tag{10.4}$$

We can rewrite the ground-state energy by

$$E_0 = E_{\text{ref}} + \Delta E, \tag{10.5}$$

where the reference energy E_{ref} is given by the expectation value with respect to the reference state

$$E_{\text{ref}} = \langle\Phi|\hat{H}|\Phi\rangle. \tag{10.6}$$

Furthermore, we call ΔE the *correlation energy*. We define the normal-ordered Hamiltonian by

$$\hat{H}_{\text{NO}} = \hat{H} - E_{\text{ref}} \tag{10.7}$$

Inserting eq. (10.1), the definition of the ground-state energy eq. (10.5) and the definition of the normal-ordered Hamiltonian eq. (10.7) into the stationary Schrödinger equation eq. (10.4) and multiplying both sides with $e^{-\hat{T}}$ yields

$$\hat{\bar{H}}_{\text{NO}}|\Phi\rangle = \Delta E|\Phi\rangle, \tag{10.8}$$

where we defined the similarity-transformed Hamiltonian by

$$\begin{aligned}\hat{\bar{H}}_{\text{NO}} &= e^{-\hat{T}}\hat{H}_{\text{NO}}e^{\hat{T}}, \\ &= \left(\hat{H}_{\text{NO}}e^{\hat{T}}\right)_{\text{C}},\end{aligned} \tag{10.9}$$

where $\left(\hat{H}_{\text{NO}}e^{\hat{T}}\right)_{\text{C}}$ denotes the connected component of the corresponding operator obtained by fully contracting $\hat{H}_{\text{NO}}e^{\hat{T}}$. We obtain a system of equations for the cluster-amplitudes by projecting eq. (10.8) onto excited reference states

$$|\Phi^{r_1\dots r_k}_{a_1\dots a_k}\rangle = \hat{a}^\dagger_{r_1}\dots\hat{a}^\dagger_{r_k}\hat{a}_{a_k}\dots\hat{a}_{a_1}|\Phi\rangle, \tag{10.10}$$

yielding

$$\begin{aligned}\langle\Phi^{r_1}_{a_1}|\hat{\bar{H}}_{\text{N}}|\Phi\rangle &= 0 \\ \langle\Phi^{r_1r_2}_{a_1a_2}|\hat{\bar{H}}_{\text{N}}|\Phi\rangle &= 0 \\ &\vdots \\ \langle\Phi^{r_1\dots r_A}_{a_1\dots a_A}|\hat{\bar{H}}_{\text{N}}|\Phi\rangle &= 0.\end{aligned} \tag{10.11}$$

Note that projecting the reference state $|\Phi\rangle$ on eq. (10.8) gives

$$\Delta E = \langle\Phi|\hat{\bar{H}}_{\text{NO}}|\Phi\rangle. \tag{10.12}$$

Solving the system of equation for the cluster-amplitudes yields an exact solution for the ground-state energy by

$$E_0 = E_{\text{ref}} + \langle\Phi|\hat{\bar{H}}|\Phi\rangle. \tag{10.13}$$

Expansion in Single and Double Excitations

The above treatment yields an exact solution of the stationary Schrödinger equation. However, in practical applications we do not take every term of the cluster-operator $\hat{T}$ into account. In order to

expand the analysis to more complicated systems we truncate the number of particle-hole excitation operators up to $2p2h$-excitations. This is the so called CCSD approach, where the cluster-operator is given by

$$\hat{T}^{(\mathrm{CCSD})} = \hat{T}_1 + \hat{T}_2, \tag{10.14}$$

with corresponding one-body operator

$$\hat{T}_1 = \sum_{r,a} \hat{a}_r^\dagger \hat{a}_a, \tag{10.15}$$

and two-body operator

$$\hat{T}_2 = \frac{1}{4} \sum_{\substack{a_1,\, a_2 \\ r_1,\, r_2}} t_{a_1 a_2}^{r_1 r_2} \hat{a}_{r_1}^\dagger \hat{a}_{r_2}^\dagger \hat{a}_{a_1} \hat{a}_{a_2}, \tag{10.16}$$

respectively. The CC equations within the CCSD approximation are obtained using the similarity-transformed normal-ordered Hamiltonian with truncated cluster-operator and limiting the projections in to $2p2h$ excitations,

$$\langle \Phi_{a_1}^{r_1} | e^{-(\hat{T}_1+\hat{T}_2)} \hat{H}_{\mathrm{NO}} e^{\hat{T}_1+\hat{T}_2} | \Phi \rangle = 0 \tag{10.17}$$

$$\langle \Phi_{a_1 a_2}^{r_1 r_2} | e^{-(\hat{T}_1+\hat{T}_2)} \hat{H}_{\mathrm{NO}} e^{\hat{T}_1+\hat{T}_2} | \Phi \rangle = 0 \tag{10.18}$$

After determining the cluster amplitudes of $\hat{T}_1$ and $\hat{T}_2$ we write down the ground-state energy in CCSD approximation,

$$E^{(\mathrm{CCSD})} = E_{\mathrm{ref}} + \Delta E^{(\mathrm{CCSD})}, \tag{10.19}$$

where again $\Delta E^{(CCSD)}$ is given by the expectation value with respect to the reference state

$$\Delta E^{(\mathrm{CCSD})} = \langle \Phi | e^{-(\hat{T}_1+\hat{T}_2)} \hat{H}_{\mathrm{NO}} e^{\hat{T}_1+\hat{T}_2} | \Phi \rangle. \tag{10.20}$$

Inclusion of Triple Excitations

The above description of a truncation of the cluster operator to $2p2h$ excitations is feasible even for heavy nuclei. However, it turns out that for an accurate description of particular properties of nuclei, like binding energies, the CCSD approach does not suffice. To extend the description we also take triple excitations into account. Unfortunetaly, including all kind of triply excited states is unmanagable. In this context there exists different approaches including triples in the desciption [18], e.g., CCSD(T), ΛCCSD(T) [44, 45, 4, 3] or CR-CC(2,3) [30]. The approach that is used to prove consistency of the results from perturbation theory is ΛCCSD(T). The derivation of the corresponding ΛCCSD(T) equations may be found in [4].

Chapter 11

Computational Aspect

Before discussing the results of our calculations we briefly describe the techniques used in increasing the performance of the algorithm to derive low-order perturbation corrections.

11.1 Limitations

The main problem when dealing with high-order perturbation calculations is memory. When calculating 30th order energy correction for a closed shell nucleus like ^{40}Ca in large model spaces, this requires a simultaneous storage of up to 100 million basis states. This becomes feasible only on supercomputers and one is left to deal with this problem by massive paralellization techniques. When working in floating point arithmetics, this corresponds to several hundreds gigabyte of memory. Note that we want to perform those calculations mainly on the RAM because reading from the hrad disk is much slower. Additionally even a recursive treatment of high perturbation order for model spaces this large would yield several weeks of runtime.

So if one wants to investigate heavier nuclei without using very small model spaces one must take another route. Since there are closed formulas available for perturbation order up to three we will use explicit summation to obtain low-order results even for heavy nuclei. Unfortunenately, a naive approach using explicit loops over all quantum numbers is insufficient. We will now discuss how this problem can be dealt with more sophisticatedly.

11.2 Improving Low-Order Summation

A general feature of perturbative calculations is the fact that they become much more involved order by order. So the amount of work one has to spend to derive the next order is far from being linear. This statement does not only account for mathematical complexity for the involved formula, e.g., the the number of contributing diagrams, but also for the computational effort, that is necessary to deal with the next correction.

Recall that the third order energy correction in particle hole formalism is given

$$E_0^{(3)} = \frac{1}{8} \sum_{a,b,c,d,r,s} \frac{\langle ab|V|rs\rangle\langle rs|V|cd\rangle\langle cd|V|ab\rangle}{(\epsilon_a + \epsilon_b - \epsilon_r - \epsilon_s)(\epsilon_c + \epsilon_d - \epsilon_r - \epsilon_s)} + \frac{1}{8} \sum_{a,b,r,s,t,u} \frac{\langle ab|V|rs\rangle\langle rs|V|tu\rangle\langle tu|V|ab\rangle}{(\epsilon_a + \epsilon_b - \epsilon_r - \epsilon_s)(\epsilon_a + \epsilon_b - \epsilon_t - \epsilon_u)} + \sum_{a,b,c,r,s,t} \frac{\langle ab|V|rs\rangle\langle cs|V|tb\rangle\langle rt|V|ac\rangle}{(\epsilon_a + \epsilon_b - \epsilon_r - \epsilon_s)(\epsilon_a + \epsilon_c - \epsilon_r - \epsilon_t)}. \tag{11.1}$$

The third order term involves three different contributions. Each of them involves six summations over single-particle states. As said before the most naive way is to loop over all possible single -particle quantum numbers. Every single-particle state is described by a radial quantum number n, orbital angular-momentum quantum number l, total angular-momentum quantum number$j$, projection of the total angular-momentum quantum number j_m and isospin-projection quantum number t. Even after imposing parity invariance and the restricted coupling of different angular momenta this is still not feasible larger quantum numbers.

When first dealing with this problem we analyzed the sparsity of the problem, i.e., the number of non-vanishing matrix elements. This quantity is of course dependend on the particular nucleus and model space. However it turned out that the sparsity of the matrix ranges from 0.1% to 10%, i.e. most matrix elements vanished. Finally one is left with finding a strategy that decreases both runtime and required memory. We explain how this is done in the following. We start with a discussion on improving runtime performance. The main idea is to use BLAS libraries, a collection of highly optimized routines designed to solve basic linear algebra problems. The routines may be divided into three categories. Level 1 is used for the optimization of vector-vector operations like scalar products or vector addition. Level 2 increases the performance of matrix-vector operation, like matrix multiplication with a vector and Level 3 optimizes matrix-matrix operations, i.e. in particular products of matrices. In our case we only used Level 3 routines. To see why this is helpful consider two matrices $A, B \in Mat_{n\times n}$. The product of these two matrices is then defined via

$$A \cdot B = \sum_{j=1}^{n} a_{ij} b_{ji}. \tag{11.2}$$

If we compare this with the structure of the third energy correction, we see that the product of matrix elements in the numerator may be interpreted as a double matrix product. Take, for instance,

$$\sum_{rs} \langle ab|V|rs\rangle\langle rs|V|cd\rangle. \tag{11.3}$$

Since the states within the matrix elements consist of two single-particle states we must construct a collective two-particle index from the variables r, s. When doing so we can write the above

expression as

$$\sum_J \langle I|V|J\rangle\langle J|V|K\rangle, \tag{11.4}$$

where we denote with I denoted the two particle index corrspond to ab and with J, K the one corresponding to rs and cd respectively. With this in mind, we have refomulated the third order contribution partially as a matrix multiplication. Unfortunately this procedure is only directly useful for the first two terms. Observe that the third part of the correction is given by

$$E^{(3)}_{0,ph} = \sum_{a,b,c,r,s,t} \frac{\langle ab|V|rs\rangle\langle cs|V|tb\rangle\langle rt|V|ac\rangle}{(\epsilon_a + \epsilon_b - \epsilon_r - \epsilon_s)(\epsilon_a + \epsilon_c - \epsilon_r - \epsilon_t)}, \tag{11.5}$$

where the lower index 'ph' indicates the socalled ph-correction. The problem is that the variables corresponding to the labels of the intermediate states are not equal, i.e., the states $|rs\rangle$ and $\langle cs|$ differ in a single-particle state. Therefore, it is impossible to construct a collective two-particle index that we can use to formulate this as a matrix multiplication. One possibility to overcome this is to integrate out one hole state and one particle state. That means we must explicitly loop over two of the six single-particle states. In the above equation partial summation over the variables b, s yields

$$\sum_{b,s} \frac{\langle ab|V|rs\rangle\langle cs|V|tb\rangle}{(\epsilon_a + \epsilon_b - \epsilon_r - \epsilon_s)} = M^{rt}_{ac}, \tag{11.6}$$

where we denote by M^{rt}_{ac} a quantity that depends on two hole indices and two particle indices. Now we are able to reformulate this as a matrix multiplication

$$\sum_{rt} M^{rt}_{ac} \cdot N^{rt}_{ab}, \tag{11.7}$$

where we defined

$$N^{rt}_{ab} = \frac{\langle rt|V|ab\rangle}{(\epsilon_a + \epsilon_b - \epsilon_r - \epsilon_t)}. \tag{11.8}$$

Afterwars we simply have to build the trace of the matrix product $M \cdot N$ which corresponds to the summation over a, b. By using two explicit summations in terms of loops, we are able to cast the problem into a form which is accesible for a BLAS implementation.

After doing so we performed some benchmark calculations in order the compare the results of an explicit loop calculation against the BLAS interface. It appeared, that for increasing model space, i.e., increasing $e_{\max}$ the acceleration factor for the pp- and hh-contributions was of the order 10^3. So we were able to improve the runtime by a factor ~ 1000. Unfortunenately the ph-contribution reduces this effect. Since we need to explicitly loop over two single particle states the overall acceleration factor is lowered to roughly ten. This factor tends to increase for heavier nuclei. But for problems with more than 40 nucleons there was no data to compare to, so we expect BLAS to be more effective in the heavy mass region.

Besides the problem of feasible runtime for heavy nuclei we had to deal with the storage of

matrix elements. When using BLAS implementations matrix elements must be cast into arrays in order to be used by the routines. This means we must initialize very huge matrices, therefore producing storage problems when working in double precision. One possibility is to make use of the symmetries of the interaction. The Hamiltonian we are working with is parity conserving. So we will contruct a two body index that uses a block diagonal structure of the matrix with resprect to the parity quantum number and total orbital angular momentum. So when performing matrix products we only perform them in a subspace with fixed parity π and total angular momentum J. We will compute the energy correction for a fixed (J, π) subspace, store the result for the energy and free the matrices arising from that particular (J, π) block. After iterating this procedure for all possible (J, π) blocks we get the entire energy correction by summing over all values obtained from one block. So the maximal storage needed is bounded from above by the largest matrix that one gets in a particular configuration for parity and total angular momentum. Fortunately, these matrices have dimension of at most 5000, which is accessible on a single node.

One of the next steps in increasing computational performance would be multi-threaded paralellization. It is possible to distribute the problem on several nodes in such a way that every node calculates the energy correction from a particular (J, π) block. Since only very little communication between different nodes is required this would tremendously decrease the runtime of low order perturbative calculations. However, this method has not been implemented so far.

Chapter 12

Results

After discussing in detail several approaches aiming at sudies of atomic nuclei, we now turn to the analysis of physical problems. This section is mainly divided into two parts. First of all we consider the approach based on resummation theory and the use of sequence transformations. This involves both benchmark problems like the quantum anharmonic oscillator and physical examples like high-order perturbation theory for light nuclei. After that we discuss the influence of a change of basis, i.e., a different partitioning, on the convergence pattern of perturbation series. We do not further restrict ourselves to light nuclei and investigate closed-shell nuclei over the entire nuclear chart up to ^{208}Pb. However, we can not derive perturbative corrections up to 30th order for medium-mass nuclei. Instead we compute the first three orders in Hartree-Fock basis via an explicit summation scheme.

12.1 Resummation Theory

We start the discussion with an analysis of the quantum anharmonic oscillator and the determination of its ground-state energy in terms of resummation schemes. The advantage of a having a closed-form solution to the coefficients of the perturbation series available cannot be overemphasized. We see how this affects the analysis of nuclei.

12.1.1 The quantum anharmonic oscillator

In chapter 4 we provided a perturbative treatment of the anharmonic oscillator and derived the first corrections explicitly. Most important, we found that a asymptotic expansion for the perturbation series for the ground state energy exists, i.e.,

$$E_0(\lambda) \sim \sqrt{\frac{6}{\pi^2}} \sum_{n=0}^{\infty} (-1)^{n+1} \Gamma(n+\frac{1}{2}) 3^n \lambda^n. \tag{12.1}$$

Since the Γ-function interpolates the factorial function, the above expression is factorially divergent. This is obvious when looking at fig. 12.1. As we can see, the contribution heavily diverges and it is meaningless to derive the sequence of partial sums to get a value for the ground-state energy. Furthermore, note that we cannot use the Shanks transformation directly, since by construction this only yields better results for series oscillating around a limit. However, we can use as a first step

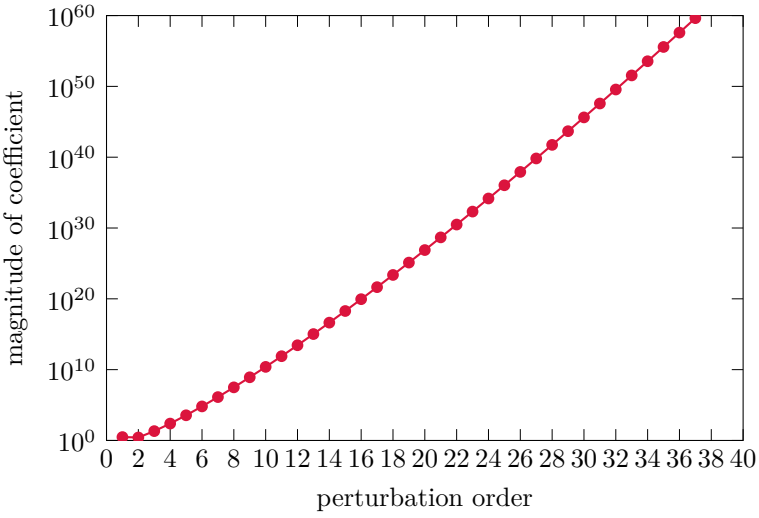

Figure 12.1: Logarithmic plot of the absolute value of the perturbative corrections of the quantum anharmonic oscillator with $\hat{x}^4$ perturbation, i.e., $\hat{H} = \hat{p}^2 + \frac{1}{2}\hat{x}^2 + \frac{1}{4}\lambda\hat{x}^4$. All physical quantities are set to one.

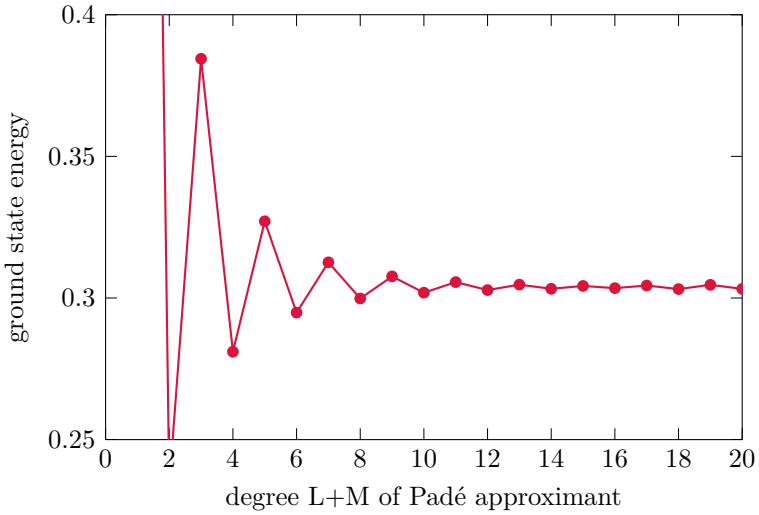

Figure 12.2: Plot of the Padé main sequence constructed from the partial sums of the quantum anharmonic oscillator with $\hat{x}^4$ perturbation, i.e., $\hat{H} = \hat{p}^2 + \frac{1}{2}\hat{x}^2 + \frac{1}{4}\lambda\hat{x}^4$. All physical quantities are set to one.

Padé approximants to obtain a transformed sequence. The results are shown in fig. 12.2. The Padé main sequence yields a convergent sequence with a limit of roughly 0.3. On top we see that the two subsequence consisting of the diagonal and subdiagonal Padé approximants converge in a monotone fashion to the limiting value. This reflects the Stieltjes property of the perturbation series. In fact one can prove that the Carleman condition of theorem 5 is fulfilled for the anharmonic oscillator with quartic perturbation. Up to this point we made huge progress compared to the sequence of partial sums. We were left with a strongly diverging series [6] from which we could not derive any information and we transformed it into a convergent one [46]. However, for determining the ground-state energy up to one percent accuracy we need 20 coefficients from the perturbation series. As already mentioned before, it is no problem to obtain corrections up to order 50 in the

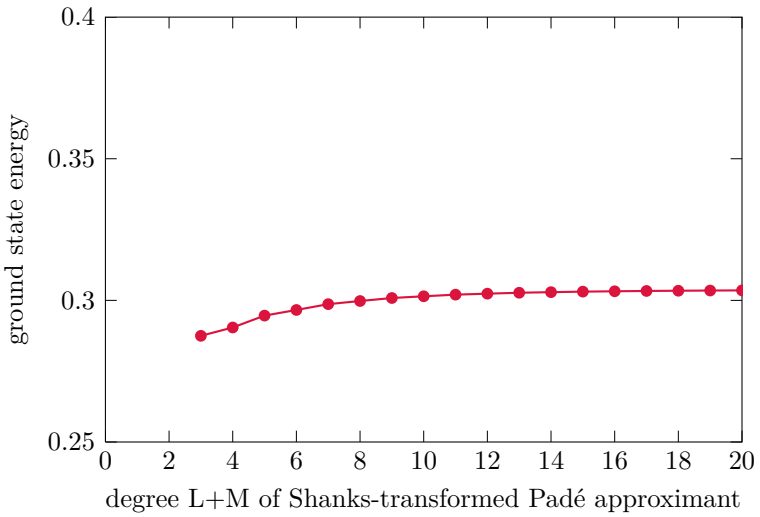

Figure 12.3: Plot of the Shanks-transformed Padé main sequence constructed from the partial sums of the quantum anharmonic oscillator with x^4 perturbation, i.e. $\hat{H} = \hat{p}^2 + \frac{1}{2}\hat{x}^2 + \frac{1}{4}\hat{x}^4$. All physical quantities are set to one.

case of the anharmonic oscillator, but similar calculations for nuclei need much more effort. It would be desirable to improve these results such that we obtain the same accuracy within less than 10 perturbation orders. One possibility is the use of the Shanks transformation. Note that after transforming the perturbation series into the Padé main sequence, we are left with an expression that is particularly well suited to the Shanks transformation, because the Padé main sequence fulfills all conditions needed for the Shanks transform, .i.e., oscillation around a limiting value as already discussed in chapter 9. The improved results by the combined use of Padé approximants and Shanks transformation are shown in fig. 12.3. Obviously the use of the Shanks transformation enables us to deduce the ground-state energy within less than ten orders of the perturbation series within acceptable accuracy. Since now, none of the used methods was particuclarly constructed for the resummation of the bare resummation series. We expect to get even further improved results when taking the asymptotic behaviour of the perturbation series into account, i.e., using a resummation method tailored to treat facorially divergent expansions. One example is the Levin-Weniger transformation. The results are shown in fig. 12.4. Note that in the definition of the Levin-Weniger transformation a real-valued parameter β is introduced that may be adjusted to achieve the best convergence,

$$\mathcal{L}(\beta) = \frac{\sum_{j=0}^{k}(-1)^j \binom{k}{j} \frac{(\beta+n+j)^{k-1}}{(\beta+n+k)^{k-1}} \frac{p_{n+j}}{\omega_{m+j}}}{\sum_{j=0}^{k}(-1)^j \binom{k}{j} \frac{(\beta+n+j)^{k-1}}{(\beta+n+k)^{k-1}} \frac{1}{\omega_{m+j}}},$$

where p_n is the n-th partial sum and ω_n the n-th energy correction. Figure 12.4 shows that there exist an optimal parameter for this transformation. When choosing β too small or too large one ends up with worse convergence properties. The intermediate value of $\beta = 2$ corresponds to the optimal choice. In this case we obtain a precise value for the ground-state energy within four orders in perturbation theory. This highlights the increased rate of convergence compared to a combined Shanks-Padé resummation method. Recall that we were only able to reduce the needed information

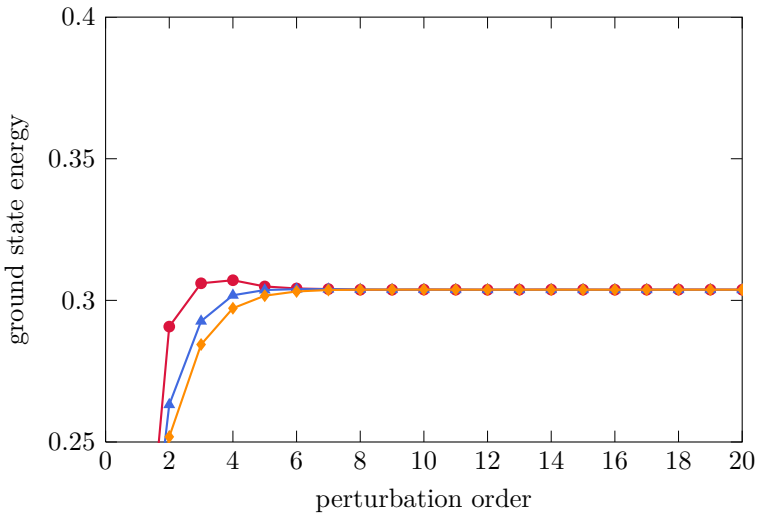

Figure 12.4: Plot of the Levin-Weniger transformed sequence of partial sums of the quantum anharmonic oscillator. Different colors correspond to different values of the parameter, $\beta = 1$(●), $\beta = 2$(▲) and $\beta = 3$(◆)

because we used a transformation that is constructed to resum factorially divergent series. The precise knowledge of the asymptotic behaviour makes a particular resummation method work. We see later how this affects our analysis in nuclei.

12.2 High-Order Perturbation Theory for Nuclei

When working on the quantum anharmonic oscillator we saw some typcial problems that arise in many-body perturbation theory. There is not always a convergent bare perturbation series, i.e., we cannot extract any information directly from the sequence of partial sums. In this case we have two options: We may either construct a particular resummation method that uses the structure of the perturbation series, or we alter the unperturbed problem and investigate the convergence properties with respect to the new basis as discussed in chapter 7.

12.2.1 Truncation Schemes

First of all we need to introduce some notation and conventions. Since in general the many-body Hilbert space is infinite dimensional we must define a truncation to make the computations feasible. This involves a number of different truncations.

1. **ph-excitations** This truncation restricts the number of particles that are simultaneously excited relative to the ground-state. When dealing with a nucleus containing A nucleons, there is in general the possibility to excite all nucleons at the same time, i.e., an exact computation for ^{4}He involves up to $4p4h$- excitations and ^{208}Pb in principle up to $208p208h$ excitations. So this quantity refers to neglecting all excitations that exceed a particular value of simultaneous excitations.

2. $\mathbf{e_{max}}$ This is a single-particle truncation. The HO energy quantum number is given by $e = 2n + l$, where n is the radial quantum number and l the orbital angular momentum

quantum number. Using a $e_{\max}$ truncation means that we neglect particle excitations that are greater than the single-particle energy quantum number e_{Max}.

3. $\mathbf{N_{max}}$ This is a many-particle quantity truncating the model space to excitations whose sum over the single-particle quantum number excitations with respect to the reference state does not exceed $N_{\max}$.

After introducing the relevant truncations for the many-body Hilbert space, we are ready to investigate realistic interactions. This section consists of a discussion of perturbative results on light and medium-light closed shell nuclei. We analyze both Harmonic Oscillator (HO) and Hartee-Fock (HF) basis sets.

12.2.2 Harmonic-Oscillator Basis

Harmonic-oscillator perturbation theory up to high order has already been discussed in several contexts with similar results. In most cases the perturbation series with respect to HO basis functions leads to divergent results. We start with an analysis of ^{4}He. This is the simplest closed shell nucleus and the only one which we can handle up to arbitrary ph-excitations. The results for a SRG-evolved NN-interaction with flow parameter $\alpha = 0.02\mathrm{fm}^4$ and $4p4h$-excitations is shown in fig. 12.5 and for $\alpha = 0.08\mathrm{fm}^4$ in fig. 12.6. Obviously, the perturbation series itself is already convergent and increasing the $e_{\max}$-truncation lowers the value of the limit. Nevertheless we can use Padé approximants to obtain a transformed sequence. The results are shown in fig. 12.7. One can see that the convergence properties are even better for the Padé approximants and there is no need to use an additional Shanks transformation to accelerate convergence. However, it has already been observed that perturbation series for ^{4}He usually do not converge [35]. The same

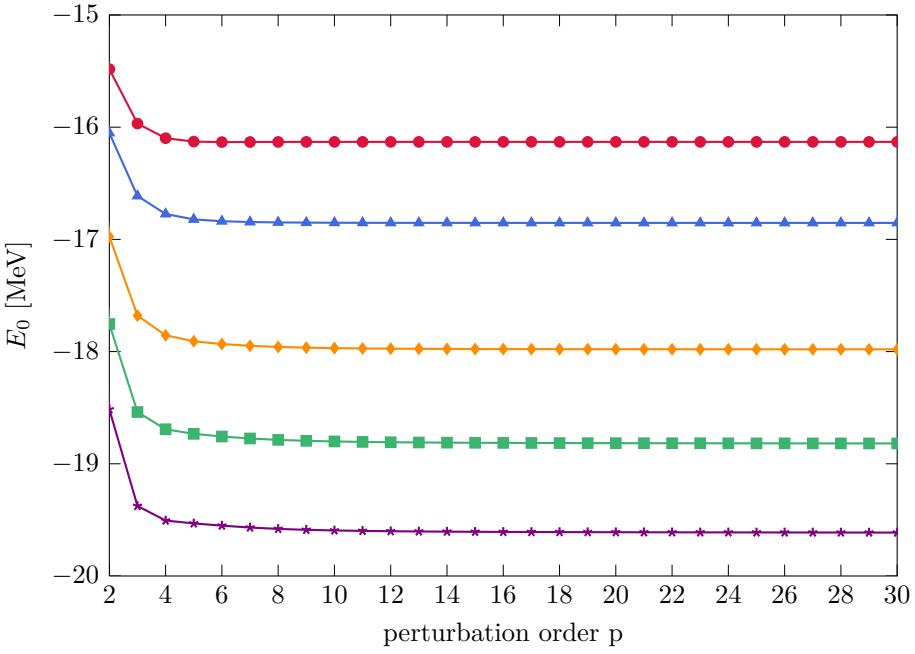

Figure 12.5: Plot of high-order perturbative corrections of ^{4}He for $\alpha = 0.08\mathrm{fm}^4$, oscillator frequency $\hbar\Omega = 20\mathrm{MeV}$ and increasing values of $e_{\max}$: $e_{\max} = 2$ (●),$e_{\max} = 4$ (▲), $e_{\max} = 6$ (◆), $e_{\max} = 8$ (■) and $e_{\max} = 10$ (★)

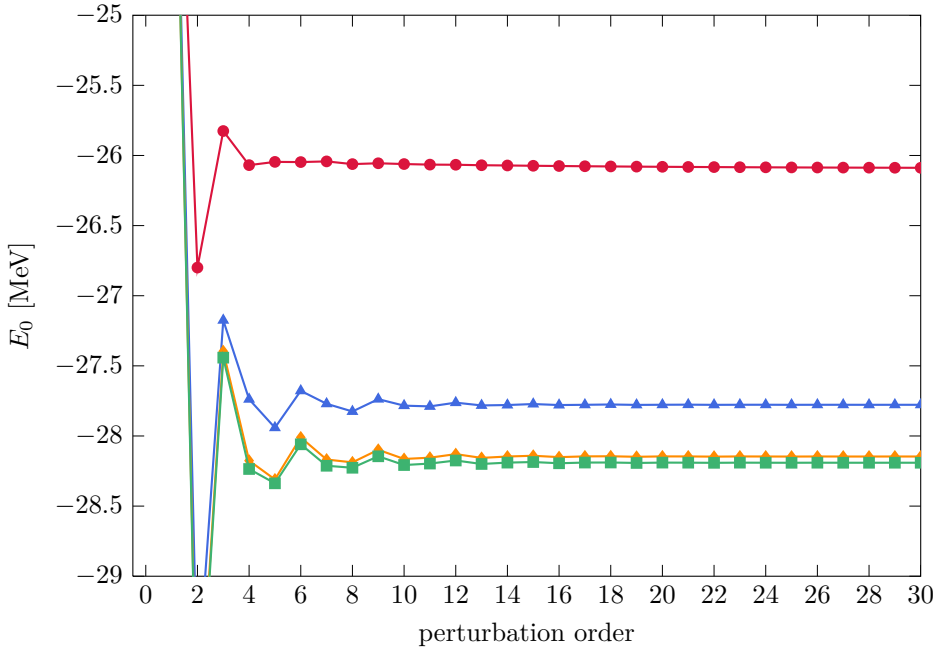

Figure 12.6: Plot of partial sums of ^{4}He with respect to HO basis for $\alpha = 0.02\text{fm}^4$, oscillator frequency $\hbar\Omega = 20\text{MeV}$, 4p4h-excitations and increasing values of $e_{\max}$: $e_{\max} = 2$ (●), $e_{\max} = 4$ (▲), $e_{\max} = 6$ (◆) and $e_{\max} = 8$ (■). Due to high computational effort, all model spaces were additionally $N_{\max}$ truncated with the same value as the $e_{\max}$ truncation.

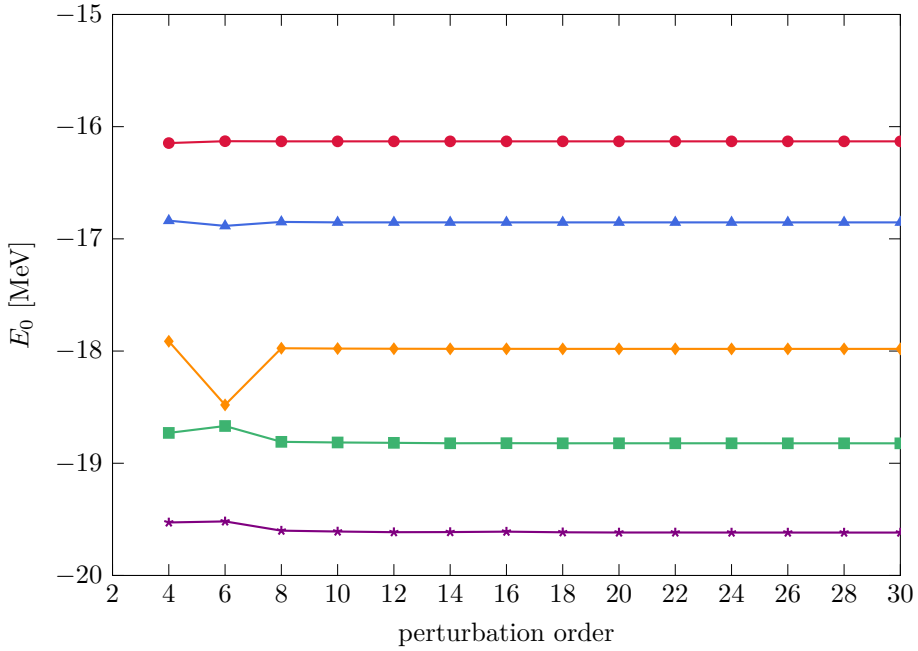

Figure 12.7: Plot of Padé main sequence of ^{4}He with respect to HO basis for $\alpha = 0.02\text{fm}^4$, oscillator frequency $\hbar\Omega = 20\text{MeV}$, 4p4h-excitations and increasing values of $e_{\max}$: $e_{\max} = 2$ (●), $e_{\max} = 4$ (▲), $e_{\max} = 6$ (◆), $e_{\max} = 8$ (■) and $e_{\max} = 10$ (★). Due to high computational effort, alo model spaces were additionally $N_{\max}$ truncated with the same value as the $e_{\max}$ truncation.

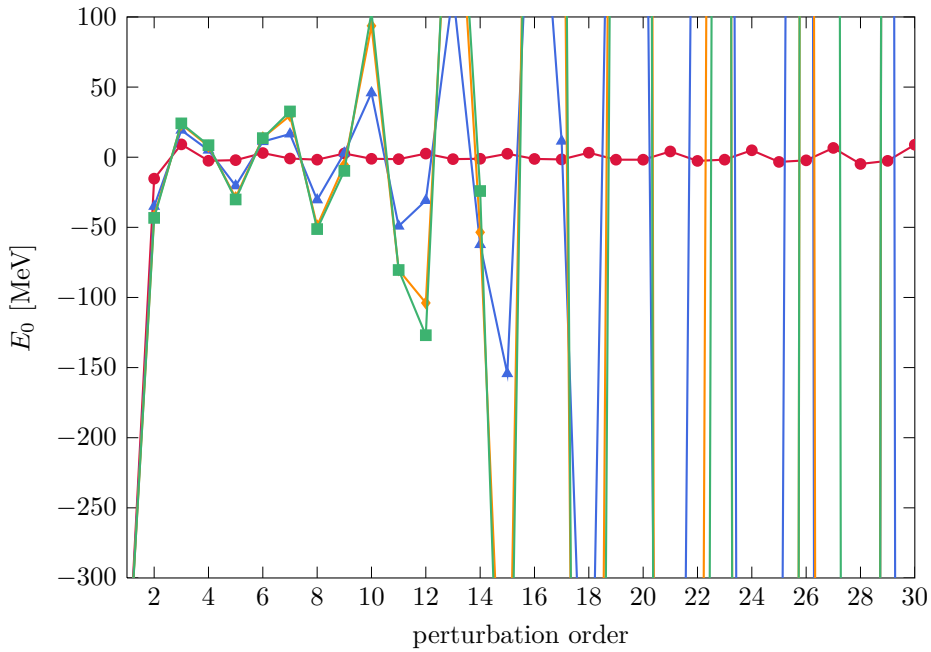

Figure 12.8: Plot of high order perturbative corrections of ^{16}O with respect to HO basis for $\alpha = 0.08\text{fm}^4$, oscillator frequency $\hbar\Omega = 20\text{MeV}$ and increasing values of $e_{\max}$: $e_{\max} = 4$ (●), $e_{\max} = 4$ (▲), $e_{\max} = 6$ (◆) and $e_{\max} = 8$ (■).

holds for ^{16}O. The results are depicted in fig. 12.8. Even though for small spaces the first order energy corrections lie near the exact results, higher orders tend to diverge wildly. This behaviour is more present for larger model spaces. This might lead to the conclusion, that contributions from a larger model space result in stronger divergences that do not occur in small model spaces.

Impact of the SRG parameter

We conclude the discussion of HO perturbation theory with a remark on SRG evolution parameter. Increasing the value of the flow parameter yields better convergence results with respect to model-space size. However, it does not improve the convergence behaviour of the series itself. Fig.(12.9) depicts the dependence of the sequence of partial sums for increasing values of α. Altering the flow parameter does not affect the qualitative behaviour of the perturbation series in HO basis. Therefore, we rely on resummation methods to extract the ground-state energy from the diverging series [21].

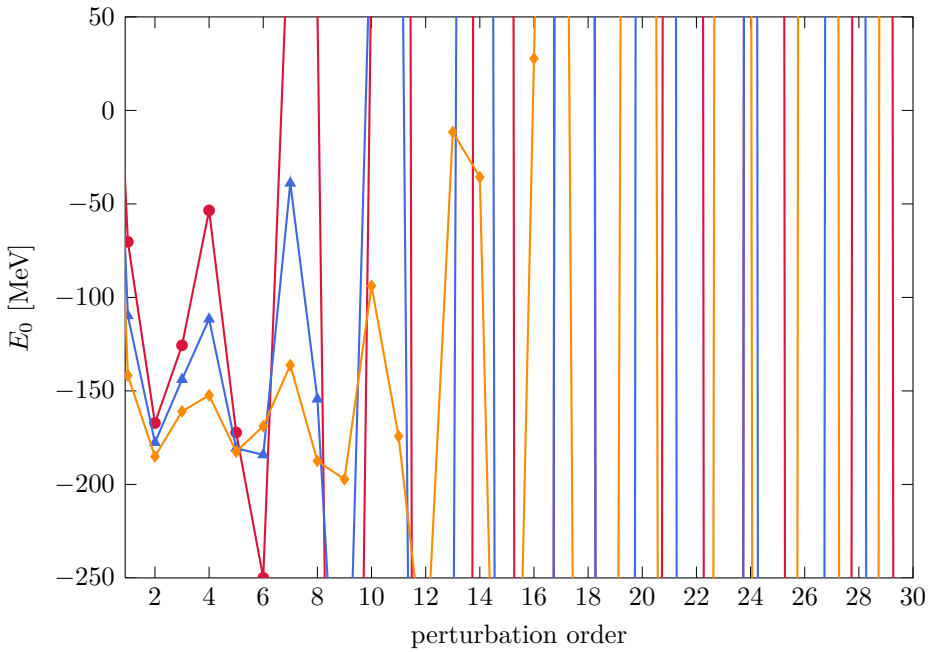

Figure 12.9: Plot of the sequence of partial sums of ^{16}O with rspect to HF basis for $e_{\max} = 8$, $2p2h$-excitations and oscillator frequency $\hbar\Omega = 20$MeV. The plots correspond to SRG flow parameters $\alpha = 0.02\text{fm}^4$(●), $\alpha = 0.04\text{fm}^4$(▲) and $\alpha = 0.08\text{fm}^4$(◆).

12.2.3 Hartree-Fock Basis

After discussing perturbation theory in terms of a HO basis we analyze the impact of a change in partitioning. In the following we compare different SRG-evolution parameters and different truncation schemes for ^{4}He. We investigate both the bare perturbation series and the Padé approximants. The results are shown in fig. 12.10. First of all, we note the convergent perturbation series. There appears not a single case in which a perturbation series tends to diverge or even oscillates in fig. 12.10. Note that for lower values of α it becomes more important to include larger model spaces, that is the difference between an $\text{N}_{\max} = 8$ and $\text{N}_{\max} = 10$ truncated spaces is most present in the case of $\alpha = 0.02\text{fm}^4$, where the difference is roughly 2 MeV, whereas for $\alpha = 0.16\text{fm}^4$ it is less than 1 MeV. Obviously interactions with a smaller evolution parameter are less good converged with respect to the model-space size. The general conclusion is that for a fixed set of parameters the partial sums converge within the first five orders up to very high precision. Next will provide an analysis of the next closed-shell nucleus, namely ^{16}O. With increasing number of nucleons, calculations get computationally very demanding. So we cannot treat this nucleus within arbitrary number of excitations. Note that this would require to take $16p16h$ excitations into account. We restrict ourselves to lower excitations, i.e., $2p2h$ and $4p4h$ excitations. We start with considering $2p2h$ excitations. We use different truncation schemes. First we adapt a $e_{\max}$ truncation only and afterwards a truncation with fixed $e_{\max}$ and increasing $N_{\max}$. In fig. 12.11 the results are shown for SRG flow parameter $\alpha = 0.08\text{fm}^4$ and increasing values of $e_{\max}$. We see that HF perturbation theory provides convergent partial sums - in contrast to HO perturbation theory. We also see that there is still the pattern that with increasing truncation parameter the results decrease in energy. Especially for larger values of $e_{\max}$ a damped oscillatory behaviour for the first

ten orders appears. We can compare this picture to the case of a less evolved interaction with SRG parameter $\alpha = 0.02\text{fm}^4$. The results are shown in fig. 12.12. The comparison of fig. 12.11 and fig. 12.12 illustrates the impact of SRG evolution to perturbation theory. For SRG-evolution parameter $\alpha = 200\text{fm}^4$ and small model spaces, i.e., $e_{\max} = 2, 4$ the partial sums show an oscillatory behaviour, while increasing the model space to values up $e_{\max} = 10$ yields wildy diverging energy corrections. This may be devoted to the SRG-evolution that accounts for correlations of the interaction. This clearly shows that we must be very careful when setting a particular model space. Especially small values of the SRG parameter make it difficult to treat the problem perturbatively. However, we cannot say that this divergences come from the SRG evolution alone. Since ^{16}O is a much more complicated nucleus than ^{4}He, in the sense as that there are much more simultaneous excitations, this divergences might be as well caused by the missing npnh excitations when n exceeds four. We cannnot derive high order perturbation series for those large model spaces and when exploring heavier nuclei we must use a different approach. Nevertheless using HF basis sets instead of HO basis sets we get improved results regarding convergence properties. By now the collected data lacks statistical significance and we must expand our treatment to different nuclei.

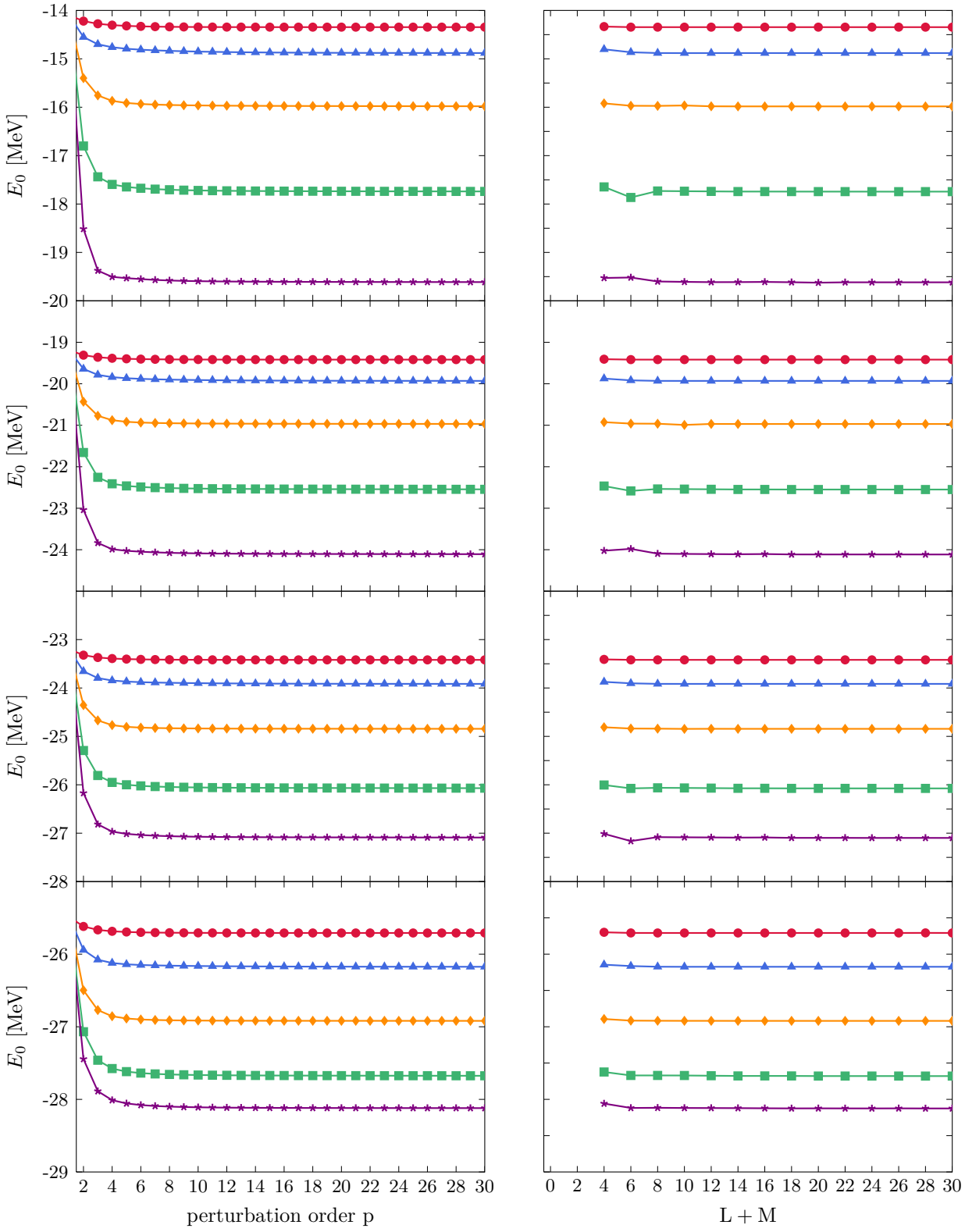

Figure 12.10: Plot of the sequence of partial sums (left) and the diagonal Padé approximants (right) of ^{4}He with respect to HF basis for $\alpha = 0.02\text{fm}^4$, 0.04fm^4, 0.08fm^4 and 0.16fm^4(going from top to bottom), oscillator frequency $\hbar\Omega = 20\text{MeV}$, $e_{\max} = 10$ and increasing values of $N_{\max}$: $N_{\max} = 2$ (●), $N_{\max} = 4$ (▲), $N_{\max} = 6$ (◆), $N_{\max} = 8$ (■) and $N_{\max} = 10$ (★). The first calculated Padé approximant is $P[2/2]$ corresponding to a perturbation order of four.

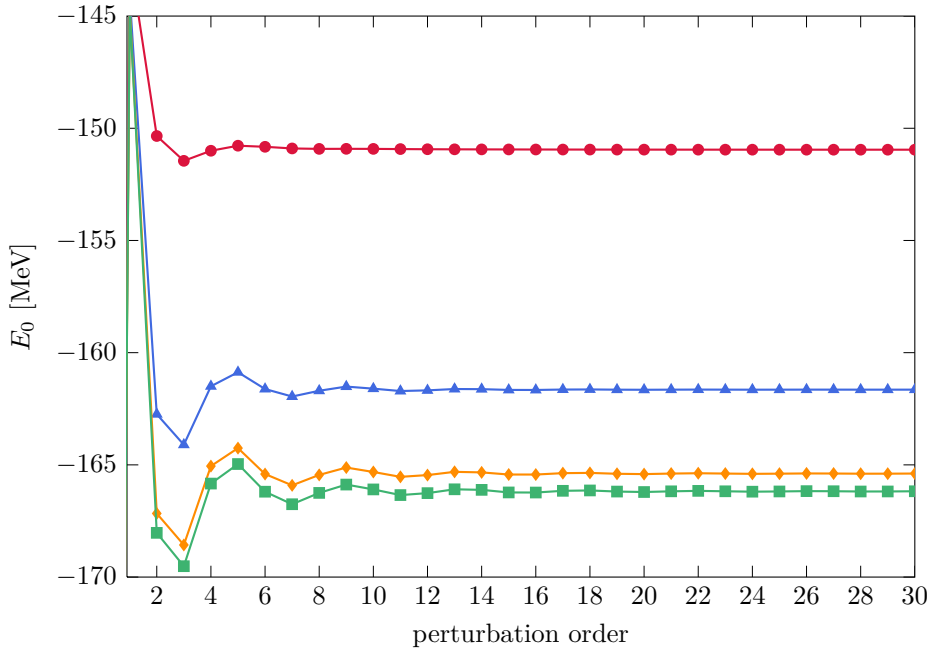

Figure 12.11: Plot of the sequence of partial sums of ^{16}O for $\alpha = 0.08\text{fm}^4$, oscillator frequence $\hbar\Omega = 20\text{MeV}$ and $2p2h$-excitations for increasing values of $e_{\max}$: $eMax = 2$ (●),$e_{\max} = 4$ (▲),$e_{\max} = 6$ (◆) and $e_{\max} = 8$ (■).

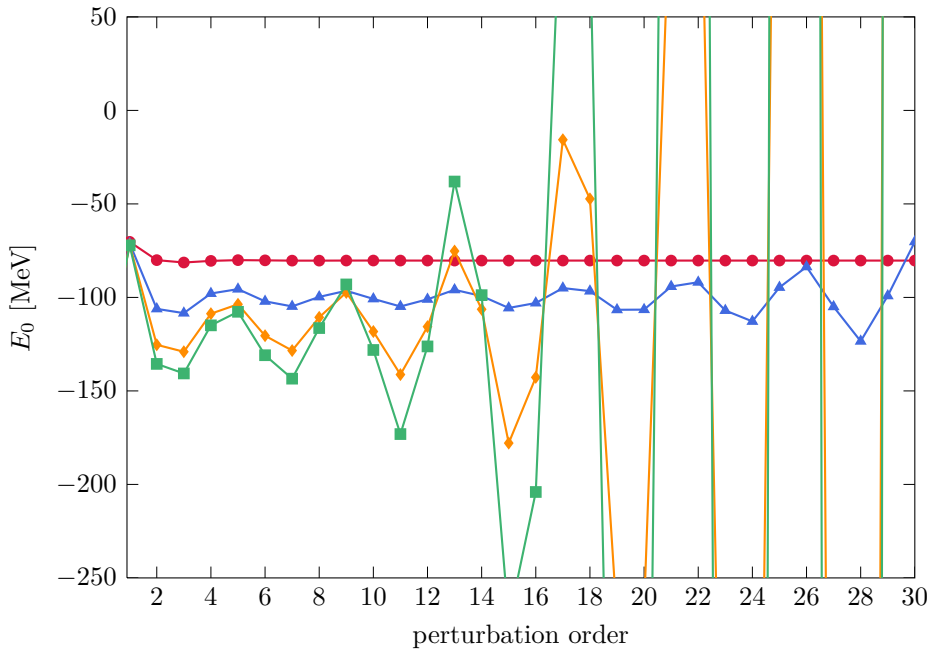

Figure 12.12: Plot of the sequence of partial sums of ^{16}O for $\alpha = 0.02\text{fm}^4$, oscillator frequency $\hbar\Omega = 20\text{MeV}$ and $2p2h$-excitations for increasing values of $e_{\max}$: $e_{\max} = 2$ (●), $e_{\max} = 4$ (▲), $e_{\max} = 6$ (◆) and $e_{\max} = 8$ (■).

Impact of SRG Evolution

SRG evolution is used to obtain better convergence with respect to the model-space size. However, fig. 12.13 shows that it may also improve the convergence properties of the the perturbation series itself for a fixed model space in terms of a HF basis. For low values of the SRG flow parameter we obtain diverging perturbation series, whereas an evolution with $\alpha = 0.08\text{fm}^4$ yields a convergent sequence of partial sums. This property makes the HF basis superior to the HO basis. Note that we investigated the dependence on the SRG flow parameter for the same nucleus within the same model-space for the HO basis in fig. 12.9. In that case SRG evolution does not affect convergence properties of the series itself, but only increases the convergence properties with respect to the model space if the perturbation series is already convergent.

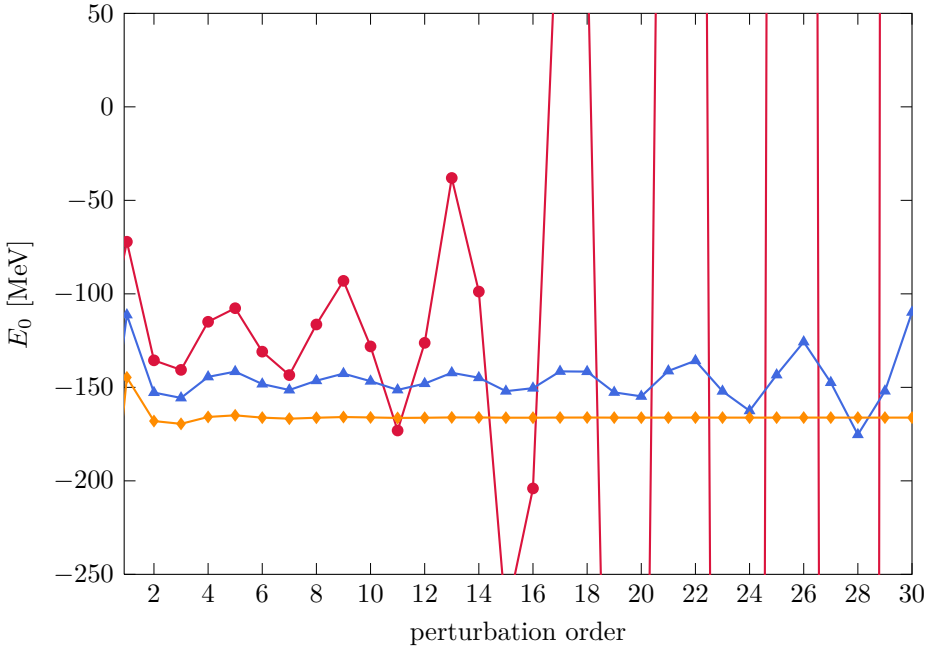

Figure 12.13: Plot of the sequence of partial sums of ^{16}O with rspect to HF basis for $e_{\max} = 8$, $2p2h$-excitations and oscillator frequency $\hbar\Omega = 20\text{MeV}$. The plots correspond to SRG flow parameters $\alpha = 0.02\text{fm}^4$(●), $\alpha = 0.04\text{fm}^4$(▲) and $\alpha = 0.08\text{fm}^4$(◆).

Summary of High-Order Perturbation Theory

The previous analysis shows that the divergence of the perturbation series appearing in HO basis can be overcome by changing the partitioning. Most perturbation series diverge in terms of the HO basis, making methods like Padé resummation inevitable. Although we only discuss HO perturbation theory for closed-shell nuclei it was shown that this is also true for open-shell nuclei and the use of degenerate perturbation theory [21]. However, when using HF basis states typically the perturbation series itself converges, compare fig. 12.14, making resummation methods superflous. Even though it may appear that in HF basis the perturbation series is divergent. It turns out that we can obtain a convergent perturbation series by further evolving the interaction. The feature that increasing the SRG flow parameter not only improves convergence with respect to model-space size but also the convergence of the perturbation series is only present in HF basis and was not

observed in HO basis. Since these preliminary results show that most perturbation series in HF basis are convergent this motivates the use of low-order perturbation theory. By considering only corrections up to order three we are able to investigate heavy nuclei. Note that this step is not justified in terms of HO basis, since for a divergent perturbation series it makes no sense to expect the third partial sum to be a reasonable appoximation to ground-state energy. However, in terms of HF basis we have numerical evidence for the perturbation series to converge, therefore, expecting the third partial sum to be a good approximation of the ground-state energy. This motivates to investigate low-order perturbation series from heavy nuclei in terms of HF bases. Note that we are restricted to closed-shell nuclei and even medium-mass nuclei like ^{40}Ca cannot be treated in terms of high-order perturbation theory for larger model spaces.

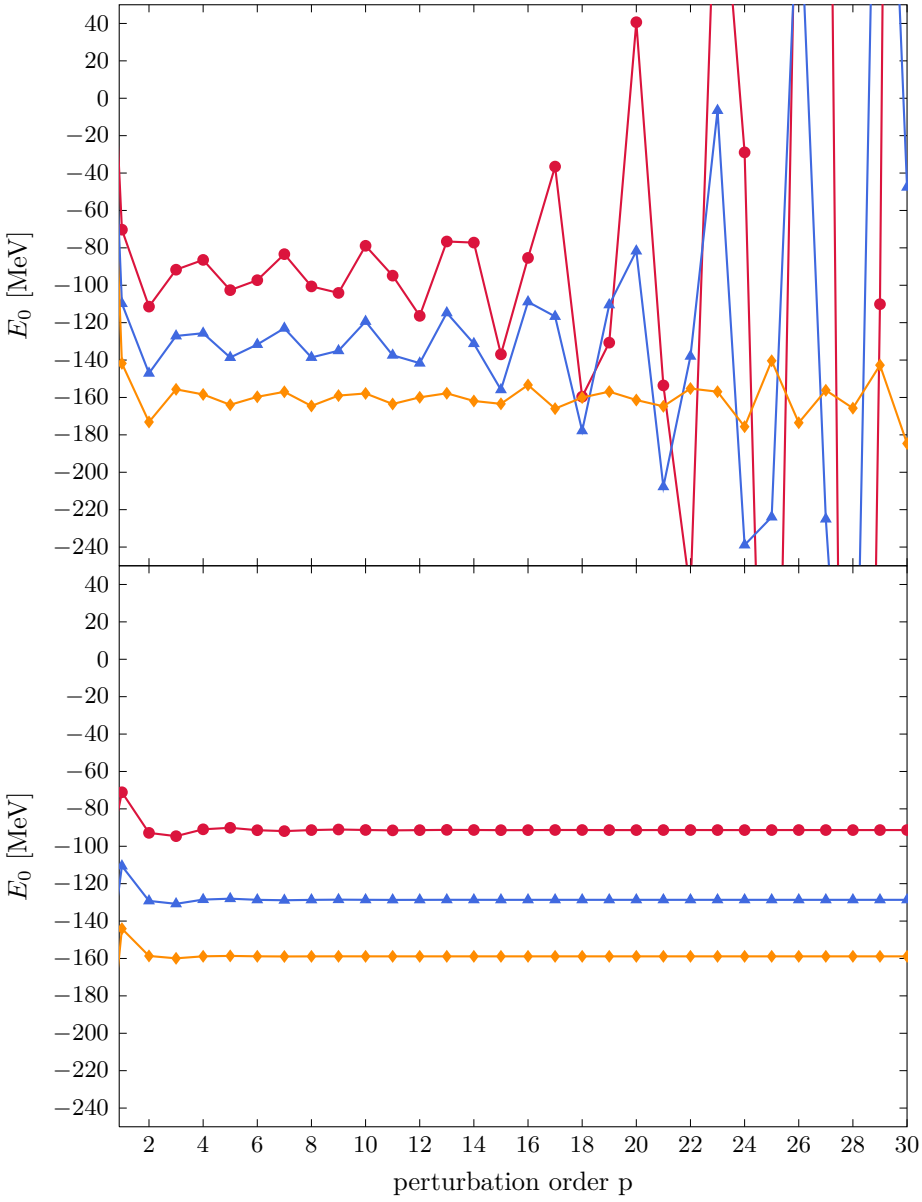

Figure 12.14: Plot of the sequence of partial sums of ^{16}O with respect to HO basis (top) and HF basis (bottom) for $e_{\max} = 8$, $4p4h$-excitations and oscillator frequency $\hbar\Omega = 20$MeV. The plots correspond to SRG flow parameters $\alpha = 0.02\text{fm}^4$(●), $\alpha = 0.04\text{fm}^4$(▲) and $\alpha = 0.08\text{fm}^4$(◆)

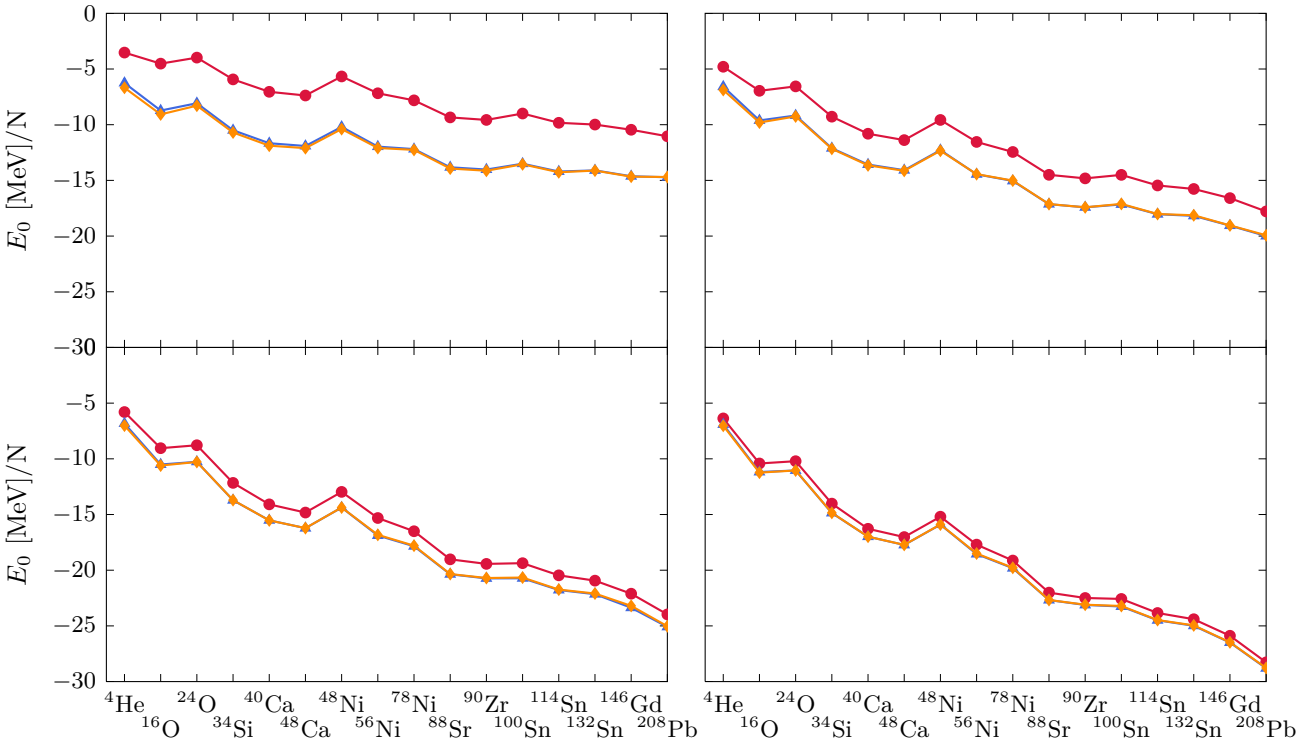

Figure 12.15: Plot of the energy per nucleon perturbative corrections up to third order. Shown are the Hartree-Fock energy (●), $E_{\mathrm{HF}} + E_0^{(2)}$ (▲) and $E_{\mathrm{HF}} + E_0^{(2)} + E_0^{(3)}$ (◆). All calculatationx are performed in a model space with $e_{\max} = 10$ and $\hbar\Omega = 20$MeV. The four plots correspond to different SRG parameters, $\alpha = 0.02\mathrm{fm}^4$(upper left),$\alpha = 0.04\mathrm{fm}^4$(upper right), $\alpha = 0.08\mathrm{fm}^4$(lower left) and $\alpha = 0.16\mathrm{fm}^4$(lower right).

12.3 Low-Order Perturbation Theory

As already explained in chapter 11 there are several limitations in the use of high-order perturbation theory. We investigate energy corrections up to third order over the whole mass range. By the use of BLAS libraries and optimized storage schemes we are able to calculate energy corrections up to third order of closed-shell nuclei up to ^{208}Pb. In this case we will not restrict ourselves to a particular number of particle-hole excitation, but use the value of $e_{\max}$ as the only truncation parameter of the model space. Recall that this is a single-particle truncation. Most of the analysis was done for a frequency of $\hbar\Omega = 20$MeV. A plot of the energy correction of selected closed-shell nuclei is shown in fig. 12.15. Note that the third-order energy corrections are much smaller compared to the second-order corrections. For most nuclei the difference between a second-order and a third-order expansion of the ground-state energy is indistingushable. However for smaller SRG parameters one can see a greater impact of second order contribations. Note that the gap between the Hartree-Fock energy and the second-order energy contribution increases for smaller values of α. Additionally for all SRG aprameters the binding energy per nucleon is decreasing for heavier nuclei in contrast to the experimentally observed saturation to a value of about 8MeV/N. Recall that we are only working with a two-body interaction and this overbinding for heavier nuclei is due to the missing three-body contributions. In table 12.1 we summarize the results for an SRG parameter $\alpha = 0.08\mathrm{fm}^4$. Up to now these are the first calculations involving third order

Nucleus	Hartree-Fock energy	2nd order correction	3rd order correction
^{4}He	- 5.80	-1.03	-0.19
^{16}O	- 9.04	-1.47	-0.09
^{24}O	- 8.78	-1.49	-0.01
^{34}Si	-12.16	-1.56	0.01
^{40}Ca	-14.09	-1.43	-0.01
^{48}Ca	-14.82	-1.40	<0.01
^{48}Ni	-12.97	-1.41	<0.01
^{56}Ni	-15.31	-1.57	0.06
^{78}Ni	-16.50	-1.35	0.05
^{88}Sr	-19.02	-1.34	0.02
^{90}Zr	-19.43	-1.30	0.03
^{100}Sn	-19.37	-1.36	0.07
^{114}Sn	-20.46	-1.32	0.04
^{132}Sn	-20.94	-1.22	0.06
^{156}Gd	-22.11	-1.26	0.17
^{208}Pb	-23.97	-1.12	0.06

Table 12.1: Hartree-Fock energy, second-order and third-order partial sums for selected closed-shell nuclei for SRG parameter $\alpha = 0.08\text{fm}^4$ and oscillator frequence $\hbar\Omega = 20\text{MeV}$

contributions from many-body perturbation theory for heavy nuclei. From table 12.1 we see that with every further perturbation order the size of the corrections decreases by at least one order of magnitude. Of course, this is not a proof of convergence but it gives at least a numerical hint for the behavior of HF perturbation series.

12.3.1 Comparison to Coupled-Cluster Techniques

By now we only discussed different approaches within the framework of perturbation theory. Next we compare these results to ab-initio nuclear-structure techniques. We use the Coupled-Cluster approach to test our calculations on consistency. Fig. 12.16 shows the excellent agreement between the Coupled-Cluster approach and perturbation techniques. Obviously, both methods are in very good agreement with each other. We will investigate this in more detail via table table 12.2. This shows the excellent agreement between these two methods. Note that the relative deviation between the Coupled-Cluster results and and the summed contributions up to third order differ by less than one percent providing strong numerical evidence for perturbation theory being consistent with the Coupled-Cluster approach.

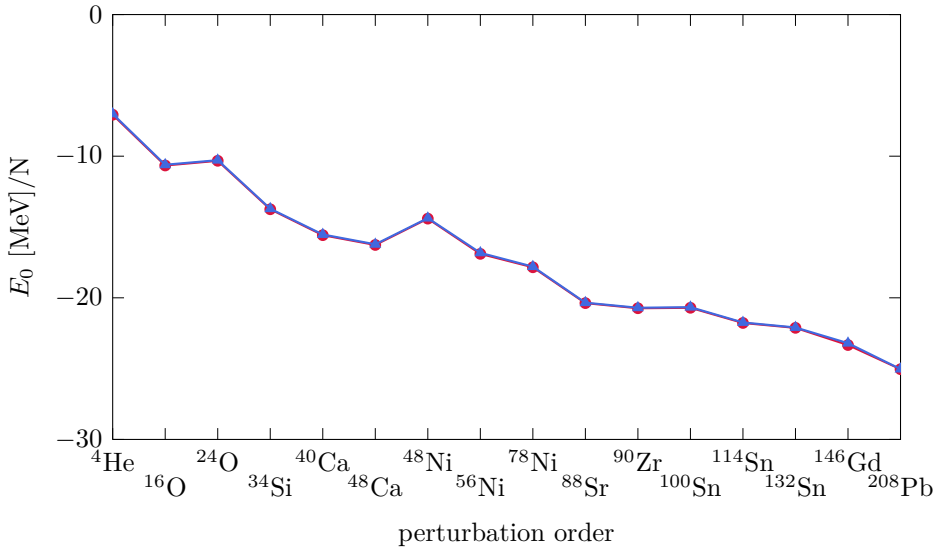

Figure 12.16: Comparison between results obtained via ΛCCSD (●) and perturbation theory (▲). Calculations were performed for $\alpha = 0.8\text{fm}^4$ and oscillator frequency $\hbar\Omega = 20\text{MeV}$ in a $e_{\max} = 10$ truncated model space. Both curves are almost indistingushable.

Nucleus	$E_{HF} + E^{(2)} + E^{(3)}$	ΛCCSD	rel. deviation in %
^{4}He	-7.01	-7.07	0.85
^{16}O	-10.60	-10.66	0.50
^{24}O	-10.28	-10.33	0.44
^{34}Si	-13.71	-13.75	0.30
^{40}Ca	-15.53	-15.58	0.32
^{48}Ca	-16.22	-16.27	0.29
^{48}Ni	-14.37	-14.41	0.27
^{56}Ni	-16.82	-16.90	0.44
^{78}Ni	-17.80	-17.84	0.27
^{88}Sr	-20.34	-20.37	0.15
^{90}Zr	-20.70	-20.74	0.17
^{100}Sn	-20.66	-20.70	0.22
^{114}Sn	-21.74	-21.78	0.17
^{132}Sn	-22.09	-22.12	0.13
^{156}Gd	-23.20	-23.34	0.57
^{208}Pb	-25.03	-25.04	0.04

Table 12.2: Comparison between Hartree-Fock-energy with second- and third-order energy corrections and Coupled-Cluster results (ΛCCSD). Both methods used SRG parameter $\alpha = 0.08\text{fm}^4$, oscillator frequence $\hbar\Omega = 20$ and $e_{\max} = 20$. The energy is given in MeV/N The relative deviation between the calculations is given in the last row.

12.3.2 Impact of SRG Evolution on Convergence Behaviour

After comparing perturbation theory to ab-initio methods we now discuss the effect of SRG evolution on the perturbative corrections in more detail. We have already seen that decreasing the flow parameter leads to increasing values for the second- and third-order energy contributions. This fact becomes more obvious from fig. 12.17. Note the sensitivity of the correlation energy to the flow parameter. For values of $\alpha = 0.02\text{fm}^4$ compared to $\alpha = 0.16\text{fm}^4$ there is a factor five between the magnitude of the correlation energy. This implies that the Hartree-Fock energy is a less good approximation to the exact ground-state energy which is a direct consequence of the Hartree-Fock approximation. For another point of view compare fig. 12.18. We see again the hirarchy between subsequent perturbation orders. The relative magnitude of the third order contribution compared to the third order correlation energy is quite small - independent of the value of the flow parameter. However, note the different scaling of the energy axis in the fig. 12.18.

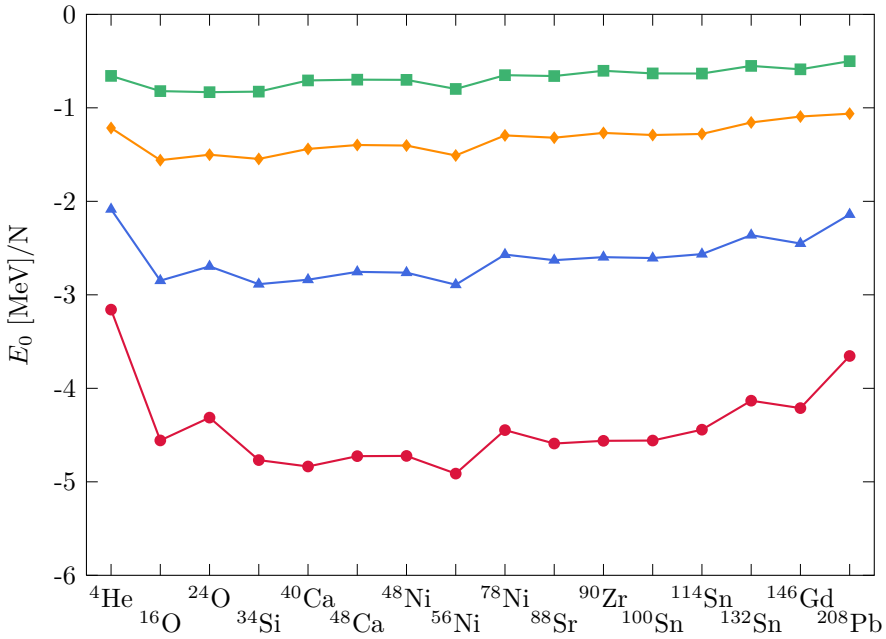

Figure 12.17: Plot of the correlation energy, i.e. the $E^{(2)} + E^{(3)}$ for different values of α, in MeV/N. We used a $e_{\max} = 10$ model space with oscillator frequence $\hbar\Omega = 20$MeV. The different colors correspond to $\alpha = 0.02\text{fm}^4$ (●), $\alpha = 0.04\text{fm}^4$ (▲), $\alpha = 0.08\text{fm}^4$ (◆) and $\alpha = 0.16\text{fm}^4$ (■)

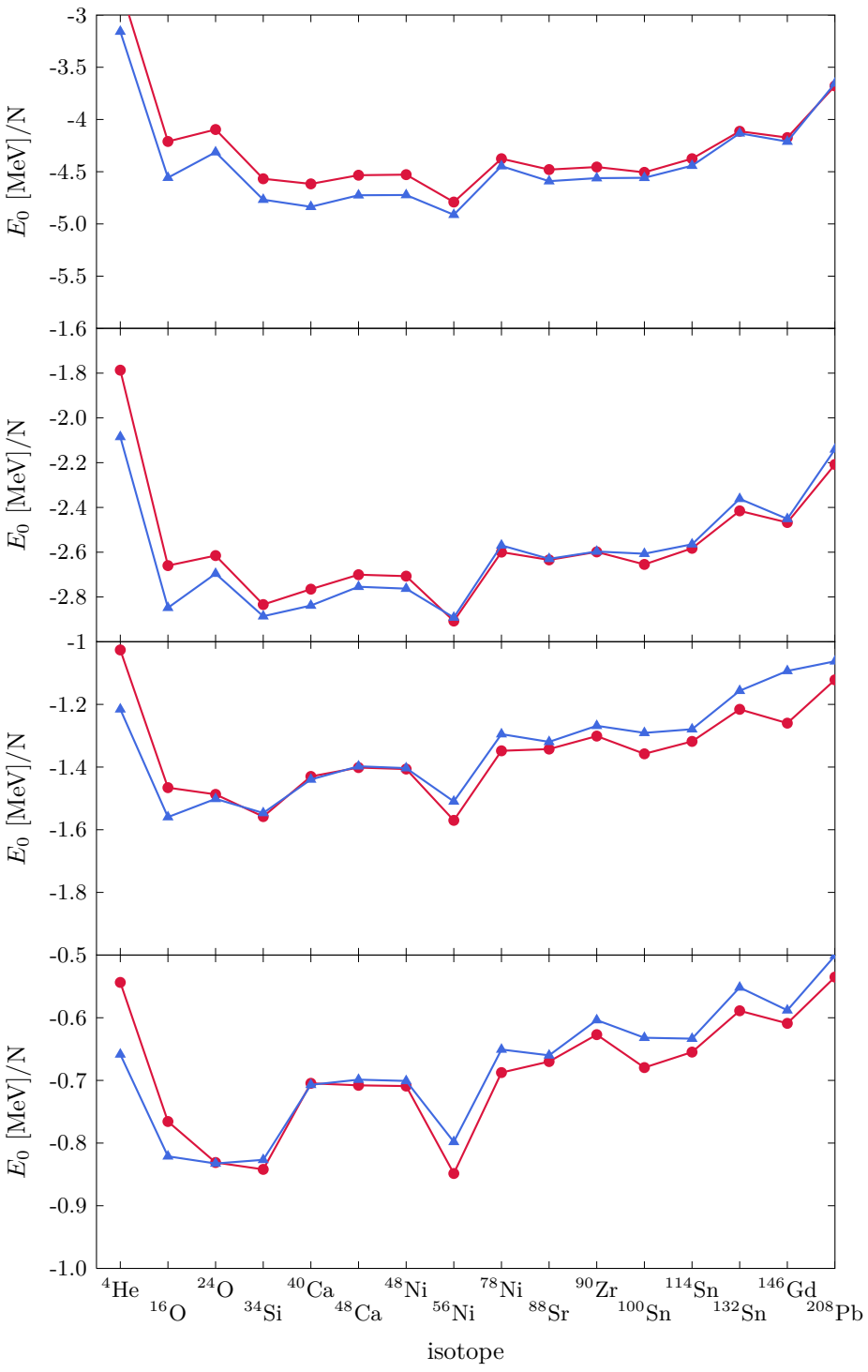

Figure 12.18: Plot of the correlation energy, i.e., the $E^{(2)} + E^{(3)}$ (▲) and the second order contribution $E^{(2)}$ (●) for different SRG parameters $\alpha = 0.02$, 0.04, 0.08 and 0.16fm^4 (from top to bottom) . Again we used $e_{\max} = 10$ model space with oscillator frequence $\hbar\Omega = 20$MeV.

Chapter 13

Conclusion and Outlook

Many-Body perturbation theory has shown to be a powerful method for the solution of the stationary Schrödinger equation. However, it may appear that even for simple analytic potential the resulting perturbation series is divergent. This behaviour is also present when investigating realistic interaction in terms of HO perturbation theory [21]. To overcome the divergences we investigated two different approaches. On one hand we alter the partitioning, i.e., change the basis set to expand the solution in. On the other hand we investigated resummation schemes and transformed the perturbation series into a new sequence with better convergence properties. It was already known that the use of Padé approximants leads to a convergent sequence which yields accurate results for the ground-state energy for both closed- and open-shell nuclei in terms of HO perturbation theory [21]. However, when using Padé approximants we need roughly the first ten energy corrections to construct enough Padé approximants to work with acceptible accuracy. The first attempt was to construct new kinds of sequence transformation which converge faster than the Padé main sequence. Unfortunately, this is only possible if there are precise remainder estimates available. This is the case for the quantum anharmonic oscillator which we studied as a benchmark case. Using the Levin-Weniger transformation enabled us to derive accurate results for the ground-state energy within four perturbation orders. However, it is not possible to extend this kind of analysis to a generic two-body interaction.

Therefore, we focused on high-order Hartree-Fock perturbation theory for closed-shell nuclei. Up to this point there was no treatment of high-order oerturbation theory for HF bases states. It was appearent that perturbation series arising from HF bases states are in many times convergent in contrast to HO bases states. We were able to derive accurate results for the ground-state energy of ^{4}He and ^{16}O from the bare perturbation series. Using HF perturbation theory obviates the use of resumamtion schemes. Furthermore, it appears that HF perturbation series have another nice property, i.e., their dependence on the SRG-evolution parameter. SRG evolution is a tool to increase the convergence properties with respect to model space size which is inevitable in MBPT. Evolved Hamiltonians have already been used in HO perturbation theory. For fixed model space the SRG evolution does not change the convergence pattern of HO perturbation series. However, preliminary results for ^{16}O show that a further evolution of the nuclear Hamiltonian improves the convergence properties of HF perturbation series for fixed model space. More precisely, we have seen that a perturbation series that was divergent for $\alpha = 0.02\text{fm}^4$ was cast to a convergent

expansion in the same model space with flow parameter $\alpha = 0.08\text{fm}^4$. Up to this point we did not find any diverging HF perturbation series for SRG parameter $\alpha = 0.08\text{fm}^4$.

The highly improved convergence properties of HF perturbation series motivated the use of HF bases states for the use of low-order calculations. By analyzing diagrammatic perturbation theory and in particular Hugenholtz diagrams, we are able to derive explicit formulas for low-order energy corrections in particle-hole formalism. Since we expect from high-order perturbation theory the HF perturbation series to converge, the sequence of partial sums formed from the three lowest orders will be a reasonable approximation. Restricting ourselves to third order contributions enabled us to investigate closed-shell nuclei over the entire nuclear chart. Comparison of the results from HF perturbation theory with Coupled-Cluster results obtained from λCCSD(T) calculations showed the excellent agreement with modern ab-initio approaches. Furthermore, we analyzed the dependence of the correlation energy with increasing SRG evolution parameter. It appeared that the corrections arising from second- and third-order perturbation theory increase with decreasing values of the α.

These preliminary results show than HF perturbation theory is more effective that the combintion of HO perturbation theory with resummation schemes like Padé approximants. However, for a systematic treatment the number of investigated nuclei is too small. For a detailed analysis of HF perturbation series we need to implement HF perturbation theory for off-shell nuclei. This extends the use of high-order perturbation theory to a large number of isotopes. Even though, this is already done for HO perturbation theory [21] there is no formulation in terms of HF basis states. Exploring degenerate HF perturbation theory is the next major step in the analysis of MBPT. Additionally all calculations within this thesis are performed with a two-body interaction only. Developments in nuclear structure from the last two decades have shown that the inclusion of three-body interactions is important for an adequate description of nuclear properties. It seems straightforward ton include normal-ordered interactions in two-body approximation, whereas an inclusion of a full three-body interaction will be much more complicated. Aside from extending HF perturbation theory to new physical grounds we need to improve computational performance. Mainly this involves implementation and optimization of multi-threaded paralellization routines making larger model spaces available. Furthermore, perturbation theory for off-shell nuclei requires full diagonalization within the degenerate subspaces. Development of degenerate HF perturbation theory with inclusion of three-body forces and implementation of effective algorithms will be a challenging task for further studies.

Chapter 14

Appendix A - Watson's Theorem

In the derivation of the Borel transform we encountered an upprotunity to assign a integral representation to a asymptotic series. This is the so-called Watson's theorem. In the following we state it without proof and use it to deduce the Borel sum of a divergent series.

Theorem 7 (Watson's Theorem)**.** *Let $f(t)$ be a continous function on the intervall $[0, b]$ with asymptotic relation*

$$f(t) \sim t^{\alpha} \sum_{n=0}^{\infty} a_n t^{\beta n}, \tag{14.1}$$

for $t \to 0^+$. Furthermore, let

$$I(x) = \int_0^b f(t) e^{-xt} dt \tag{14.2}$$

a convergent integral. Then it holds

$$I(x) \sim \sum_{n=0}^{\infty} \frac{a_n \Gamma(\alpha + \beta n + 1)}{x^{\alpha+\beta n+1}}, \tag{14.3}$$

for $x \to \infty$.

Note that we defined the Borel transformed by

$$B(x) = \int_0^{\infty} e^{-t} \phi(xt) dt, \tag{14.4}$$

with $\phi(x) = \sum_{n=0}^{\infty} \frac{a_n}{n!} x^n$. Substitution yields

$$\begin{aligned} B(x) &= \int_0^{\infty} e^{-\frac{\tau}{x}} \phi(\tau) d\tau \frac{1}{x}, \\ &= \int_0^{\infty} e^{-\frac{\tau}{x}} \sum_{n=0}^{\infty} \frac{a_n}{n!} \tau^n d\tau \frac{1}{x} \\ &\sim \sum_{n=0}^{\infty} \frac{a_n}{n!} \int_0^{\infty} e^{-\frac{\tau}{x}} \tau^n d\tau \frac{1}{x} \end{aligned} \tag{14.5}$$

Substitution with $s = \tau/x$ yields

$$\begin{aligned} B(x) &\sim \sum_{n=0}^{\infty} \frac{a_n}{n!} \int_0^{\infty} e^{-\frac{s}{x}} s^n ds x^n \\ &\sim \sum_{n=0}^{\infty} \frac{a_n}{n!} \Gamma(n+1) x^n \\ &\sim \sum_{n=0}^{\infty} a_n x^n. \end{aligned} \tag{14.6}$$

So the Borel transform is indeed asymptotic to the original divergent series. The Borel sum is given by the integral eq. (14.4) evaluated at $x = 1$. For the original paper see [47] and [2] applications on the asymptotic behaviour of integrals.

Bibliography

[1] George A. Baker and Peter Graves-Morris. *Pade Approximants. Part 1: Basic Theory. Part 2: Extensions and Applications. (Encyclopedia of Mathematics and Its Applications, Vols. 13-14)*. Addison-Wesley, 1981.

[2] Carl M. Bender and Steven A. Orszag. *Advanced Mathematical Methods for Scientists and Engineers: Asymptotic Methods and Perturbation Theory (v. 1)*. Springer, 1999.

[3] Sven Binder. PhD thesis, 2014. In preparation.

[4] Sven Binder, Piotr Piecuch, Angelo Calci, Joachim Langhammer, Petr Navrátil, and Robert Roth. Extension of coupled-cluster theory with a noniterative treatment of connected triply excited clusters to three-body Hamiltonians. *Physical Review C*, 88(5):054319, November 2013.

[5] JP Boyd. The devil's invention: Asymptotic, superasymptotic and hyperasymptotic series. *Acta Applicandae Mathematica*, 193995:1–98, 1999.

[6] T. Wu C. Bender. Anharmonic Oscillator. *Physical Review*, 186, 1969.

[7] Torsten Carleman. Les fonctions quasi analytiques. 1926.

[8] Ana C. Matos Claude Brezinski. A Derivation of Extrapolation Algorithms Based on Error Estimates. 1993.

[9] Reinhard Diestel. *Graph Theory (Graduate Texts in Mathematics)*. Springer, 2010.

[10] D. R. Entem and R. Machleidt. Accurate charge-dependent nucleon-nucleon potential at fourth order of chiral perturbation theory. *Physical Review C*, 68(4):041001, October 2003.

[11] Evgeny Epelbaum. Few-nucleon forces and systems in chiral effective field theory. *Progress in Particle and Nuclear Physics*, 57(2):654–741, October 2006.

[12] Leonhard Euler. Inventio summae cuiusque seriei ex dato termino generali.

[13] Philippe Gaudreau, Richard M. Slevinsky, and Hassan Safouhi. An asymptotic expansion for energy eigenvalues of anharmonic oscillators. *Annals of Physics*, 337:261–277, 2013.

[14] Godfrey Harold Hardy. *Divergent Series*. 1991.

[15] Einar Hille. Review: G. Doetsch, Handbuch der Laplace-Transformation. Vol. 1. Theorie der Laplace-Transformation. *Bulletin of the American Mathematical Society*, 58(6):670–673, November 1952.

[16] Ulrich Jentschura, Andrey Surzhykov, and Jean Zinn-Justin. Unified Treatment of Even and Odd Anharmonic Oscillators of Arbitrary Degree. *Physical Review Letters*, 102(1):011601, January 2009.

[17] George A. Baker Jr. *Essentials of Padé Approximants*. Academic Press, 1975.

[18] Jean-Pierre Julien, Jean Maruani, Didier Mayou, and Gerard Delgado-Barrio. *Recent Advances in the Theory of Chemical and Physical Systems: Proceedings of the 9th European Workshop on Quantum Systems in Chemistry and Physics ... in Theoretical Chemistry and Physics)*. Springer, 2006.

[19] ED Jurgenson, P Navratil, and RJ Furnstahl. Evolution of nuclear many-body forces with the similarity renormalization group. *Physical review letters*, 103(8):2–5, August 2009.

[20] Volker Koch. Aspects of Chiral Symmetry. *International Journal of Modern Physics E*, 06(02):203–249, June 1997.

[21] Joachim Langhammer, Robert Roth, and Christina Stumpf. Spectra of open-shell nuclei with Padé-resummed degenerate perturbation theory. *Physical Review C*, 86(5):054315, November 2012.

[22] David Levin. Development of non-linear transformations for improving convergence of sequences. *International Journal of Computer Mathematics*, 3(1-4):371–388, January 1972.

[23] J. Lyons, D. Moncrieff, and S. Wilson. Diagrammatic many-body perturbation expansion for atoms and molecules. *Computer Physics Communications*, 84(1):91–101, 1994.

[24] R. Machleidt and D.R. Entem. Chiral effective field theory and nuclear forces. *Physics Reports*, 503(1):1–75, June 2011.

[25] V. I. Mel'nik. Tauberian theorems foe Borel-type methods of summability. *Ukrainian Mathematical Journal*, 30(2):133–139, 1978.

[26] Jesus Navarro. *Microscopic Quantum Many-Body Theories and Their Applications: Proceedings of a European Summer School, (Lecture Notes in Physics)*. Springer, 2013.

[27] Wolfgang Nolting. *Grundkurs Theoretische Physik 5/2: Quantenmechanik - Methoden und Anwendungen (Springer-Lehrbuch) (German Edition)*. Springer, 2012.

[28] J. Paldus and H.C. Wong. Computer generation of Feynman diagrams for perturbation theory I. General algorithm. *Computer Physics Communications*, 6(1):1–7, July 1973.

[29] A Pich. Effective field theory. *arXiv preprint hep-ph/9806303*, (June 1998), 1998.

[30] Piotr Piecuch and Marta Włoch. Renormalized coupled-cluster methods exploiting left eigenstates of the similarity-transformed Hamiltonian. *The Journal of chemical physics*, 123(22):224105, December 2005.

[31] Jorge Rezende. A note on Borel summability. *Journal of Mathematical Physics*, 34(9):4330, September 1993.

[32] Robert Roth, Angelo Calci, Joachim Langhammer, and Sven Binder. Evolved Chiral NN+3N Hamiltonians for Ab Initio Nuclear Structure Calculations. November 2013.

[33] Robert Roth, Jeffrey Gour, and Piotr Piecuch. Ab initio coupled-cluster and configuration interaction calculations for O16 using the VUCOM interaction. *Physical Review C*, 79(5):054325, May 2009.

[34] Robert Roth and Joachim Langhammer. Padé-resummed high-order perturbation theory for nuclear structure calculations. *Physics Letters B*, 683(4-5):272–277, January 2010.

[35] Robert Roth and Joachim Langhammer. Padé-resummed high-order perturbation theory for nuclear structure calculations. *Physics Letters B*, 683(4-5):272–277, January 2010.

[36] Robert Roth, Joachim Langhammer, Angelo Calci, Sven Binder, and Petr Navrátil. Similarity-Transformed Chiral NN+3N Interactions for the Ab Initio Description of ˆ{12}C and ˆ{16}O. *Physical Review Letters*, 107(7):072501, August 2011.

[37] Robert Roth, Sabine Reinhardt, and Heiko Hergert. Unitary correlation operator method and similarity renormalization group: Connections and differences. *Physical Review C*, 77(6):064003, June 2008.

[38] J. J. Sakurai. *Modern Quantum Mechanics (Revised Edition)*. Addison Wesley, 1993.

[39] Isaiah Shavitt and Rodney J. Bartlett. *Many-Body Methods in Chemistry and Physics: MBPT and Coupled-Cluster Theory (Cambridge Molecular Science)*. Cambridge University Press, 2009.

[40] Bruce Shawyer and Bruce B. Watson. *Borel's Methods of Summability: Theory and Applications*. 1994.

[41] Avram Sidi. Acceleration of convergence of general linear sequences by the Shanks transformation. *Numerische Mathematik*, 119(4):725–764, July 2011.

[42] Ian Stewart. *Galois Theory, Third Edition (Chapman & Hall/CRC Mathematics)*. Chapman and Hall/CRC, 2003.

[43] Attila Szabo and Neil S. Ostlund. *Modern Quantum Chemistry: Introduction to Advanced Electronic Structure Theory (Dover Books on Chemistry)*. Dover Publications, 1996.

[44] Andrew G Taube and Rodney J Bartlett. Improving upon CCSD(T): LambdaCCSD(T). I. Potential energy surfaces. *The Journal of chemical physics*, 128(4):044110, January 2008.

[45] Andrew G Taube and Rodney J Bartlett. Improving upon CCSD(T): LambdaCCSD(T). II. Stationary formulation and derivatives. *The Journal of chemical physics*, 128(4):044111, January 2008.

[46] G. Turchetti. Classical limit and stieltjes properties of perturbation series for anharmonic oscillators. *Il Nuovo Cimento B*, 82(2):203–213, August 1984.

[47] G. N. Watson. The harmonic functions associated with the parabolic cylinder. 2(17):116–148, 1918.

[48] Steven Weinberg. Effective chiral lagrangians for nucleon-pion interactions and nuclear forces. *Nuclear Physics B*, 363(1):3–18, 1991.

[49] EJ Weniger. Summation of divergent power series by means of factorial series. *Applied numerical mathematics*, 2010.

[50] Ernst Joachim Weniger. Nonlinear Sequence Transformations for the Acceleration of Convergence and the Summation of Divergent Series. 1989.

[51] E. T. Whittaker and G. N. Watson. *A Course of Modern Analysis*. 1927.

[52] H.C. Wong and J. Paldus. Computer generation of Feynman diagrams for perturbation theory II. Program description. *Computer Physics Communications*, 6(1):9–16, July 1973.

Erklärung zur Eigenständigkeit

Hiermit versichere ich, die vorliegende Master-Thesis ohne Hilfe Dritter nur mit den angegebenen Quellen und Hilfsmitteln angefertigt zu haben. Alle Stellen, die aus diesen Quellen entnommen wurden, sind als solche kenntlich gemacht worden. Diese Arbeit hat in gleicher oder ähnlicher Form noch keiner Prüfungsbehörde vorgelegen.

Ort und Datum

Alexander Tichai